USZ Universitäts Spital Zürich

24th Day of Clinical Research

Sepsis – eine multidisziplinäre Herausforderung

Donnerstag, 22. Mai 2025, 8.15 – 16.00 Uhr
Grosser Hörsaal OST, Universitätsspital Zürich

Verleihung Day of Clinical Research Preis 2025
Georg-Friedrich-Götz Preisverleihung 2025
19. Hartmann-Müller Gedächtnisvorlesung 2025

Committee Day of Clinical Research

Cinelli Paolo, PD Dr.
Distler Oliver, Prof. Dr.
Moch Holger, Prof. Dr.
Schneider Robin
Speck Roberto, Prof. Dr
Van den Broek Maries, Prof. Dr.
von Eckardstein Arnold, Prof. Dr.
Wegener Susanne, Prof. Dr.
Weller Michael, Prof. Dr.
Witzel Isabell, Prof. Dr.
Zinkernagel Annelies, Prof. Dr.

Table of contents

Cover Figure:

Institute of Intensive Care Medicine, University Hospital Zurich

Programm

Donnerstag, 22. Mai 2025

Grosser Hörsaal Ost

08.15 Uhr **Begrüssung – Day of Clinical Research**
Dr. Monika Jänicke, CEO, Universitätsspital Zürich

Veranstaltungsthema: «Sepsis – eine multidisziplinäre Herausforderung»

08.20 Uhr **Einführung in das Veranstaltungsthema und Moderation**
Prof. Dr. Dr. med. Silvio Brugger, Klinik für Infektionskrankheiten und Spitalhygiene, Universitätsspital Zürich

08.25 Uhr **Mechanismen der Sepsis und Antibiotikaresistenzen sowie neue Ansätze zur Bekämpfung**
Überblick über Mechanismen der Sepsis und der Antibiotikaresistenz, Mikrobiota-basierte Therapien
Prof. Dr. Dr. med. Silvio Brugger, Klinik für Infektionskrankheiten und Spitalhygiene, Universitätsspital Zürich

08.40 Uhr **Wie verbessern wir die Resistenzsituation? Ein europäischer Ansatz**
REVERSE – Strategien und Werkzeuge zur Prävention und Behandlung von Infektionen durch multiresistente Erreger
Prof. Dr. med. Walter Zingg, Klinik für Infektionskrankheiten und Spitalhygiene, Universitätsspital Zürich

08.55 Uhr **Diagnostik und Frühtherapie: Früherkennung der Sepsis**
Überblick über neue Methoden zur Erkennung von Sepsis und Stabilisierung des Patienten
Prof. Dr. Dr. med. Sina Coldewey, Institut für Anästhesiologie und Perioperative Medizin, Universitätsspital Zürich

09.10 Uhr **Sepsis-Therapie 2025: Neue Optionen in der Sepsisbehandlung**
Moderne Ansätze und alternative Therapien bei Sepsis
Prof. Dr. med. Sascha David, Institut für Intensivmedizin, Universitätsspital Zürich

09.25 Uhr **Coffee Break**

09.45 Uhr **Intensivmedizin & Chirurgie**
Prognostische Marker für Sepsis nach schwerem Trauma: Erkenntnisse basierend auf Omics-Profilen
PD Dr. sc. nat. Paolo Cinelli, Zentrum Forschung Chirurgie, Universitätsspital Zürich

10.00 Uhr **Sepsis und Gender: Geschlechtsspezifische Unterschiede in Prävention, Diagnose und Behandlung**
Untersuchung geschlechtsspezifischer Unterschiede bei der Sepsisentstehung, Diagnose und Therapie
PD Dr. med. Giovanna Brandi, Institut für Intensivmedizin, Universitätsspital Zürich

10.15 Uhr **Postakute Behandlung: Sepsis-assoziierte Enzephalopathie – Pathophysiologie, Diagnose und therapeutische Ansätze**
Pathophysiologie und Diagnostik der Sepsis-assoziierten Enzephalopathie
Dr. med. Macellina Häberlin, Klinik für Neurologie, Universitätsspital Zürich
Dr. med. Francesco Capecchi, Klinik für Neurochirurgie, Universitätsspital Zürich

10.30 Uhr **Individualisierte Rehabilitationsstrategien nach Sepsis: Von der Intensivstation zurück ins Leben**
Entwicklung personalisierter Therapiepläne zur Förderung der Genesung und Verbesserung der Lebensqualität nach Sepsis
Prof. Dr. med. Matthias Hänggi, Institut für Intensivmedizin, Universitätsspital Zürich

Day of Clinical Research - Preisverleihung

10.50 Uhr **Einführung – Day of Clinical Research, Preisverleihung**
Prof. Dr. Dr. med. Silvio Brugger, Klinik für Infektionskrankheiten und Spitalhygiene, USZ

10.55 Uhr **Session 1: Cardiovascular/Metabolism/Endocrinology**
Plasma Proteomics Identify Molecular Features and Biomarkers of Fulminant Myocarditis
Yuxiao Hu, MD, PhD, Zentrum für translationale und experimentelle Kardiologie (CTEC),
Klinik für Kardiologie, Universitätsspital Zürich, Universität Zürich

11.05 Uhr **Session 2: Hematology/Oncology**
Dual-CAR T cells against NKG2D ligands and VEGFR2 accumulate in orthotopically implanted glioma and prolong survival of immunocompetent glioma-bearing mice
Dr. med. Dr. sc. nat. Maximilian Mastall, Klinik für Neurologie, Universitätsspital Zürich

11.15 Uhr **Session 3: Head Region/Neuroscience**
Relapse activity in pregnancy and the postpartum year in women with multiple sclerosis
Dr. med. Lea Walter, Klinik für Neurologie, Universitätsspital Zürich

11.25 Uhr **Session 4: Infection/Immunity/Inflammation/Systemic Diseases**
HIV superinfections and dolutegravir resistance in South Africa: a modelling study
Gioia Wick, BSc, Klinik für Infektionskrankheiten und Spitalhygiene, Universitätsspital Zürich,
Institut für Medizinische Virologie, Universität Zürich

11.35 Uhr **Session 5: Mixed Topics**
Limitations of SpO2/FiO2-Ratio for Classification and Monitoring of Acute Respiratory Distress Syndrome
Dr. med. Rolf Erlebach, Institut für Intensivmedizin, Universitätsspital Zürich & Universität Zürich,
Dr. Una Pale, Institut für Intensivmedizin, Universitätsspital Zürich & Universität Zürich

11.50 Uhr **Lunch / Poster tour**

Götz-Preis-Verleihung

14.05 Uhr **Begrüssung der Gäste**
Prof. Dr. med. Hanns Ulrich Zeilhofer,
Stellvertretender Dekan Medizinische Fakultät,
Universität Zürich

14.10 Uhr **Einführung und Würdigung der Preisträgerin Prof. Dr. med. Jana Ellegast**
Prof. Dr. med. Beatrice Beck Schimmer,
Direktorin Universitäre Medizin Zürich

14.15 Uhr **Kurzreferat Prof. Dr. med. Jana Ellegast**
Zellintrinsische Inflammation als Strategie gegen AML-Zellen
Klinik für Medizinische Onkologie und Hämatologie, Universitätsspital Zürich

14.30 Uhr **Preisverleihung durch Prof. Dr. med. Hanns Ulrich Zeilhofer**
Stellvertretender Dekan Medizinische Fakultät, Universität Zürich

14.35 Uhr **Einführung und Würdigung des Preisträgers Dr. Jiang-An Yin**
Prof. Dr. med. Beatrice Beck Schimmer,
Direktorin Universitäre Medizin Zürich

14.40 Uhr **Kurzreferat von Dr. Jiang-An Yin**
Quadruple-Guide Arrayed CRISPR Libraries and Novel Genetic Modifiers for Parkinson's and Prion Diseases
Institut für Neuropathologie, Universitätsspital Zürich

14.55 Uhr **Preisverleihung durch Prof. Dr. med. Hanns Ulrich Zeilhofer**
Stellvertretender Dekan Medizinische Fakultät, Universität Zürich

Verleihung 19. Hartmann Müller Gedächtnisvorlesung

15.05 Uhr **Einführung und Preisverleihung durch Prof. Dr. med. Felix Beuschlein,**
Stiftungsrat Hartmann Müller-Stiftung

15.15 Uhr **Vortrag der Preisträgerin**
Trinken und Kuscheln – der unsichtbare Einfluss von Hormonen
Prof. Dr. med. Mirjam Christ-Crain, Klinische Forschung, Universität Basel

16.00 Uhr **Ende der Veranstaltung**

Cardiovascular / Metabolism / Endocrinology

Basic Research

733
L. Rings, R. Boulos, V. Ntinopoulos, A. Haeussler, H. Rodriguez Cetina Biefer, O. Dzemali
Normothermic Circulatory Arrest with Antegrade Cerebral Perfusion for Type A Aortic Dissection

734
L. Rings, R. Boulos, A. Haeussler, I. Tudorache, S. Dushaj, H. Rodriguez Cetina Biefer, O. Dzemali
Right Anterior-Lateral Thoracotomy vs. Partial Upper Sternotomy for SAVR: A Comparative Analysis of Minimally Invasive Approaches

735
Y. Gong, M. Generali, H. Renikunta, C. Balbi, Y. Wang, S. Mohammed, E. Gorica, A. Mongelli, F. Ruschitzka, U. Landmesser, S. Costantino, F. Paneni, P. Jakob
MiRNA-519e promotes cardiomyocyte cell division accompanied by pro-angiogenic capacity and anti-apoptotic effects

747
F. Klingebiel, Y. Kalbas, S. Halvachizadeh, M. Teuben, B. Ganse, P. Cinelli, H. Pape, R. Pfeifer
Metabolomics after polytrauma – A biobank analysis of 97 patients over the time course of 10 days

750
L. Di Venanzio, E. Gorica, M. Shafeeq, N. Atzemian, V. Masciovecchio, S. Costantino, F. Ruschitzka, F. Paneni
Epigenetic editing of BET proteins restores autophagy and cardiac function in cardiometabolic heart failure with preserved ejection fraction

752
S. Mohammed, P. Enz, N. Atzemian, E. Gorica, M. Telesca, G. Panteloglou, F. Ruschitzka, S. Costantino, F. Paneni
The BET Protein Inhibitor Apabetalone rescues Doxorubicin-Induced Endothelial Senescence and Vascular Dysfunction

754
V. Masciovecchio, E. Gorica, J. Spezzini, M. Telesca, I. Papadopoulou, S. Mohammed, L. Di Venanzio, F. Paneni, B. Ludewig, F. Ruschitzka, S. Costantino
Metabolic Stress in Alveolar Macrophages Enhanced Inflammation and Pyroptosis

757
Y. Hu, L. Yang, J. Cai, X. Zhou, Y. Liu
Plasma Proteomics Identify Molecular Features and Biomarkers of Fulminant Myocarditis

759
T. Diteepeng, Y. Puspitasari, S. Ministrini, M. Telesca, D. Vdovenko, A. Akhmedov, J. Beer, S. Costantino, F. Ruschitzka, F. Paneni, G. Camici, M. Luciani
Unfolding the Link Between Protein Misfolding and Stroke-Heart Syndrome

760
E. Gorica, S. Costantino, S. Mohammed, M. Telesca, A. Mongelli, F. Ruschitzka, N. Hamdani, F. Paneni
The BET inhibitor Apabetalone Protects Against Heart Failure with Preserved Ejection Fraction by Suppressing Myocardial Inflammation

764
N. Atzemian, S. Mohammed, E. Gorica, L. Di Venanzio, S. Costantino, F. Ruschitzka, F. Paneni
Epigenetic and transcriptional landscape of the kidney in heart failure with preserved ejection fraction

765
A. Mongelli, I. Papadopoulou, A. Mengozzi, E. Gorica Hoxha, S. Mohammed, H. Rodriguez Cetina Biefer, O. Dzemali, S. Costantino, L. Burkhard, F. Ruschitzka, F. Paneni
Role of paracardial fat in heart failure with preserved ejection fraction

766
A. Mongelli, A. Farsetti, N. Hamdani, F. Ruschitzka, C. Gaetano, F. Paneni
Epigenetic Age of the Male and Female Heart: Insights into Cardiovascular Risk Assessment across Sexes

767
A. Mongelli, A. Mengozzi, E. Gorica Hoxha, S. Mohammed, M. Telesca, C. Matter, F. Ruschitzka, F. Paneni, S. Costantino
Long non-coding RNA PANDA promotes endothelial senescence and oxidative damage through the interaction with NRF2

780
J. Feiereisen, R. Boulos, Y. Kalbas, H-C. Pape, O. Dzemali, H. Rodriguez Cetina Biefer
Traumatic Intracranial Hemorrhage in Mechanical Heart Valve Patients: A Retrospective Analysis of Incidence and Outcomes

798
D. Moysidis, DB. Benz, M. Gajic, A. Pazhenkottil, P. Kaufmann, R. Buechel, AG. Giannopoulos
Rationale and Development of the Computed Tomography Simulated Pressure Loss Index (CTSPLI)

813
M. Telesca, V. Masciovecchio, I. Papadopoulou, SA. Mohammed, E. Gorica, J. Spezzini, A. Mongelli, K. Urbanek, A. De Angelis, L. Berrino, L. Burkhard, F. Paneni, F. Ruschitzka, S. Costantino
Employing Epi-drugs to Rescue Lung Microenvironmental Changes in Heart Failure with Preserved Ejection Fraction

Clinical Trials

749
S. Gruber, M. Cavusoglu, I. Sudano, C. Rossi, F. Beuschlein
Short-Term Effect on Tissue Sodium Distribution in Hypertensive Patients Following Sodium Loading Test: a Sodium MRI study

769
TG. Donati, F. Ortelli, A. Protonotarios, Q. Chen, M. Hebeisen, NE. Winkler, G. Montrasio, K. Savvatis, PAS. Olsen, C. Brunckhorst, F. Duru, AM. Saguner, PM. Elliott, KH. Haugaa, FC. Tanner
Right ventricular outflow tract diameter for diagnosis of arrhythmogenic right ventricular cardiomyopathy

770
TG. Donati, F. Ortelli, A. Protonotarios, Q. Chen, M. Hebeisen, NE. Winkler, D. Cener, G. Montrasio, K. Savvatis, PAS. Olsen, C. Brunckhorst, F. Duru, AM. Saguner, PM. Elliott, KH. Haugaa, FC. Tanner
Prognostic proprieties of echocardiographic right ventricular outflow tract diameter in arrhythmogenic right ventricular cardiomyopathy

786
Q. Chen, T. Donati, M. Hebeisen, N. Winkler, J. Michel, B. Stähli, A. Kasel, F. Tanner
A Prospective Cohort Based Preprocedural Prediction Model for One-year Survival After Transcatheter Aortic Valve Implantation

788
V. Reber, S. Lengsfeld, N. Varghese, Y. Emara, L. Probst, C. Bathelt, L. Werlen, A. Eckert, B. Winzeler
Effects of dulaglutide on oxytocin plasma levels in healthy men: a secondary analysis of a randomized, double-blind, placebo-controlled crossover study

800
L. Ilcheva, A. Janenko, A. Tobias, O. Dragan, P. Nestor, H. Rodriguez Cetina Biefer, O. Dzemali
Efficacy of a Novel Protocol for Eliminating Mycobacterium chimaera in Heater-Cooler Units: Single Center Clinical Study

805

NE. Winkler, G. Tsiourantani, Q. Chen, TG. Donati, M. Hebeisen, J. Michel, B. Stähli, AM. Kasel, FC. Tanner

Clinical Significance of Dilated Left Ventricular Outflow Tract in patients undergoing Transcatheter Aortic Valve Implantation

Hematology / Oncology

Basic Research

725
R. Roggo, A. Ghosh, P. Gueguen, V. Haunerdinger, E. Ramelyte, F. Sella, M. Esposito, P. Turko, M. Levesque, R. Dummer, A. Tastanova
Single-cell multiomics identifies distinct central memory phenotypes in CTCL - transition from blood to skin

729
S. Brunn, C. Magnani
Combining CAR T Cell Therapy and Inhibitory Receptor Targeting for the Treatment of AML

758
L. Leuenberger, L. Isenegger, Y. Chen, M. Burri, S. Kollar, L. Planas-Paz, P. Bode, A. Wozniak, S. Bauer, P. Schöffski, C. Pauli, C. Britschgi
Identifying Novel Vulnerabilities in Clear Cell Sarcoma Through Functional and Genomic Screening

773
C. Meisel, R. Destefani, I. Valookkaran, A. Batavia, F. Catto, N. Rupp, T. Mitsiadis, C. Porcheri
The Notch1/Delta-like-4 axis is crucial for the initiation and progression of Oral Squamous Cell Carcinoma

787
B. Ohm, K. Kurowski, V. Veal, J. Heyer, P. Bronsert, W. Jungraithmayr
CD26 as a target for combination therapy with immune checkpoint inhibition in thymic epithelial tumors

796
S. Traxel, F. Schmidt, C. Beerli, D. Vuong, R. Speck, S. Bredl
Turning tumors hot: Reprogramming the tumor microenvironment using engineered macrophages expressing a chimeric cytokine receptor

799
C. Arnaud-Boissel, K. Zielinska, LC. Hinte, C. Nombela-Arrieta, F. von Meyenn
Trained immunity and inflammatory memory in the bone marrow

801
M. Soballa, M. Mastall, D. Villars, L. Hänsch, M. Mayoux, S. Tugues, M. Weller, P. Roth
ICAM-1 CAR T cells enhance survival and remodel the tumor microenvironment in glioma mouse models

810
M. Mastall, G. Dunkel, N. Okada, T. Weiss, B. Weigelin, M. Weller, P. Roth
Dual-CAR T cells against NKG2D ligands and VEGFR2 accumulate in orthotopically implanted glioma and prolong survival of immunocompetent glioma-bearing mice

815
T. Vancsik, C. Rossel Dorca, M. Ronner, F. Schläpfer, LR. Herrador, S. Arni, M. Meerang, H. Gehart, I. Opitz
Patient-Derived Tumoroid Xenograft Models for Preclinical Validation of Therapeutics for Pleural Mesothelioma

817
A. Kraft, A. Tönz, F. Schläpfer, M. Ronner, V. Orlowski, MB. Kirschner, V. Boeva, I. Opitz, M. Meerang
Exosomal RNA Profiling Identifies GAS5 and Other Long Noncoding RNAs as Circulating Diagnostic Biomarkers for Pleural Mesothelioma

Clinical Trials

739
P. Rahimzadeh, N. Miglino, J. Bachir, N. Bodmer, A. Gircys, Q. Li, M. Iovino, S. Juritz, B. Maier, L. Rudofsky, A. Wolfer, E. Zaninotto, M. Zosso-Pavic, U. Rohr, A. Wicki
From Trials to Approvals: The Evolution of Cancer Drug Approvals in Switzerland with the Rise of Biomarker-Associated Therapies, 2001-2020

803
K. Hofer, N. Sievi, F. Schmidt, A. Egli, J. Deuel
Real-time breath analysis for the detection of invasive fungal infections in neutropenic high-risk patients (REDEFINE)

811
M. Meerang, M. Glettig, MB. Couger, F. Barkmann, V. Boeva, R. Bueno, I. Opitz
Pipeline establishment for reliable single nuclei RNA-sequencing analysis of banked frozen pleural mesothelioma tumors

824
C. Steinack, P. Baumgartner, GM. Monsch, D. Schneiter, S. Oh, E. Samara, I. Opitz, C. Clarenbach, S. Ulrich, M. Kohler, T. Gaisl
Impact of Robotic-Assisted Bronchoscopy with Integrated Cone-Beam CT on Stage Shift in Peripheral Pulmonary Lesions at a Lung Cancer Centre

826
C. Steinack, P. Baumgartner, G. Monsch, D. Schneiter, S. Oh, E. Samara, I. Opitz, C. Clarenbach, S. Ulrich, M. Kohler, T. Gaisl
Robotic-Assisted Bronchoscopy with Integrated Cone-Beam CT vs. Conventional Bronchoscopy for Diagnosing Peripheral Pulmonary Lesions: An Open-Label Randomized Controlled Trial

Head Region / Neuroscience

Basic Research

741
W. Lackinger, F. Scholkmann
Cerebral and peripheral fNIRS signals provide additional vascular information and show a surprising correlation

772
IM. Bugueno, V. Platania, G. Alastra, F. Machla, N. Tavernaraki, S. Svanberg, K. Kodonas, P. Dittrich, TA. Mitsiadis
Development of tooth-on-chip models for simulating human dental tissues

781
M. Graure, N. Nierobisch, A. De Vere-Tyndall, V. Kana, P. Roth, M. Herwerth
Clinical Profile and Treatment Outcome in Chronic Relapsing Inflammatory Optic Neuropathy: a Longitudinal Retrospective Study

785
D. Balun, S. Drack, S. Kling, H. Walt, H. Essig
Validation of a trifold methodology for the diagnosis of oral squamous cell carcinoma in comparison to the conventional histopathological examination.

792
E. Voloviceva, S. Bernhard, S. Goetze, A. Othman, A. von Eckardstein, J. Robert
Brain apoE particle composition defines its functions

802
N. Ziak, A. Abidi Ostorero, M. Generali, T. Hornemann, M. A. Lone
Understanding the selective neurotoxicity of Serine-palmitoyltransferase mutations towards motor and sensory neurons

806
A. Buck, S. Lee, R. Wegmann, I. Sakic, J. Mena, F. Vasella, J. Friesen, E. Le Rhun, A. Zeitlberger, N. Tatari, L. Regli, G. Hutter, M. Neidert, M. Weller, B. Snijder, T. Weiss
Spatially resolved functional profiling for glioblastoma

807
I. Sakic, E. Uijttewaal, R. De Luca, E. Puca, M. Weller, D. Neri, U. Elling, T. Weiss
CRISPR-guided optimization of tumor-targeted cytokine therapy against glioblastoma

818
K. Lehmann, T. Schweizer, G. Kadler, A. Kalyanov, H. Walt, H. Essig
Zirconium dental implants as optical waveguides in antimicrobial photodynamic therapy

820
F. Davidhi, F. Costa, D. Ledergerber, I. Indiveri, L. Imbach, J. Sarnthein
Event-based seizure detection in iEEG using neuromorphic hardware

Clinical Trials

753
LI. Walter, V. Kana, M. Herwerth, S. Hösli, P. Roth
Relapse activity in pregnancy and the postpartum year in women with multiple sclerosis

789
B. Beyersdorf, S. Voglis, Z. Guoming, J. Sarnthein, L. Regli, M. Germans
Treatment Outcomes and the Role of the DES scheme in the Appropriate Treatment Selection for High Grade Dural Arteriovenous Fistulas

812
M. Germans, J. Rohr, C. Globas, T. Schubert, A. Kaserer, G. Brandi, J. Studt, M. Greutmann, K. Geiling, L. Verweij, L. Regli
Challenges in Coagulation Management in Neurosurgical Diseases: A Scoping Review, Development, and Implementation of Coagulation Management Strategies

821
D. Dimakopoulos, JJB. Teurlings, D. Ledergerber, L. Imbach, J. Sarnthein
Human ripples underlying working memory lateralize to healthy hippocampus

822
V. Mavrodiev, C. Bockisch, W. Weber, F. Fierz
Investigating differences in the early visual response to a moving visual field in patients with visual dependency

823
V. Mavrodiev, C. Bockisch, K. Weber, F. Fierz
Vestibular rotation cancellation perception by vision in patients with increased visual dependency

Infection / Immunity / Inflammation / Systemic Diseases

Basic Research

724
M. Pivard, J. Bär, S. Mairpady-Shambat, A. Zinkernagel
Role of the agr-type on the virulence regulation of Staphylococcus aureus

726
D.K. Partl, N. Anderegg, E.E. Müller, V. Maseko, T. Kufa, K. Oliveira Roster, Y.H. Grad, P. Abel zur Wiesch, R.D. Kouyos, N. Low
Neisseria gonorrhoeae Antimicrobial Resistance in South Africa, 2007 – 2023: Implications for National Sentinel Surveillance

728
J. Heuss, A. Tarnutzer, F. Andreoni, AS. Zinkernagel
Culture medium composition influences oxacillin minimal inhibitory concentration and heteroresistance in methicillin-resistant S. aureus clinical isolates

732
V. Schmidtchen, A. Zinkernagel, B. Hasse, S. Brugger
Investigating the phenotypic and genotypic properties of colonising and invasive bacterial isolate pairs in infective endocarditis

736
M. Yang, W. Staiger, W. Barcik, S. Brugger
Microbiota engineering for respiratory health - novel treatment and prevention strategies against pathogens

746
E. Gorica, L. Di Venanzio, I. Papadopoulou, SA. Mohammed, N. Atzemian, A. Mengozzi, V. Masciovecchio, M. Telesca, A. Mongelli, HW. Cheng, B. Ludewig, F. Ruschitzka, N. Hamdani, S. Costantino, F. Paneni
NCOR1-Driven Macrophage Inflammation in HFpEF: a translational study

748
P. Goeller, V. Ihle, H. Seth-Smith, F. Imkamp, S. Mancini, M. Kälin, A. Egli, O. Nolte, V. Hinic
A novel Nocardia species in disseminated nocardiosis: diagnostic challenges in a post-transplant patient with non-responsive pneumonia

775
W. Barcik, M. Soyka, W. Staiger, S. Brugger
The role of bacteria-derived histamine in allergy associated airway diseases

776
S. Hertegonne, A. Gomez-Mejia, A. Tarnutzer, CC. Chang, A. Kempchinksy, E. Parietti, S. Mairpady Shambat, A. Zinkernagel
Stress adapted Staphylococcus aureus modulates neutrophil effector response for its survival during infection

777
P. Laphanuwat, E. Camarillo-Retamosa, C. Seiler, C. Ospelt
Unveiling Synovial Fibroblast Morphology Using Cell Painting Imaging for Drug Screening

782
A.L. Leblond, B. Helmchen, M. Ankavay, D. Lenggenhager, J. Jetzer, F. Helmchen, H. Yurtsever, R. Parrotta, M. Healy, A. Pöschel, E. Markkanen, N. Semmo, M. Ferrie, L. Cocquerel, H. Seeger, H. Hopfer, M. Beat, J. Gouttenoire, D. Moradpour, A. Gaspert, A. Weber
HEV ORF2 protein-antibody complex deposits are associated with glomerulonephritis in hepatitis E with reduced immune status

791
J. Baum, C. Boggon, N. Ranzoni, D. Megias Ramos, L. Isa, S. Brugger
Microbiota engineering for the eradication of Staphylococcus aureus

793
Y. Gütlin, A. Egli
Toward sustainable and reproducible MALDI-TOF MS: Impact of target selection and hardware maintenance on mass spectral quality

794
B. Siedentop, M. Papadimitriou-Olivgeris, J. Epprecht, P. Monney, G. Tzimas, M. Frank, P. Tozzi, M. Kirsch, M. van Hemelrijck, O. Dzemali, R. Kouyos, B. Hasse
Using machine learning to create a new diagnostic algorithm for infective endocarditis

804
G. Wick, T. Loosli, N. Han, S.E. Chaudron, L. Johnson, H. Günthard, M. Egger, R. Lessells, R. Kouyos
HIV superinfections and dolutegravir resistance in South Africa: a modelling study

814
A. Rooney, Y. Yi Li, A. Diversi, K. Haldimann, A. Andrade Barrios, J. Scherrer, D. Albertos Torres, P. Göller, A. Egli
Swab comparison for ease-of-use assessment and oral microbiota characterization

819
Z. Germuskova, E. Pronzini, T. Roloff, E.M. Broens, K. Søgaard, F. Renzi, A. Egli
Emerging evidence of antimicrobial resistance in Capnocytophaga canimorsus and the implications for empiric treatment choices

825
J. Epprecht, B. Siedentop, M. Papadimitriou-Olivgeris, P. Monney, M. Frank, B. Ledergerber, G. Tzimas, P. Tozzi, M. Kirsch, M. van Hemelrijck, O. Dzemali, B. Hasse
No gender disparities in surgical treatment of infective endocarditis: a Swiss multicenter study

Clinical Trials

722
K. Castrezana Lopez, S. von Moos, L. Weidmann, D. Harmacek, E. Rho, B. George, T. Schachtner
The Effect of Tocilizumab on Biopsy-Based Transcriptomics in Kidney Transplant Recipients with Chronic Active Antibody-Mediated Rejection

727
A. Zaugg, J. Zoellin, P. Roth, I. Jelcic, R. Martin, V. Kana
Reduction in fatigue in RRMS after autologous hematopoietic stem cell transplantation

742
J. Zoellin, D. Mattle, D. Agostino, F. Fierz, J. Ruder, A. Zaugg, J. Gartlehner, P. Roth, I. Jelcic, R. Martin, V. Kana
Stability of retinal layers in relapsing remitting multiple sclerosis after autologous hematopoietic stem cell transplantation

762
E. Parietti, A. Gómez Mejia, CC. Chang, S. Mairpady Shambat, AS. Zinkernagel
Rifampicin impairs intracellular eradication of Staphylococcus aureus by human macrophages

771
E. Parietti, D. Bivona, A. Tarnutzer, D. Bongiorno, N. Musso, S. Stefani, S. Mairpady Shambat, S. Zinkernagel
Assessment of Staphylococcus aureus phenotypic heterogeneity mediated by small colony variant formation

774
C. Dollé, T. Tutumlu, J. Nemeth
Multiomic Analysis of Bacille Calmette-Guérin (BCG)'s Immunomodulatory Effects in People with HIV

Mixed Topics

Basic Research

730
P. Wolint, I. Miescher, A. Mechakra, P. Jäger, J. Rieber, G. Meier Bürgisser, M. Calcagni, P. Giovanoli, V. Vogel, JG. Snedeker, J. Buschmann
Comparison of secretome of co-cultured mesenchymal stem cells and tenocytes versus secretome of mesenchymal stem cells alone for the treatment of tendon injuries: determination of composition and functional characterization

731
J. Rieber, RK. Niederhauser, P. Giovanoli, J. Buschmann
Fabrication and characterization of electrospun DegraPol® tubes releasing TIMP-1 protein to modulate tendon healing

737
N. Han, T. Loosli, N. Anderegg, A. Hauser, J. Josi, M. Davies, L. Johnson, R. Lessells, H. Günthard, R. Kouyos
The evolution of resistance during the tail phase of long-acting cabotegravir and rilpivirine: a modelling study

744
E. Sosa, AG. Monsalve, K. Haldimann, D. Albertos Torres, J. Halter, SM. Mueller, A. Egli
Culturomics insights into phenotypic antimicrobial resistance evolution in the gut microbiota of allogenic stem cell transplant patients

745
S. Changkhong, M. Ronner, F. Schläpfer, E. Felley-Bosco, M. Meerang, I. Opitz
Characterization of Live Cell Repository for Pleural Mesothelioma Cells and Cancer Associated Fibroblasts

756
R. Boulos, L. Rings, P. Risteski, F. Paneni, O. Dzemali, H. Rodriguez Cetina Biefer
Platelet Dysfunction and Altered Immune Response in Acute Aortic Dissection Type A: Insights from RNA-Seq Analysis

761
J. Rieber, G. Meier Bürgisser, P. Wolint, I. Miescher, JG. Snedeker, M. Calcagni, P. Giovanoli, J. Buschmann
Synergistic Effect of IGF-1 and PDGF-BB in Tendon Healing

763
RR. Penna, S. Pascolo
Ic-siRNA: Developing A Trifunctional Therapeutic Integrating RNA Interference, Chemotherapy, and Immunostimulation for Cancer Treatment

768
J. Jang, S. Guerra, D. Bochicchio, E. Breuer, A. Charlton, P. Dutkowski, P. Clavien, B. Humar
Histological scoring and non-invasive assessment of ischemic injury in pretransplant uterus grafts

778
TB. Beck, E. Keller
ICUCockpit: IT infrastructure for the collection of multi-modal, high-resolution patient data and online validation of predictive algorithms in a live data stream

779
M. Labarile, M. Huber, K. Leuzinger, M. Perreau, A. Ramette, S. Yerly, M. Cavassini, M. Stöckle, A. Rauch, A. Calmy, J. Notter, E. Bernasconi, HF. Günthard, C. Pasin, RD. Kouyos
HIV Transmission Dynamics in the Swiss HIV Cohort Study

795
M. Sun, A. Mohammed, D. Villars, K. Portmann, M. Mastall, M. Bouzereau, A. Köpp, T. Look, P. Westarp, P. Roth, K. Eyer, S. Pascolo, M. Weller, K. Joesph, V. Ravi, T. Weiss
Rapid generation of multitargeting CAR-PBMCs: a novel immunotherapeutic strategy against glioblastoma

816
V. Ntinopoulos, H. Rodriguez Cetina Biefer, P. Risteski, L. Rings, S. Dushaj, O. Dzemali
Performance of an open-source, offline-capable large language model in data extraction from unstructured electronic health records

Clinical Trials

723
V. Attanasio, C. Zuccarella-Hackl, A. Pazhenkottil, S. Zirngast1, A. Menzi, R. Altwegg, L. Nager, M. Dörner, L. Guth, R. von Känel, M. Princip
Heart Drawings Reflect Illness Perceptions and Are Associated with Quality of Life, Depression, Anxiety and Post-Traumatic Stress Symptoms in ICD Patients

751
R. Erlebach, U. Pale, T. Beck, S. Markovic, M. Seric, S. David, E. Keller
Limitations of SpO2 / FiO2 - Ratio for Classification and Monitoring of Acute Respiratory Distress Syndrome

808
F. Westphal, D. Harmacek, R. Elena, L. Weidmann, K. Castrezana Lopez, B. George, S. von Moos, T. Schachtner
Correlation of activity, and chronicity indices derived from Banff lesion scores with injury dimension scores from biopsy-based transcript diagnostics

722

K. Castrezana Lopez[1], S. von Moos[1], L. Weidmann[1], D. Harmacek[1], E. Rho[1], B. George[1], T. Schachtner[1]

The Effect of Tocilizumab on Biopsy-Based Transcriptomics in Kidney Transplant Recipients with Chronic Active Antibody-Mediated Rejection

University Hospital Zurich, Division of Nephrology[1]

Introduction:
Chronic active antibody-mediated rejection (caAMR) is a leading cause of late allograft failure in kidney transplant recipients (KTRs), with limited effective treatment options. Tocilizumab (TCZ), an interleukin-6 monoclonal antibody, has been proposed as a potential therapy improving long-term outcome. We examined gene expression changes in follow-up biopsies after TCZ treatment in comparison to optimized standard immunosuppression (sIS) alone.

Methods:
KTRs with biopsy-proven caAMR >6 months post-transplantation and available follow-up biopsies were included. Biopsy-based transcriptomics were assessed using the Molecular Microscope Diagnostic System (MMDx). Six KTRs received monthly TCZ (8 mg/kg IV) for 6-12 months plus optimized sIS (tacrolimus/mycophenolic acid/prednisone), and three KTRs received sIS only.

Results:
In the TCZ group, there was a decrease in injury and repair-associated transcripts in the follow-up biopsies compared to the first biopsy (IRAAT, median 0.24; 0.03) and a slight decrease in atrophy-fibrosis transcripts (IFTA, median 0.65; 0.51). Rejection classifier scores (median 0.66; 0.6) and AMR classifier scores (median 0.51; 0.58) remained stable, with a marginal decrease in all AMR score (median 0.92; 0.81). The rejection archetype cluster significantly evolved from early-stage AMR (R4 score, median 0.53; 0.23; p=0.004) to fully developed AMR (R5 score, median 0.27; 0.47; p=0.041). In contrast, in the sIS group, IRAATs (median -0.11; 0.40) and IFTA (median 0.22; 0.60) increased. Rejection classifier (median 0.81; 0.65) and AMR classifier scores (median 0.79; 0.45) decreased, with no change in AMR archetypes.

Conclusion:
TCZ compared to sIS alone did not improve molecular AMR activity or halt progression from early to fully developed AMR. However, it reduced IRAAT scores, which are linked to graft failure, suggesting potential benefits. Further investigation in a larger cohort is needed to determine whether IRAAT scores could serve as early markers of treatment response.

723

V. Attanasio[1], C. Zuccarella-Hackl[1], A. Pazhenkottil[1], S. Zirngast1[1], A. Menzi[1], R. Altwegg[1], L. Nager[1], M. Dörner[1, 2], L. Guth[1], R. von Känel[1], M. Princip[1]

Heart Drawings Reflect Illness Perceptions and Are Associated with Quality of Life, Depression, Anxiety and Post-Traumatic Stress Symptoms in ICD Patients

USZ Klinik für Konsiliarpsychiatrie und Psychosomatik[1], USZ Klinik für Nuklearmedizin[2]

Introduction:
Cardiovascular disease is the leading cause of mortality in Switzerland, and the implantable cardioverter defibrillator significantly reduces mortality in patients with life-threatening arrhythmias. However, many patients experience anxiety, depression, post-traumatic stress, and negative illness perceptions after implantation, resulting in a lower quality of life. Heart drawings are a novel and promising method for assessing illness perceptions and health status, yet their use in ICD patients remains unexplored. The aim of this study was to investigate how heart drawings reflect illness perception, mental health, and quality of life of ICD patients.

Methods:
421 ICD patients aged 18 to 80 were recruited at the University Hospital Zurich between January 2020 and November 2023. Participants completed the European Quality of Life 5 Dimensions 5 Levels (EuroQoL-5D-5L), the Patient Health Questionnaire-8 (PHQ-8), the General Anxiety Disorder-7 (GAD-7), the Post-traumatic Diagnostic Scale (PDS), the Brief Illness Perception Questionnaire (B-IPQ), and produced heart drawings. Heart drawings were categorized as “positive, negative, or neutral” and “anatomy, emotions, size, or damage”. Group differences were tested using the Chi-square and Kruskal-Wallis tests with a significance level of $p = 0.05$.

Results:
75.4% of patients had a neutral perception of their heart-health status, 19.5% a negative perception, and 5.9% a positive one. Most patients had low levels of depression, anxiety, and post-traumatic stress, perceived control over their illness, and expressed confidence in their treatment. Heart drawings reflected health perceptions, with associations found between the drawing categories and quality of life, anxiety, depression, post-traumatic stress, and dimensions of illness perception such as consequences, identity, and control.

Conclusion:
Heart drawings reflected health perceptions and mental health of ICD patients, with negative perceptions being associated with lower quality of life, increased anxiety, depression, and post-traumatic stress. This suggests that targeted therapeutic interventions could be developed to improve patient well-being and support the prognosis of heart patients.

724

M. Pivard[1], J. Bär[1], S. Mairpady-Shambat[1], A. Zinkernagel[1]

Role of the agr-type on the virulence regulation of Staphylococcus aureus

UniversitätsSpital Zürich[1]

Introduction:
Staphylococcus aureus is a pathobiont, colonizing up to 30% of humans but also causes diverse infections, such as pneumonia, abscesses, or sepsis. The ability of S. aureus to successfully invade and colonize infection sites relies on the tightly regulated production of virulence factors such as adhesion proteins, toxins and innate immune evasion factors. The time environment dependent regulation is orchestrated by a complex network of genetic systems, with the accessory gene regulator (agr) system at its core. The agr system, a quorum-sensing system, is activated by the accumulation of an autoinducing peptide (AIP) in a population density-dependent manner. Each S. aureus strain belongs to one of four agr types (agr-I to agr-IV), distinguished by their unique AIP sequence. Although specific agr types have been associated with specific infection profiles—such as agr-IV with exfoliative syndromes or agr-III with toxic shock syndrome—these findings are confounded by the genetic diversity among strains. It remains unclear whether the observed differences in virulence are attributable to the agr type itself or the broader genetic background of the strain.

Methods:
To disentangle the influence of agr type from genetic background, we employed six congenic strains within the genetic background of the Newman strain: wild-type (agr-I), Newman Δagr and Newman with its agr system replaced by agr-I, agr-II, agr-III, or agr-IV from different S. aureus strains. RNA sequencing was performed on cultures sampled at exponential phase (1h30, low agr activation) and early stationary phase (6h, high agr activation). Differential gene expression analysis will compare the transcriptomes of each agr type to the Δagr strain and among themselves to identify agr-type-specific regulatory patterns.

Results:
Previous studies have linked certain S. aureus infections to specific agr types, yet the specific effect of agr type remains confounded by genetic variation. With this study we expect to, for the first time, unravel the specific role of the agr type in the regulation of virulence factors expression and other cellular pathways, independently of the genetic background. We anticipate our findings will align with one of three scenarios: 1) Distinct transcriptomic profiles emerge between agr types, suggesting a strong impact on the virulence capacity of the strains depending on its agr type. 2) Minimal differences are observed, suggesting the genetic background predominates over agr type in shaping virulence. 3) A hybrid scenario arises where certain virulence factors are agr-type-specific while others are genetically determined, indicating a nuanced interplay between agr type and genetic background.

Conclusion:
This study addresses a critical gap in understanding the role of agr type in S. aureus virulence regulation, independent of genetic background. Our results will provide a robust foundation for future research and contribute to clinical decision-making by shedding light on agr-type-specific virulence profiles. The public release of our RNAseq data will facilitate broader analysis and collaboration in the field. If agr-type-specific expression of virulence factors is confirmed, agr typing in clinical settings could offer novel diagnostic and prognostic tools to optimize infection management and improve patient outcomes.

725

R. Roggo[1, 4], A. Ghosh[2, 3], P. Gueguen[2], V. Haunerdinger[1, 4], E. Ramelyte[1], F. Sella[1], M. Esposito[1, 4], P. Turko[1, 4], M. Levesque[1, 4], R. Dummer[4], A. Tastanova[1, 4]

Single-cell multiomics identifies distinct central memory phenotypes in CTCL - transition from blood to skin

Department of Dermatology, University Hospital Zurich, Zurich, Switzerland[1], Functional Genomics Center Zurich, University of Zurich and ETH Zurich, 8057 Zurich, Switzerland[2], Institute of Food, Nutrition and Health, ETH Zurich, Schwerzenbach, Switzerland[3], Medical Faculty, University of Zurich, Zurich, Switzerland[4]

Introduction:
Cutaneous T-cell lymphoma (CTCL) is a malignancy characterised by neoplastic lymphocytes accumulating in the skin. In patients with the aggressive Sézary Syndrome, malignant T-cells are detected in both the blood circulation and skin lesions. Therefore, different phenotypes of T-cells can be studied in both local cutaneous and systemic environments. Circulating T-cells extravasate and accumulate in the skin where they form an immunologic memory. Using skin and blood of CTCL patients, we studied the influence of skin microenvironment on the initiation of malignant T-cell homing, memory formation and their immunological function.

Methods:
To characterise malignant phenotypes and the tumor microenvironment, we employed CITE-seq and scATAC-seq, obtaining data across three omics layers: surface proteome, whole transcriptome paired with TCR repertoire and accessible chromatin regions. Identified cellular phenotypes and markers were further investigated in the skin using single cell spatial transcriptomics (scST) on the Xenium platform and orthogonally validated through flow cytometry and targeted serum proteome profiling.

Results:
We identified a heterogeneous malignant population with two T-central memory (TCM) phenotypes in blood (n=8) and skin (n=10). The phenotypes consisted of a heterogeneous non-polarized (TCM-NP) and a homogeneous polarized (TCM-P) population. Serum proteomics and sc profiling identified a predominant TCM-NP signature in the blood, and predominant TCM-P in the skin. TCM-NP showed a broader spectrum of differentiation potential while TCM-P was terminally differentiated, suggesting a phenotypic transition upon skin homing. scST (n=12) and external scCTCL datasets confirmed high TCM-P abundance in skin.TCM signature, identified in sc protein differential abundance, was validated in an independent CTCL blood cohort (n=15) and allowed for discrimination of those two phenotypes. Furthermore those two phenotypes were monitored in longitudinal CTCL samples under systemic treatment and showed dynamic changes in TCM-NP population in responders and non-responders.

Conclusion:
Surface protein expression, spectrum of differentiation, and presence of terminally differentiated phenotype in skin supports the role of immunologic memory in skin homing and enhanced extravasation of polarized malignant T-cell population in CTCL. Monitoring the abundance of two distinct malignant TCM populations using the TCM signature to assess treatment response in both blood and skin is a potential strategy for managing CTCL.

726

D. Partl[3, 4, 7], N. Anderegg[4], E. Müller[2], V. Maseko[2], T. Kufa[2, 5], K. Oliveira Roster[1], Y.H. Grad[1], P. Abel zur Wiesch[6], R. Kouyos[3, 7], N. Low[4]

Neisseria gonorrhoeae Antimicrobial Resistance in South Africa, 2007 – 2023: Implications for National Sentinel Surveillance

Harvard University[1], National Institute For Communicable Diseases Of South Africa[2], University Hospital Zurich[3], University of Bern[4], University of the Witwatersrand[5], University of Tromsø[6], University of Zurich[7]

Introduction:
South Africa has among the highest levels of gonorrhea worldwide. *Neisseria gonorrhoeae* resistance develops readily and recommended first line gonorrhea treatments in South Africa have changed accordingly: in 2008, from ciprofloxacin to cefixime, and in 2014 to ceftriaxone. Azithromycin has been in the regimen for genital discharge syndrome since 2014.

Methods:
We analyzed sentinel surveillance data collected by the South African National Institute for Communicable Diseases from 2007 to 2023. Samples from patients with male urethritis syndrome were cultured. Confirmed *N. gonorrhoeae* isolates had minimum inhibitory concentrations (MIC, mg/L) of antimicrobials determined by Etest or agar dilution, interpreted using European Committee on Antimicrobial Susceptibility Testing (EUCAST) breakpoints. We described MICs using medians (interquartile range, IQR) and percentages resistant (95% confidence intervals, CI). For antimicrobials with sufficient data, we estimated resistance trends using logistic regression models, incorporating splines to allow flexibility in the shape of the distribution.

Results:
MIC data were available for: ceftriaxone (n=4844, 2007-2023), cefixime (n=4496, 2008-2023), ciprofloxacin (n=2121, 2007-2016) and azithromycin (n=2824, 2011 and 2014-2023). MIC distributions were stable for ceftriaxone (2023 median 0.004 mg/L, IQR 0.002-0.004) and cefixime (0.016, 0.016-0.016), with the last resistant isolate in 2019 (cefixime, 0.25) (Figure). Ciprofloxacin resistance increased from 27% (95% CI 21-35%) in 2007 to 75% (69-80%) in 2016 and was predicted at 91% (69-98%) in 2023. Azithromycin resistance increased from 0.2% (0-0.6%) in 2020 to 3.3% (1.5-5.2%) in 2023.

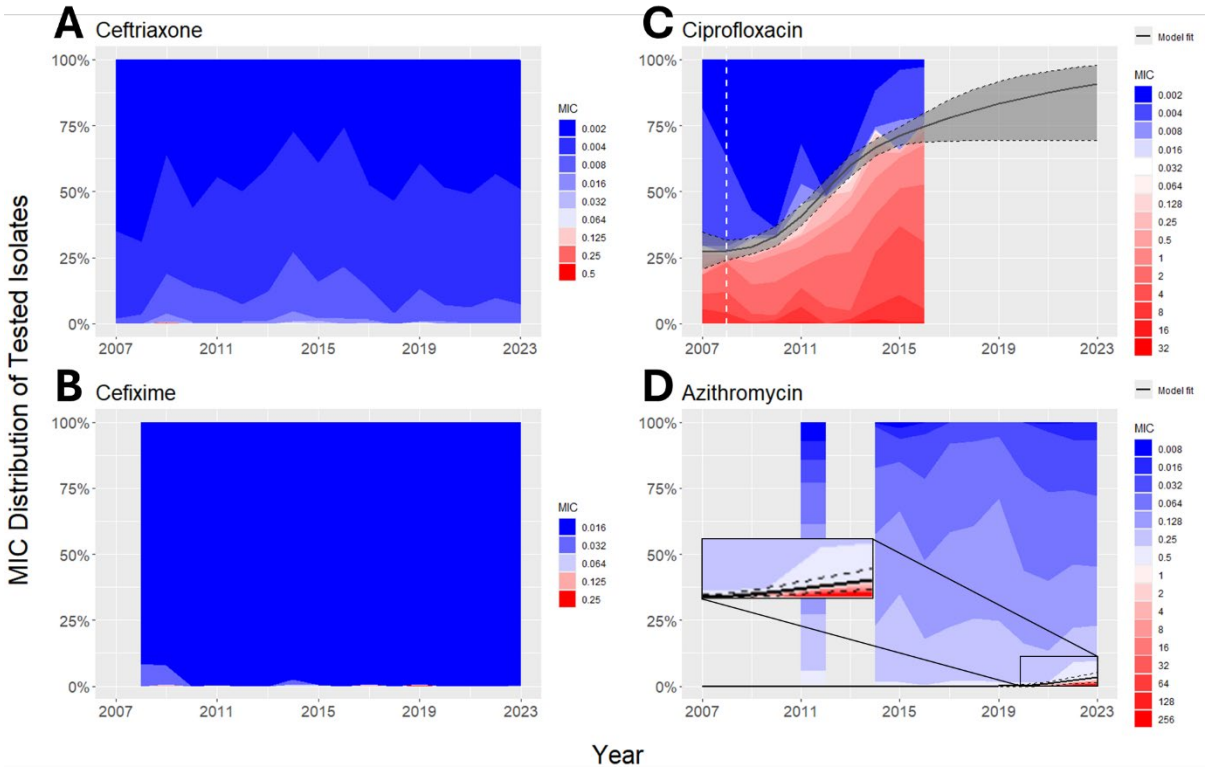

Figure: MICs for *N. gonorrhoeae* isolates from patients with male urethritis syndrome in South Africa, for ceftriaxone (panel A), cefixime (B), ciprofloxacin (C) and azithromycin (D). Colored areas from blue through red show proportions of isolates with MIC at each doubling dilution for years with available data. Panels C and D: black lines show the predicted proportion of resistance (EUCAST breakpoints) from logistic regression models, incorporating splines; confidence intervals shown as grey shaded area bordered by black dashed lines for ciprofloxacin, extrapolated to 2023 (panel C) and azithromycin, with inset enlarged for 2020-2023 (D). The white dashed line in panel C in 2008 is when ciprofloxacin was removed from treatment guidelines.

Conclusion:

N. gonorrhoeae MICs to ceftriaxone are not increasing in South Africa. Azithromycin resistance is increasing, reducing potential effectiveness of a combination regimen. Nearly all *N. gonorrhoeae* isolates were predicted to be resistant to ciprofloxacin by 2023. This finding is consistent with reports of ongoing prescribing, despite its longstanding absence from guidelines. Routine enhancement of sentinel surveillance with prescription data, and interventions for South African physicians could improve antimicrobial stewardship.

727

A. Zaugg[1], J. Zoellin[1], P. Roth[1], I. Jelcic[1], R. Martin[1, 2], V. Kana[1]

Reduction in fatigue in RRMS after autologous hematopoietic stem cell transplantation

Department of Neurology, University Hospital, Zurich, Switzerland[1], Institute of Experimental Immunology, University of Zurich, Zurich, Switzerland[2]

Introduction:
Fatigue is one of the most common symptoms in multiple sclerosis (MS). Besides disease severity and depression, fatigue is one of the key factors leading to reduced quality of life. While the pathophysiology of fatigue in MS is thought to be multifactorial, the majority of patients with autoimmune disorders suffer from fatigue, indicating that dysregulation of the immune system may have a major impact on fatigue development. Since fatigue is more common in patients suffering from autoimmune diseases, immunomodulatory treatment might lead to reduction of fatigue. Autologous hematopoietic stem cell transplantation (aHSCT) is thought to halt autoimmunity by eradicating autoreactive lymphocytes and is a treatment option in aggressive and treatment-refractory MS. Previous data indicate that aHSCT decreases fatigue in relapsing remitting MS (RRMS), but the amount of data is limited, and the effect on fatigue in progressive MS forms is not known.

Methods:
Fatigue Severity Scale (FSS) was used to asses fatigue in 28 RRMS, 9 SPMS and 9 PPMS patients from the Swiss aHSCT registry at pre-treatment, and 1, 6, 12, 24, and 36 months after aHSCT. Clinical measures included Expanded Disability Status Scale (EDSS), the Multiple Sclerosis Impact Scale-29 (MSIS-29) and the Multiple Sclerosis Quality of Life (MUSIQoL). R software (version R 4.3.3) was used for statistical analysis. Missing values were removed and not considered in the analysis. Nonparametric tests with Bonferroni correction for multiple testing were used to assess differences in medians and multiple linear regression to check for dependencies. The p-value for significance was set at a threshold of 5%.

Results:
FSS was significantly correlated with MSIS-29 ($p < 2.2 \times 10^{-16}$) and MUSIQoL ($p < 2.2 \times 10^{-16}$). The amount of no evidence of disease activity (NEDA-3) after aHSCT was comparable with values found in the literature for RRMS, SPMS and PPMS respectively. Fatigue levels did not differ between RRMS, SPMS and PPMS before aHSCT. After aHSCT the FSS values in RRMS were significantly reduced compared to PPMS ($p = 0.00045$). In RRMS, the decrease of fatigue was most pronounced in the first year after transplantation ($p = 0.075$). FSS values did not change in SPMS and tended to increase in PPMS after aHSCT, although not significantly. Females compared to males ($p = 2.3 \times 10^{-5}$), higher EDSS at baseline ($p = 4.3 \times 10^{-6}$), older patients ($p = 0.04$), fewer relapses ($p = 8.2 \times 10^{-6}$) and Natalizumab-treatment instead of Ocrelizumab before aHSCT ($p = 0.02$) were significantly correlated with higher FSS scores in RRMS. Disease duration or EBV/CMV reactivation did not significantly affect the FSS score in RRMS. No significant effect of disease duration, baseline-EDSS, gender, relapses, age or CMV reactivation was found in SPMS patients. In PPMS patients shorter disease duration ($p = 0.001$), higher EDSS ($p = 0.002$), CMV reactivation ($p = 0.007$) and Fingolimod therapy instead of Ocrelizumab ($p = 0.002$) were significantly associated with a higher FSS in PPMS patients.

Conclusion:
aHSCT reduced fatigue in relapsing-remitting, but not in progressive MS. Although still limited, our data suggest that aHSCT can reduce inflammation-induced fatigue, but not fatigue predominantly caused by neurodegeneration.

728

J. Heuss[1], A. Tarnutzer[1], F. Andreoni[1], AS. Zinkernagel[1]

Culture medium composition influences oxacillin minimal inhibitory concentration and heteroresistance in methicillin-resistant S. aureus clinical isolates

Department of Infectious Diseases and Hospital Epidemiology, University Hospital Zurich, University of Zürich[1]

Introduction:
Methicillin-resistant Staphylococcus aureus (MRSA) pose a substantial threat to public health due to their resistance to beta-lactams. Methicillin-resistance is often expressed in a heterogenous way, a phenomenon called heteroresistance, which possibly leads to treatment failure.

Methods:
To assess whether culture medium composition influences antibiotic susceptibility in general as well as heteroresistance, we tested the beta-lactam antibiotic oxacillin minimum inhibitory concentration (MIC) of 47 clinical MRSA isolates collected at the University Hospital of Zurich, Switzerland, by broth microdilution and Etests in four defined media (cation-adjusted Müller-Hinton (CA-MH), tryptic soy broth (TSB), TSB-NaCl and RPMI-1640). Heteroresistance was assessed by population analysis profiles in ten isolates displaying signs of heteroresistance (distinct colonies inside the inhibition zone of the E-test) and oxacillin MICs ≤2µg/ml on TSB E-test plates.

Results:
Median oxacillin MICs decreased in RPMI-1640 (1µg/ml) and TSB (8µg/ml) compared to CA-MH (64µg/ml). To assess whether the salt concentration influences antibiotic susceptibility, 2% NaCl was added to TSB leading to a trend towards higher MICs (16µg/ml). Population analysis profiles of ten isolates revealed that while all strains showed heteroresistance on RPMI-1640, TSB and TSB-NaCl, the heteroresistance phenotype was lost in six strains on CA-MH.

Conclusion:
This study shows that oxacillin susceptibility and heteroresistance expression in clinical MRSA isolates are medium-dependent and that the NaCl concentration affects both phenomena in a strain-dependent manner. Future research should aim at elucidating the connection between heteroresistance and susceptibility profiles.

729

S. Brunn[1], C. Magnani[1]

Combining CAR T Cell Therapy and Inhibitory Receptor Targeting for the Treatment of AML

USZ - Department of Medical Oncology and Hematology[1]

Introduction:
Acute myeloid leukemia (AML) is a malignant disorder of the hematopoietic system initiated by oncogenic transformation of hematopoietic stem and progenitor cells. Even though treatment opportunities for AML have continuously improved in recent decades, long-term treatment success is still poor, with a 5-year relative survival of 30%, showing the necessity of more effective treatments.

Chimeric antigen receptor (CAR) T cell therapy has recently proved effective in B-cell and plasma-cell neoplasms. This approach unleashes the anti-tumor activity of our immune system and relies on genetic engineering of T-cells with an artificial receptor recognizing surface antigens. However, potential barriers caused by the immunosuppressive tumor microenvironment and the similarity between tumor cells and hematopoietic stem and progenitor cells (HSPCs) limit the applicability of this therapy to AML.

In this context, inhibitory receptors of the leukocyte immunoglobulin-like receptor-subfamily B (LILRB) have attracted special interest in recent years as possible immune checkpoints in AML and other cancer types. Several studies have shown an effect of different LILRB subtypes on T-cell functionality and AML development. However, combinatorial treatments using CAR T-cells and LILRB2 targeting have not yet been closely investigated.

Methods:
In this project, we aim to increase the efficiency of CAR T cell therapies against AML by simultaneously targeting LILRB receptors. Genetic (CRISPR/Cas knock out and lentiviral transduction) or pharmacologic perturbation of LILRBs in combination with already established CAR T-cell approaches against AML-associated antigens are tested in vitro and in vivo. T-cell effector functions (killing, expansion, and cytokine production) and phenotype are evaluated in co-cultures with AML cell lines and patient samples and anti-leukemic activity is assessed in AML engrafted NSG mice. Furthermore, we investigate the use of CAR T-cells generated with a Sleeping Beauty transposon system directly targeting LILRBs to simultaneously tackle the leukemic blasts and the immunosuppressive microenvironment.

Results:
Flow cytometry analysis revealed overexpression of the LILRB2 subtype in AML blasts of approximately 45% of all patients and on tumor-associated myeloid cells, while being present in only 10% of healthy HSPCs. Conversely, only a small fraction of patients seemed to have overexpression of LILRB1 or LILRB4 on their blasts. CD33 CAR T cells were less efficient in controlling THP-1 target cells expressing high levels of LILRB2 compared to LILRB2^{ko}. The observed inhibition of CAR T-cell functionality by LILRB2 expression was associated to increased CAR T-cell differentiation and exhaustion. Furthermore, significantly lower levels of TNFa and IL2 were found in the supernatant of CAR T co-cultures with LILRB2^{high} target cells. Blocking of the LILRB2 signaling with neutralizing antibodies partially restored reduced CD33 CAR T cell functionality against THP-1 LILRB2^{high} target cells. CAR T cells designed to target LILRB2 showed potent anti-tumor activity against LILRB2 expressing AML cell lines in vitro and in vivo, justifying further evaluations against primary AML patient samples.

Conclusion:
LILRB2 is overexpressed on a considerable proportion of AML patient samples and CAR T cell functional response showed to be impaired by high target cell LILRB2 expression. In addition, anti-LILRB2 CAR T cells showed efficient killing of AML cells in vivo and in vitro. Altogether, this study identifies LILRB2 as a potential target for more effective CAR T-cell therapies against AML by pharmacologic inhibition or direct targeting.

730

P. Wolint[3], I. Miescher[3], A. Mechakra[1], P. Jäger[1], J. Rieber[3], G. Meier Bürgisser[3], M. Calcagni[3], P. Giovanoli[3], V. Vogel[2], JG. Snedeker[1], J. Buschmann[3]

Comparison of secretome of co-cultured mesenchymal stem cells and tenocytes versus secretome of mesenchymal stem cells alone for the treatment of tendon injuries: determination of composition and functional characterization

Institute for Biomechanics, ETH Zurich[1], Laboratory of Applied Mechanobiology, Department of Health Sciences and Technology, ETH Zurich[2], Plastic Surgery and Hand Surgery, USZ[3]

Introduction:
Tendon injuries represent a large proportion of musculoskeletal injuries, and tendon diseases affect four million new patients worldwide each year. Since tendons are hypovascular and hypocellular and have low metabolic activity, their natural healing capacity is limited. In clinical practice, surgical, rehabilitative and pharmacological treatments are still considered the gold standard. However, symptomatic pain and inflammation treatments do not improve tendon healing capacity, which can often lead to re-rupture. Intensive research is being conducted in the field of cell therapy. The aim of this study was to fully characterize the two types of secretome, co-cultured mesenchymal stem cells with tenocytes and mesenchymal stem cells cultured alone, for a systematic comparison and to examine them with regard to tendon healing.

Methods:
The comprehensive characterization included the proteomic profiling of the two secretome types produced from rabbit cells, co-cultured mesenchymal stem cells with tenocytes and mesenchymal stem cells cultured alone, and the targeted application, which was designed to mimic the in vivo situation from different perspectives. Efficacy in vitro was based on studies of gene expression, proliferation, migration and angiogenesis after appropriate stimulation of tenocytes with the respective secretome. To expose the secretomes to an inflammatory environment, the tenocytes were pre-treated with LPS. Particular attention was paid to determining the influence of soluble proteins on the ECM with a focus to improving biomechanical properties.

Results:
Analysis of the LC-MS/MS data showed that 182 proteins were significantly differently expressed in the two secretome types. In the co-cultured secretome, the concentrations of tendon-related proteins such as BGN, TNC and MMP-9 were increased in the upregulated protein fraction compared to the secretome of the single cell type. The proliferation capacity of tenocytes was increased by both secretomes, whereas the migration ability was more increased by the mesenchymal stem cells secretome. In contrast, both secretomes had a positive effect on angiogenesis. The relative gene expression levels of tenocytes treated with the two secretome types showed similar changes compared to control cells in medium, with some differences: as with IL-6, an increase was also observed in the ECM remodelling factors MMP-9 and Timp1.

Conclusion:
The comparison of the co-cultured mesenchymal stem cells with tenocytes secretome with the mesenchymal stem cells alone secretome showed that most proteins, including growth factors important for tendon healing such as FGF-2, VEGF, IGF-1 and PDGF-BB, were expressed at the same high level in both, which could explain similar results in terms of proliferation, cell migration, angiogenesis and gene expression in treated tenocytes. However, the co-cultured secretome was convincing in terms of molecular functions and biological processes associated with ECM, which may have a positive effect on tendon healing processes. According to our results, treating tendon injuries with the co-cultured secretome could be beneficial compared to single cell type secretome. This novel approach could pave the way for a cell-free therapeutic strategy for tendon injuries by interacting via paracrine mechanisms.

731

J. Rieber[1], RK. Niederhauser[1], P. Giovanoli[1], J. Buschmann[1]

Fabrication and characterization of electrospun DegraPol® tubes releasing TIMP-1 protein to modulate tendon healing

Plastic Surgery and Hand Surgery, USZ[1]

Introduction:
Tendon rupture repair is still challenging because tendons have a low cell density, and the tenocytes are metabolically not very active. Moreover, tendon tissue is practically avascular, and tenocytes receive the necessary oxygen and nutrients mostly via diffusion. In turn, tendons heal only very slowly, and tendon ruptures very often end up in inferior mechanical stability caused by fibrotic scar tissue. During the three-stage tendon repair, the remodeling of the extracellular matrix (ECM) is a key event, as proper and stable aligned fiber network has to be rebuilt, while cellular and fiber debris must be appropriately degraded and removed. Besides force-induced remodeling processes, enzymatic ECM degradation by matrix metalloproteases (MMPs) in balance with their inhibitors (tissue inhibitors of MMPs, TIMPs) plays a fundamental role. TIMP-1 can bind to several cell surface proteins, such as CD82, CD63 and LRP1, respectively, particularly in case TIMP-1 concentrations exceed MMP concentrations. TIMP-1 may act as a cytokine and triggers different signaling pathways via cell surface receptor binding; thereby activating cell growth, proliferation, and anti-apoptosis; processes that promote tendon regeneration and potentially accelerate the healing process.

Methods:
We fabricated an emulsion electrospun biodegradable and biocompatible DegraPol® fiber mesh with incorporated TIMP-1 protein and characterized the new mate-rial by assessment of fiber diameter, pore size, wall thickness with scanning electron microscopy (SEM), of Fourier-Transformed Infrared spectra (FTIR) and of static as well as dynamic water contact angles, respectively. Release kinetics were assessed as well as the impact of TIMP 1 on gene expression of rabbit Achilles tenocytes (rbTenocytes) and rabbit adipose-derived stem cells (rbASCs) in vitro. Typical tendon-related marker gene tenomodulin, proliferation marker ki67 and ECM marker Col1A1 encoding colla-gen I protein were assessed as well as alkaline phosphatase (a typical early marker dur-ing osteogenesis), the latter because TIMP-1 has been reported to act beneficially at the tendon-bone interface, the enthesis, too.

Results:
While proliferation of rbTenocytes and rbACS was not affected by TIMP-1 supplementation in vitro, gene expression of Col1A1 was increased in rbTenocytes; ki67 in both cell types; tenomodulin in both cell types at 100 ng/mL TIMP-1, and ALP significantly in rbASCs. Electrospun TIMP-1/DP fibers had a ~5 mm diameter, a ~10 mm pore size and a mesh thickness of ~200 mm. TIMP-1/DP meshes were more hydrophilic than pure DP meshes. TIMP-1 was released from the meshes with a sustained release up to 7 days.

Conclusion:
Regulating ECM remodeling in preclinical animal models of tendon rupture repair demand for implant materials that affect the ECM remodeling and composition. We have chosen the protein TIMP-1, an inhibitor of MMPs and a proliferation and anti-apoptosis promoting cytokine, and incorporated it in DP random fiber meshes by emulsion electrospinning for the first time. Based on TIMP-1 impact on gene expression of rbTenocytes and rbASCs, where TIMP-1 increased Col1A1 gene expression in rbTenocytes, ki67 gene expression in both cell types, tenomodulin in both cell types at high concentrations (100 ng/mL) and ALP gene expression in rbASCs, we judge our novel elastic electrospun tube that releases TIMP-1 in a controlled slow way as a suitable implant material to be tested in the rabbit full transection model; to get insight into its in vivo function, particularly when positioned at the bone-tendon enthesis – and potentially pave the way for subsequent clinical trials.

732

V. Schmidtchen[1], A. Zinkernagel[1], B. Hasse[1], S. Brugger[1]

Investigating the phenotypic and genotypic properties of colonising and invasive bacterial isolate pairs in infective endocarditis

Department of Infectious Diseases and Hospital Epidemiology, University Hospital and University of Zurich[1]

Introduction:
Infective endocarditis (IE) is a serious infection of the endocardium, primarily caused by bacterial pathogens, most commonly *Staphylococcus aureus*, *Streptococcus* spp., and *Enterococcus* spp.. *S. aureus*, like many bacteria, has a dual behaviour in human health, acting as both, a commensal coloniser, and a virulent pathogen. While it often resides harmlessly on the skin or mucous membranes, it can transition into an invasive pathogen, causing severe infections. This remarkable adaptability is not exclusive to *S. aureus*. Numerous bacteria, including *E. faecalis* and *E. faecium* also demonstrate the ability to shift from colonisation to invasive disease. Understanding the factors that drive these transitions is crucial for improving IE prevention and treatment. Potential contributors include bacterial virulence factors, host immune responses, and microbiome interactions. This study aimed to identify distinct genotypic and phenotypic traits associated with invasive bacterial strains.

Methods:
Factors driving the transition from colonisation to invasive disease were investigated using paired colonising and invasive bacterial isolates among 16 participants from ENVALVE, a prospective cohort study of IE patients located at the University Hospital Zurich. This cohort systematically collects and biobanks patient-derived bacterial strains for research purposes. Whole-genome sequencing was utilised to identify the multilocus sequence typing (MLST) profiles of the bacterial isolates and genomic differences between the paired strains were examined. Additionally, phenotypic characteristics such as bacterial fitness, haemolytic activity, virulence, and adherence properties were assessed to uncover traits associated with invasiveness.

Results:
Among the 16 IE patients, 12 cases of IE were caused by *Staphylococcus aureus* and four by *Enterococcus* spp. (3 *E. faecalis*, 1 *E. faecium*). Analyses of the *S. aureus* bacterial strain pairs revealed that 83 % shared the same MLST type, thus meriting deeper genomic investigation to uncover potential factors driving the transition from colonisation to invasion. The MLST profiles of the enterococcal strain pairs did not match, suggesting that the colonising strains did not cause invasive disease. However, this may be attributed to strain heterogeneity within the bio-banked samples derived from skin swabs. Nevertheless, these strains were included in further studies to explore general genotypic differences between colonising and invasive enterococci. The phenotypic analysis revealed limited adaptation of the invasive strains, as illustrated by a decline in the fitness of certain invasive strains when co-cultured with their corresponding colonising strain. A similar trend is anticipated for the other phenotypic characteristics.

Conclusion:
Preliminary analysis suggests a fitness decrease of invasive strains after transitioning from colonisation to invasion; however, the limited sample size precludes definitive conclusions. Ongoing data collection within the PRospective Swiss EndoCarditis COhort and Platform (PROSECCO) will expand the research of factors driving bacterial transition, incorporating investigations into both strain-specific traits and the microbiota's role in the transition from commensal to pathogen.

733

L. Rings[1, 2], R. Boulos[2], V. Ntinopoulos[2], A. Haeussler[1, 2], H. Rodriguez Cetina Biefer[1, 2], O. Dzemali[1, 2]

Normothermic Circulatory Arrest with Antegrade Cerebral Perfusion for Type A Aortic Dissection

Department of Cardiac Surgery City Hospital of Zurich - Site Triemli[1], Department of Cardiac Surgery University Hospital Zurich[2]

Introduction:
Deep hypothermic circulatory arrest is the standard approach for the surgical repair of acute type A aortic dissection. This study aimed to evaluate the feasibility and outcomes of normothermic circulatory arrest using antegrade cerebral perfusion as an alternative technique.

Methods:
A retrospective propensity score-matched analysis was conducted on patients undergoing surgery for acute type A aortic dissection between 2007-2023 at a single center. Outcomes were compared between patients who underwent normothermic (>35°C) versus mild hypothermic (28-34°C) circulatory arrest. The primary outcomes were 30-day mortality, new neurological deficits, and the intraoperative and postoperative parameters.

Results:
After propensity score matching, 20 pairs were analyzed. The normothermic group (NTCA) had significantly shorter aortic cross-clamp times (47.5 vs 66.5 min, p=0.013) and trends towards shorter cardiopulmonary bypass times (68 vs. 95 min, p=0.066), ICU stays (4.5 vs. 5 d, p=0.4), and intubation times (6 vs. 8 h, p=0.4). There were no significant differences in new neurological deficits (n = 6 [NTCA] vs. 4, p = 0.7), delirium (n = 5 [NTCA] vs. 6, p = 0.6), or mortality (n = 1 [NTCA] vs. 3, p = 0.6) between the groups. The normothermic group required less prothrombin complex concentrate (p=0.0012).

Conclusion:
Normothermic circulatory arrest with antegrade cerebral perfusion appears feasible and safe for hemiarch repair in acute type A aortic dissection, with the potential benefits of shorter operative times and improved coagulation profiles compared to mild hypothermia. Larger prospective studies are needed to confirm these findings.

734

L. Rings[1, 2], R. Boulos[2], A. Haeussler[1, 2], I. Tudorache[2], S. Dushaj[2], H. Rodriguez Cetina Biefer[1, 2], O. Dzemali[1, 2]

Right Anterior-Lateral Thoracotomy vs. Partial Upper Sternotomy for SAVR: A Comparative Analysis of Minimally Invasive Approaches

Department of Cardiac Surgery City Hospital of Zurich - Site Triemli[1], Department of Cardiac Surgery University Hospital Zurich[2]

Introduction:
Surgical aortic valve replacement (SAVR) remains the gold standard treatment for aortic stenosis, offering established long-term outcomes. Despite the increasing popularity of transcatheter aortic valve implantation (TAVI), concerns regarding inferior valve durability have tempered broader acceptance. To reduce surgical trauma while maintaining the durability advantages of SAVR, minimally invasive strategies have been introduced. Several techniques have emerged, notably partial upper sternotomy (PUS) and right anterolateral thoracotomy (RALT), aiming to minimize operative morbidity and expedite recovery. Here, we conducted a retrospective cohort study to compare these two minimally invasive SAVR approaches in terms of intraoperative parameters and postoperative course, thereby providing insights into optimal surgical strategies for patients requiring aortic valve replacement.

Methods:
All patients undergoing surgery for SAVR either through PUS or RALT were propensity-score matched. PUS was performed though a J-incision in the 4th intercostal space, RALT was performed through the third intercostal space. Out of 380 patients, 107 propensity score-matched pairs were selected. All patients were operated on using central aortic cannulation and peripheral venous cannulation. Retrospective statistical analysis was performed regarding: benefits in the intra- and postoperative course, need for transfusions and catecholamines postoperative infections.

Results:
No patient died In-hospital. Cumulative Bypass, Cross Clamp times and operation duration are higher in RALT but reperfusion time is lower in RALT (reperfusion p = <0.001, bypass time p = 0.061, cross clamp p = < 0.001, operation duration p =< 0.001). There was no difference in total red blood cells, fresh frozen plasma, and thrombocyte transfusions (p = 0.41). The perioperative cell saver amount was lower in the RALT group (p = 0.017 before matching and after matching still with a tendency favoring RALT (p = 0.081)). Intubation time did not differ between the groups (p = 0.46). ICU stay and length of postoperative hospital stay were significantly lower in the RALT group (ICU stay 46.38 h vs 26.68 h , p <0.001; postoperative hospital stay 11d vs 9.24 d, p = 0.014). The catecholamine dosage was significantly lower in the RALT group (p < 0.001). Two patients (n = 2) in both groups received permanent pacemakers postoperatively. There were no wound infections; pulmonary infections did not differ between groups (p = 0.4).

Conclusion:
Both minimally invasive approaches provide a safe alternative to conventional SAVR. Although RALT was associated with longer cross-clamp and operation times, it conferred shorter ICU and overall hospital stays, lower catecholamine requirements, and comparable blood transfusion needs. These findings suggest that RALT may be a beneficial approach for select patients by combining the proven durability of SAVR with reduced postoperative morbidity.

735

Y. Gong[2], M. Generali[4], H. Renikunta[3], C. Balbi[1], Y. Wang[2], S. Mohammed[2], E. Gorica[2], A. Mongelli[2], F. Ruschitzka[2], U. Landmesser[3], S. Costantino[2], F. Paneni[2], P. Jakob[2]

MiRNA-519e promotes cardiomyocyte cell division accompanied by pro-angiogenic capacity and anti-apoptotic effects

Center for Molecular Cardiology, University of Zurich[1], Center for Translational and Experimental Cardiology (CTEC), Department of Cardiology, University Hospital Zurich, University of Zurich[2], Department of Cardiology, Angiology and Intensive Care Medicine, Charité - University Medicine Berlin[3], Institute for Regenerative Medicine (IREM), University of Zurich[4]

Introduction:
MicroRNAs have the therapeutic potential for heart repair after myocardial infarction (MI). Using a functional high-throughput screening approach, we identified microRNA-519e (miR-519e) as an inducer of cell-cycling in human-derived iPSC-cardiomyocytes(hiPSC-CM).This study examines miR-519e for cell division in hiPSC-CM, additional beneficial functions in heart-related non-CMs, and direct target identification and validation in vitro and in vivo.

Methods:
MiR-519e-mimics or miR-scrambled (miR-scr) were transfected into hiPSC-CM, human aortic endothelial cells (HAEC) and human cardiac fibroblasts (cFB). Proliferative markers 5-Ethynyl-2'-deoxyuridine (EdU), Phospho-Histone H3 (H3P) and Aurora B-kinase (AURKB) and apoptotic response using 3-(4, 5-dimethylthiazolyl-2)-2, 5-diphenyltetrazolium bromide (MTT) assay after exposure to doxorubicin were assessed in hiPSC-CMs. Angiogenic capacity of HAEC was evaluated by tube formation assay and fibrotic response of cFBs using EdU and α-SMA (smooth muscle actin) staining. In vivo, a mouse myocardial infarction (MI) model with ligation of the left anterior descending followed by intramyocardial injection of miR-519e or miR-scr was used. Direct target identification of miR-519e was assessed using in silico analysis combined with RNA-Seq of miR-519e-mimic treated hiPSC-CMs and validated using Ago2-RNA immunoprecipitation (RIP) followed by qPCR.

Results:
After transfection of miR-519e-mimics in hiPSC-CM, a significant proliferative response indicative of cell division was observed in immunofluorescence staining and on protein level as compared with miR-scr treated hiPSC-CMs (EdU, H3P and AURKB, $p<0.01$). Apoptosis was blunted in miR-519e-treated hiPSC-CMs ($p<0.05$). MiR-519e-treatment of HAEC resulted in more meshes ($p<0.01$) and longer tube length ($p<0.05$), indicating enhanced pro-angiogenic capacity. Importantly, EdU-uptake and α-SMA were similar in miR-519e-treated cFB as compared to miR-scr, suggesting neutral effects of miR-519e on myofibroblast transition. In mice undergoing MI, injection of miR-519e-mimics significantly downregulated CDKN1A (Cyclin dependent kinase inhibitor 1A) /P21 ($p<0.05$ vs. miR-scr), a direct target of miR-519e and negative master regulator of cell-cycling. For further novel target identification of miR-519e, we performed in silico analysis combined with RNA-Seq data from miR-519e-treated hiPSC-CM and validation using Ago2-RIP followed by qPCR. Herein, we identified PTEN (Phosphatase and tensin homolog) and TGFBR2 (Transforming growth factor β receptor 2) that are involved in cardiomyocyte proliferation and hypoxic response, as direct targets of miR-519e.

Conclusion:
Collectively, miR-519e is a potent inducer of cell division in human cardiomyocytes, with anti-apoptotic and pro-angiogenic capacity in the absence of pro-fibrotic effects. We show that miR-519e treatment downregulates key negative cell-cycle regulators in vivo and we identified novel direct targets of miR-519e that are involved in regulatory pathways for heart regeneration.

736

M. Yang[1], W. Staiger[1], W. Barcik[1], S. Brugger[1]

Microbiota engineering for respiratory health - novel treatment and prevention strategies against pathogens

University Hospital Zurich[1]

Introduction:
Emerging antimicrobial resistance (AMR) leads to higher mortality rates and healthcare costs in bacterial diseases. *Staphylococcus* aureus is a major human pathogen associated with AMR, capable of causing various diseases, including bloodstream infections, skin and soft tissue infections, and pneumonia. *S. aureus* is also a common colonizer in the healthy human nasal passage. However, as colonization is a major risk factor for invasive disease, decolonization strategies have been established. Unfortunately, currently available protocols are inefficient and increase selection pressure for AMR. Previous studies on upper respiratory microbiota have suggested that commensals *Dolosigranulum pigrum* and *Corynebacterium* spp. exhibit antagonism towards *S. aureus* both *in vitro* and *in vivo*. Therefore, we aim to investigate the therapeutic efficacy of commensals *D. pigrum* and *Corynebacterium* spp. against pathogens *S. aureus* using a humanized 3D organotypic airway tissue model (ATM).

Methods:
To evaluate if commensals *D. pigrum* and *C. pseudodiphtheriticum* can reduce the re-ocurrence of the *S. aureus* infection *ex vivo*, nasal swabs from human donors colonized with *S. aureus* were collected and inoculated onto the ATM containing layers of human fibroblasts and human epithelial cell exposed to air. As the first step, mupirocin was added to the ATM to eradicate *S. aureus*. Following this, commensalswere introduced to the ATM to establish colonization and the model was subsequently challenged with *S. aureus* mimicking the recolonization process. The colony-forming units (CFU) of *S. aureus* on the ATM were then measured to evaluate pathogen recovery.

Results:
Inoculating the ATM with commensals *D. pigrum* and *C. pseudodiphtheriticum* after mupirocin treatment resulted in a threefold reduction in *S. aureus* recolonization (CFU/ml) compared to the ATM without commensal inoculation. However, inoculating *D. pigrum* or *C. pseudodiphtheriticum* alone did not show a significant change in *S. aureus* recolonization.

Conclusion:
Our finding demonstrates that commensals *D. pigrum* and *C. pseudodiphtheriticum* might effectively reduce the reintroduction of *S. aureus*. To validate this result, further experiments need to be conducted with a larger number of donors and in a more complex *in vivo* mouse model. This study provides valuable insight for developing microbiota-targeted therapeutic and preventative strategies to combat pathogen colonization, transmission, infection, and AMR.

737

N. Han[4, 5], T. Loosli[4, 5], N. Anderegg[6], A. Hauser[3], J. Josi[4, 5], M. Davies[1], L. Johnson[1], R. Lessells[2, 7], H. Günthard[4, 5], R. Kouyos[4, 5]

The evolution of resistance during the tail phase of long-acting cabotegravir and rilpivirine: a modelling study

Centre for Infectious Disease Epidemiology and Research, University of Cape Town, Cape Town, South Africa[1], Centre for the AIDS Programme of Research in South Africa (CAPRISA), Durban, South Africa[2], Department of Epidemiology and Health Systems, Unisanté, Center for Primary Care and Public Health & University of Lausanne, Lausanne, Switzerland[3], Department of Infectious Diseases and Hospital Epidemiology, University Hospital Zürich, Zürich, Switzerland[4], Institute of Medical Virology, University of Zürich, Zürich, Switzerland[5], Institute of Social and Preventive Medicine (ISPM), University of Bern, Bern, Switzerland[6], KwaZulu-Natal Research Innovation and Sequencing Platform (KRISP), University of KwaZulu-Natal, Durban, South Africa[7]

Introduction:
Long-acting cabotegravir and rilpivirine (CAB/RPV) has emerged as a new HIV treatment option for individuals with suppressed viral loads and those facing adherence challenges in resource-rich settings. However, concerns about drug resistance arising from its lower genetic barrier relative to dolutegravir (DTG) and its prolonged tail phase warrant consideration. Further, cyclical care engagement resulting in treatment interruption may select resistance mutations during the extended tail phase when drug concentrations are suboptimal. However, the expected population impact of care disengagement on drug resistance, in the context of the programmatic use of CAB/RPV, has not been quantified and remains unclear.

Methods:
We extended the MARISA (Modelling Antiretroviral drug Resistance in South Africa) model to include the implementation of CAB/RPV in 2025 and cyclical care engagement in South Africa. CAB/RPV is implemented for new antiretroviral treatment (ART) initiation and HIV maintenance therapy for those with viral suppression, assuming a 30% CAB/RPV coverage among the population on ART by 2035. The remaining proportion of the population continues with dolutegravir (DTG)-based or protease inhibitor (PI)-based ART. Care disengagement for CAB/RPV was modelled as three stages (early, intermediate, and late). They represent distinct phases of drug resistance mutations (DRMs) selection during the tail phase: both CAB and RPV (early), only RPV (intermediate), and neither (late) select resistance due to subtherapeutic drug levels. DRMs may revert to wild-type in the absence of selection pressure. We estimated the prevalence of integrase strand transfer inhibitor (INSTI) pretreatment drug resistance (PDR) among people initiating or re-initiating ART. Furthermore, we evaluated the impact of interactions among key model parameters on the estimated population PDR level using a variance-based analysis with Sobol's method.

Results:
In our model, implementation of CAB/RPV increases INSTI PDR in 2045 from 14.2% (DTG-based treatment only) to 29.6% (Figure 1A). We find that INSTI PDR depends relatively little on the annual incidence rates of care disengagement (total Sobol's index of 0.019, 95% confidence interval [CI] 0.016 – 0.023; Figure 1B) and the length of the tail phase (total Sobol's index of 0.038, 95% CI 0.032 – 0.042), compared to other model parameters including coverage of CAB/RPV (total Sobol's index of 0.696, 95% CI 0.633 – 0.763) and INSTI mutation acquisition rates (total Sobol's index of 0.056, 95% CI 0.050 – 0.062). However, varying care disengagement rates exclusively for PWH on CAB/RPV substantially affects INSTI PDR by 2045 (range: 17.0% to 30.9%). Moreover, the increase in INSTI PDR in 2045 is attenuated notably from 29.6% to 21.8% when we assumed that resistance acquisition during the CAB/RPV tail phase can be avoided. (Figure 1A).

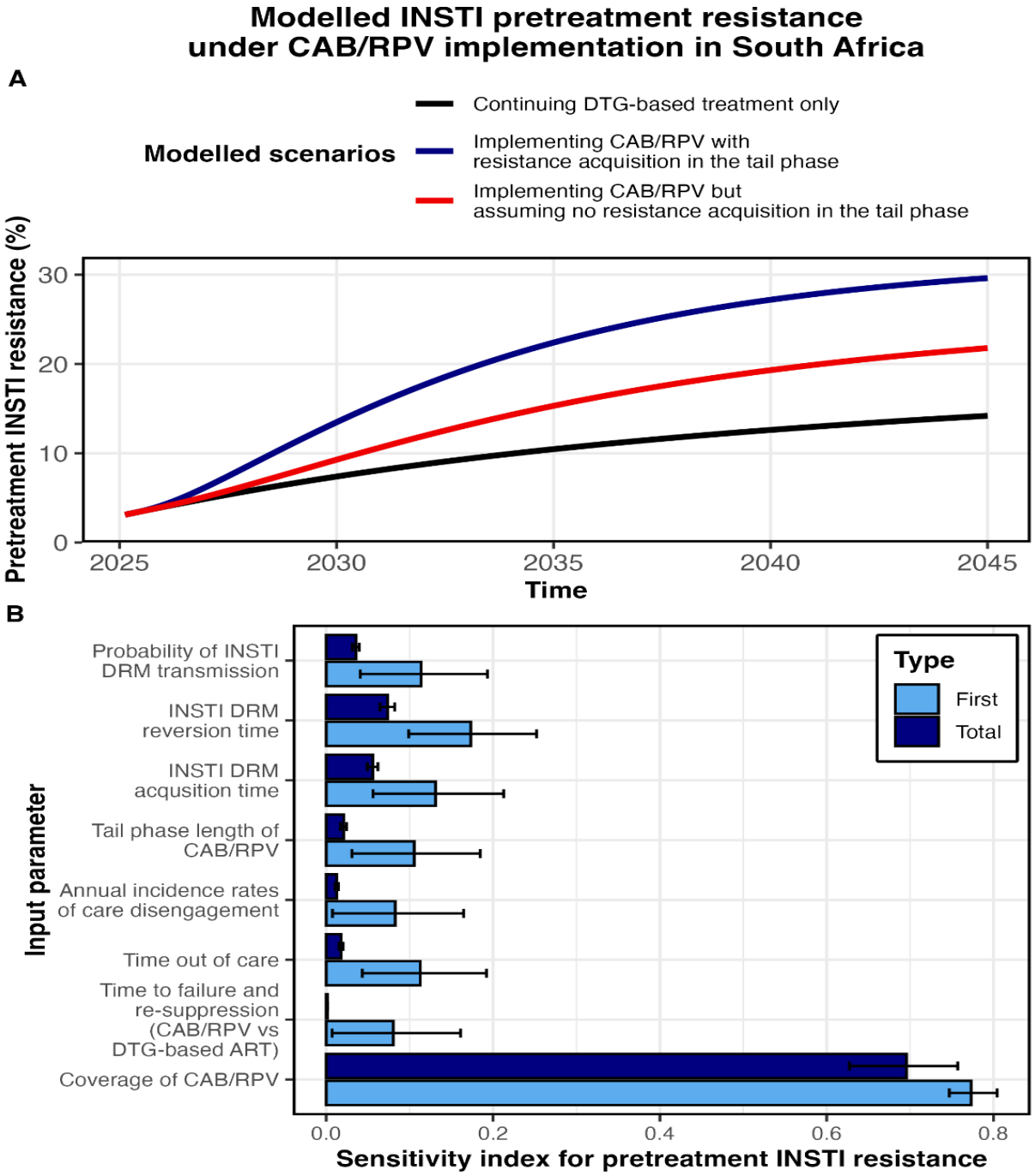

Figure 1 Modelled INSTI pretreatment resistance under CAB/RPV implementation in South Africa. (A) Predicted levels of INSTI PDR over time depending on the occurrence of resistance acquisition during the CAB/RPV tail phase. (B) Sensitivity index for pretreatment INSTI resistance.

Conclusion:
Our findings suggest that while the tail phase of CAB/RPV may contribute significantly to resistance evolution, its population-level effect is offset by mutation reversion and transmission of drug-susceptible virus during care disengagement. Nevertheless, targeted strategies and support systems should be developed to monitor the tail phase of CAB/RPV closely and to address disengagement promptly.

739

P. Rahimzadeh[4], N. Miglino[2], J. Bachir[1], N. Bodmer[1], A. Gircys[1], Q. Li[1], M. Iovino[1], S. Juritz[1], B. Maier[1], L. Rudofsky[1], A. Wolfer[3], E. Zaninotto[1], M. Zosso-Pavic[1], U. Rohr[1], A. Wicki[2, 4]

From Trials to Approvals: The Evolution of Cancer Drug Approvals in Switzerland with the Rise of Biomarker-Associated Therapies, 2001-2020

Department Clinical Assessment, Swiss Agency for Therapeutic Products (Swissmedic), Bern, Switzerland[1], Department of Medical Oncology and Hematology, University Hospital Zurich, Zurich, Switzerland[2], Department of Oncology, Geneva University Hospital, Geneva, Switzerland[3], Faculty of Medicine, University of Zurich, Zurich, Switzerland[4]

Introduction:
Cancer treatment has advanced rapidly in recent decades. Pivotal clinical trials are the backbone of new cancer drug approvals. However, data on the long-term overview and trends in approvals and clinical trial characteristics is limited. This study aims to provide a 2-decade descriptive analysis in this regard in Switzerland.

Methods:
Data on cancer drug approvals and supporting clinical trials in Switzerland, between 2001 and 2020, were collected from Swissmedic's (SMC) database. Relevant information was extracted from clinical assessment reports. We performed descriptive and moving average analyses.

Results:
SMC approved 362 cancer indications between 2001 and 2020, of which 40.6% (147) were New Active Substances (NAS) and 59.4% (215) extensions of existing approvals (indication extensions = IE). Of all approvals, 63.3% (229) were related to solid tumors, and 36.7% (133) to hematologic neoplasms. The number of approved indications increased over time: from 6 in 2001 to 34 in 2020. While most indications, 73.1% (258), were approved based on a randomized clinical trial, moving average analysis revealed a clear increasing trend towards single-arm trials, particularly in solid tumors. For hematologic neoplasms, the percentage of single-arm trials for approval was on average higher compared to solid tumors, but there was less increase over time. 38.4% (139) of indications included a biomarker in the approved regulatory indication. The proportion of biomarker-associated approvals steadily increased, from 17% in 2001 to 56% in 2020. Among biomarker-associated solid tumors, breast cancer (32 indications), lung cancer (31 indications), and gastrointestinal cancer (13 indications) had a biomarker mentioned most frequently in the approved label. In hematologic neoplasms, leukemia led with 31 indications. Over the two decades, 34.1% of biomarker-associated indications compared to 22.3% of non-biomarker-associated indications gained approval based on single-arm trials.

Conclusion:
The notable increase in solid tumor and hematologic neoplasm therapy approvals accompanied by an increased proportion of biomarker-associated approvals in solid tumors, has offered Swiss patients more diverse and tailored treatment options. While RCT served as the main basis for most approvals, the use of single-arm trials was more common for biomarker-associated approvals compared to non-biomarker-associated approvals. The growing reliance on single-arm trials, particularly in solid tumors, introduces uncertainties for regulatory agencies when assessing the benefit/risk profile of a new drug.

741

W. Lackinger[2], F. Scholkmann[1, 2, 3]

Cerebral and peripheral fNIRS signals provide additional vascular information and show a surprising correlation

Institute of Complementary and Integrative Medicine, University of Bern, Bern, Switzerland[1], Neurophotonics and Biosignal Processing Research Group, Biomedical Optics Research Laboratory, Department of Neonatology, University Hospital Zurich, University of Zurich, Zurich, Switzerland[2], Neuroscience Center Zurich, University of Zurich and ETH Zurich, Zurich, Switzerland[3]

Introduction:
The oxyhaemoglobin concentration ([HbO2]) signal measured by functional near-infrared spectroscopy (fNIRS) contains various oscillations, including a high frequency oscillatory component: the blood volume pulse (BVP). These signal components contain wealthy physiological information usually discarded in fNIRS experiments. **Aim**: We investigated the possibility of measuring and characterising the oscillations of the [HbO2] signal using systemic physiology augmented fNIRS (SPA-fNIRS).

Methods:
Resting state SPA-fNIRS measurements were performed on the head (frontal and fronto-lateral) and on the finger (age range: 24-50 years, n = 11, 3 female) using a continuous wave fNIRS device (NIRxSport2, NIRx, Berlin). In parallel, the BVP was measured on the earlobe using a photoplethysmography (PPG) device (WINGS, NIRx, Berlin, Germany) and the respiratory rate (RR) and end tidal CO2 (ETCO2) with a capnograph (Life Sense LS1-9R, Nonin Medical, Inc. Plymouth, MN USA). A newly developed algorithm was used to extract the BVP from the [HbO2] signal, determine an average BVP waveform and calculate parameters related to the state of the vascular and cardiac system. It also calculates the BVP amplitude time-series (BVPA).

Results:
The BVP and BVPA were successfully obtained from the [HbO2] signal measured by fNIRS on the head and on the finger using the new algorithm. The average BVP waveforms and the vascular parameters could also successfully be calculated. When comparing the BVPA signals with the fNIRS [O2Hb] signal, complex frequency-dependent correlations were observed.

Conclusion:
Our investigation has demonstrated that it is possible to use a commercially available fNIRS device to obtain the BVP signal and BVP waveforms (including descriptive parameters) from both the head and the finger. The complex frequency-dependent correlation of the BVPA signals with the fNIRS [O2Hb] signal are a novel finding that need further investigation.

742

J. Zoellin[1], D. Mattle[1], D. Agostino[1], F. Fierz[2], J. Ruder[1], A. Zaugg[1], J. Gartlehner[1], P. Roth[1], I. Jelcic[1], R. Martin[1, 3], V. Kana[1]

Stability of retinal layers in relapsing remitting multiple sclerosis after autologous hematopoietic stem cell transplantation

Department of Neurology, University Hospital Zurich[1], Department of Ophthalmology, University Hospital Zurich[2], Institute of Experimental Immunology, University of Zurich[3]

Introduction:
Autologous hematopoietic stem cell transplantation (aHSCT) is a highly effective treatment for aggressive, treatment-resistant multiple sclerosis (MS). While aHSCT achieves no evidence of disease activity (NEDA) in a high proportion of patients, the impact on neurodegeneration is less clear. Thinning of the peripapillary retinal nerve fiber layer (pRNFL) and the ganglion cell/inner plexiform layer (GCIPL) assessed by optical coherence tomography (OCT) is considered a marker for neurodegeneration, whereas increased inner nuclear layer (INL) is linked to inflammatory activity in MS. The value of repeated OCT measurements for assessing the effect of aHSCT is unknown. Here, we aim to assess the effect of aHSCT on changes in retinal layer thickness using repeated OCT measurements.

Methods:
OCT measurements were performed in 39 patients (23 relapsing remitting MS (RRMS), 8 secondary progressive MS (SPMS), 8 primary progressive MS (PPMS)) of the Swiss aHSCT-in MS registry during 36 months after aHSCT. Both eyes were imaged before (n=64 eyes), 3 (n=60 eyes), 12 (n=55 eyes), 24 (n=53 eyes) and 36 (n=18 eyes) months after transplantation (n=332 measurements total). Eyes with a history of optic neuritis 6 months before the first image acquisition were excluded. Linear mixed models (LMM) were used to compare the atrophy of retinal layers before and after transplantation and to evaluate baseline thickness values as predictors of post-transplant expanded disability status scale (EDSS). Furthermore, longitudinal retinal layer thickness values were compared to an observational cohort of 52 RRMS patients without aHSCT using LMM and generalized additive models.

Results:
aHSCT significantly reduced atrophy rates of pRNFL and GCIPL thickness ($p<0.01$) when compared to atrophy rates before aHSCT in RRMS, but not in SPMS and PPMS. GCIPL and pRNFL atrophy rates after aHSCT were significantly lower in RRMS patients than in the observational cohort without aHSCT ($p<0.01$). High INL thickness before transplantation was associated with a smaller likelihood of EDSS rise after transplantation in RRMS ($p<0.01$).

Conclusion:
aHSCT reduces neurodegeneration of retinal layers in relapsing-remitting, but not progressive MS. Higher INL thickness before transplantation is associated with better neurological outcomes following aHSCT, suggesting a favorable effect of high inflammatory activity before aHSCT on clinical outcome. OCT can serve as a non-invasive and accessible tool to assess potential neuroprotective effects of aHSCT in MS.

744

E. Sosa[3], AG. Monsalve[3], K. Haldimann[3], D. Albertos Torres[3], J. Halter[2], SM. Mueller[1], A. Egli[3]

Culturomics insights into phenotypic antimicrobial resistance evolution in the gut microbiota of allogenic stem cell transplant patients

Department of Dermatology, University Hospital Basel[1], Department of Hematology, University Hospital Basel[2], Institute of Medical Microbiology, University of Zurich[3]

Introduction:
Allogeneic human stem cell transplant (allo-HSCT) recipients are at high risk for bacterial infections. These patients are often exposed to prolonged antimicrobial treatment, which disrupts the gut microbiota and drives antimicrobial resistance (AMR) evolution. Despite its clinical relevance, the *in vivo* resistance dynamics of individual strains within this population's gut microbiota remain poorly understood. We aim to explore the prevalence and resistance dynamics in gut microbiota in allo-HSCT recipients at single-strain level resolution.

Methods:
We collect weekly stool samples from 100 allo-HSCT patients over six months, covering 28 timepoints in pre- and post-transplantation periods. We established a culturomics-based approach in aerobic conditions at 37°C and overnight incubation to isolate 20 random single bacterial colonies from three agar plates (COS, MacConkey, UriSelect) per stool sample each. Colonies were analysed using MALDI-TOF mass spectrometry for species identification and biobanked for further analysis. To assess phenotypic AMR changes over time, *Escherichia coli* strains were retrieved from timepoints where ≥5 replicates were available and tested using EUCAST-compliant disc diffusion assays against clinically relevant antibiotics (amikacin, ceftriaxone, levofloxacin, cefepime, piperacillin/tazobactam, and amoxicillin/clavulanate).

Results:
Our preliminary analysis identified 4178 isolates and 50 unique species. Our results reveal complex patterns at multi-strain and single-strain levels. The gut microbiota was dominated by *E.coli* (37.6%), *Enterococcus faecalis* (20.5%) and *E.faecium* (18.5%), with evidence of interspecies dominance and selection pressure shaping the microbial community structure (Fig.1). We measured among 38 *E.coli* isolates a total of 228 inhibition zones and observed changes in antibiotic sensitivity over time with decreasing inhibition zone median. For example, for levofloxacin, it decreased from 23mm (interquartile range [IQR] 17.5-28.5mm) at timepoint 18 to 10mm (IQR 10.0-10.0mm) at timepoint 26 (Fig.2).

Conclusion:
This study provides culturomics insights into AMR evolution of single bacterial isolates within the gut microbiota during allo-HSCT. Our preliminary findings highlight dynamic, strain-level adaptations to antibiotic pressure, underscoring the potential of this approach to uncover critical patterns in AMR evolution. As the study progresses, expanded sampling, phenotypic and genotypic testing across a larger patient cohort will further enhance these insights.

745

S. Changkhong[2, 3], M. Ronner[2, 3], F. Schläpfer[2, 3], E. Felley-Bosco[1], M. Meerang[2, 3], I. Opitz[2, 3]

Characterization of Live Cell Repository for Pleural Mesothelioma Cells and Cancer Associated Fibroblasts

Department of Biomedical Sciences, University of Lausanne, Lausanne, Switzerland[1], Department of Thoracic Surgery, University Hospital Zürich, Zürich, Switzerland[2], University of Zurich, Zurich, Switzerland[3]

Introduction:
Cancer-associated fibroblasts (CAFs) are a prominent component of the tumor microenvironment, exhibiting heterogeneity and functional diversity. CAFs can exhibit both tumor-suppressive and tumor-activating functions, potentially influencing cancer progression and therapeutic response. This study aims to explore the characteristics of CAFs cultivated from pleural mesothelioma (PM) in our biobank, assess their functional interactions with tumor cells, and establish in vitro co-culture models to evaluate their potential roles in anti-cancer therapy.

Methods:
Cell cultures derived from PM tissues were established. Cell cultures enriched with CAF were identified by the enrichment of spindle-shape cells coupled with negativity of epithelial marker Pan-cytokeratin (pan-CK). We performed IHC staining for expression of proteins, previously shown to enrich in different CAF subtypes, including α-Smooth Muscle Actin (α-SMA), Podoplanin (PDPN), and Vimentin (VIM). Preliminary gene expression analysis by RT-qPCR was conducted to investigate correlation between gene and protein expression. In addition, we performed co-culture experiments with two PM cell lines and four different CAF cultures that show Pan-CK negative in all cells. We used proliferation marker Phospho-histone 3 (PH3) assessed by immunofluorescent staining (IF) as readout for functional interaction in tumor (Pan-CK positive) and CAFs (pan-CK negative) fractions.

Results:
We identified 98 mesothelioma derived cell cultures enriched with fibroblasts (pan-Cytokeratin H-score <150) in our cell biobank with the median H-score of 29.8 (range 0-150). Median doubling time, assessed using colorimetric metabolic assays (MTT), was 88.28 hours. Preliminary analysis of protein expression in 14 cell lines showed that PDPN and α-SMA expression was heterogeneous, while VIM was highly expressed in all cultures. The analysis of PM tumor specimens showed that these proteins were detectable in CAF fractions within tumor nodule. Similarly, in tumor α-SMA and PDPN were heterogeneous in CAFs, whereas VIM was highly expressed in all CAFs. However, when compared to gene expression, protein and gene expression did not correlate. Preliminary data suggest that co-culture may alter proliferation of tumor cells and we are performing more analysis to confirm this finding.

Conclusion:
Our study provides an initial characterization of CAFs from mesothelioma-derived cultures and provide preliminary data on the functional aspectWe are currently performing additional assays and characterization. More data will be presented at the symposium. These fibroblast-enriched cell cultures offer a valuable model for further translational research, including the development of co-culture models.

746

E. Gorica[1, 4], L. Di Venanzio[1], I. Papadopoulou[2], SA. Mohammed[1], N. Atzemian[1], A. Mengozzi[1], V. Masciovecchio[1], M. Telesca[1], A. Mongelli[1], HW. Cheng[2], B. Ludewig[2, 4], F. Ruschitzka[1, 4], N. Hamdani[3], S. Costantino[1, 4], F. Paneni[1, 4]

NCOR1-Driven Macrophage Inflammation in HFpEF: a translational study

Center for Translational and Experimental Cardiology (CTEC), Department of Cardiology, University Hospital Zurich and University of Zürich, Zurich, Switzerland[1], Institute of Immunobiology, Kantonsspital St. Gallen, St. Gallen 9007, Switzerland[2], Institute of Physiology, Ruhr University, Bochum, Germany, Bochum, Germany[3], University Heart Center, University Hospital Zurich, Zurich, CH, Zurich, Switzerland[4]

Introduction:
Inflammatory response is a key player in heart failure with preserved ejection fraction (HFpEF), but the underlying mechanisms are poorly understood. Recent studies have shown the critical involvement of cardiac macrophage activation in myocardial remodelling, thus contributing to HFpEF.

Methods:
Human and murine left ventricular (LV) myocardial tissue, snRNA sequencing of human and murine hearts, FACS analysis of cardiac immune cells, and in vitro experiments were employed. RAW-264.7 cells exposed to palmitic acid (PA), bone marrow-derived macrophages from healthy and HFpEF mice, cardiomyocytes (H9c2), endothelial cells (HAECs), and ex vivo LV tissue analyses were used. Human LV myocardial samples evaluated macrophage pro-inflammatory activity in HFpEF mice. Cardiac function was assessed by high-resolution ultrasound imaging (Vevo3100), and LV samples studied macrophage polarization and inflammatory activity. Available RNA-seq data identified NCOR1 as crucial in macrophage inflammation, leading to the creation of the myeloid cell-specific NCOR1 knockout (Ncor1-KO) transgenic mice to study NCOR1 deletion's effects on HFpEF.

Results:
The expression of macrophage markers in human LV specimens from HFpEF patients showed an increase in pro-inflammatory macrophages (M1) and a decrease in regulatory macrophages (M2) as compared to age-matched control donors. Consistently, HFpEF mice showed increased expression of vascular adhesion molecules (ICAM1, ICAM2, E-selectin) and significant recruitment of M1 macrophages as shown by qPCR, WB, and flow cytometry analysis. Of interest, diastolic dysfunction - assessed by E/E' ratio and isovolumic relaxation time (IVRT) – and lung congestion were significantly reduced in mice with macrophage NCOR1 deletion as compared to WT littermates, while exercise tolerance was significantly improved. These findings were associated with a reduction of myocardial inflammation (TNF-a, IL6, IL-1b) in Ncor1-KO mice. In vitro assays showed that stimulation of macrophages with PA (to mimicmetabolic stress) activated macrophages, upregulated NCOR1, and consequently activated NLRP3-IL1b pathway; whereas NCOR1 depletion prevented detrimental changes of macrophage activation and secretome. Finally, NCOR1-silencing in macrophages prevented inflammation, oxidative stress, and cell death in cardiomycoytes and endothelial cells, thus suggesting a dynamic crosstalk in this setting.

Conclusion:
NCOR1 is a crucial regulator of immune response and inflammasome activation in cardiac macrophages. Our findings highlight its potential as a target for therapies aimed at preventing myocardial damage in HFpEF.

747

F. Klingebiel[2], Y. Kalbas[2], S. Halvachizadeh[2], M. Teuben[2], B. Ganse[1], P. Cinelli[2], H. Pape[2], R. Pfeifer[2]

Metabolomics after polytrauma – A biobank analysis of 97 patients over the time course of 10 days

Department of Trauma, Hand and Reconstructive Surgery, Saarland University[1], Traumatology Department, University Hospital Zürich[2]

Introduction:
Severe injury is known to have systemic effects at multiple levels, with the inflammatory response being a major focus of research in recent years. However, little is known about the perturbation of metabolic pathways after polytrauma. Therefore, we performed a metabolomic analysis of patients from our in-hospital polytrauma biobank, which contains up to ten days of samples from each patient.

Methods:
Patients from the in-house polytrauma biobank with signed ethical consent were utilized. Sample time points were baseline (hospital admission), 8h, 24h, 48h, 5d and 10 days post trauma. Untargeted mass spectrometry was performed, while metabolites reliably identified using the KEGG/HMDB database were subset-analyzed in a semitargeted approach. Metabolic changes were identified using MetaboAnalyst 6.0 to detect pathways that were particularly affected and presented using enrichment ratios. Additionally, cluster analyses were performed and metabolite dynamics over time were assessed.

Results:
97 severely injured patients (79.4% male / 20.6% female) were included in the study. The median ISS of this cohort was 29 (IQR=19). 46 metabolites were reliably identified. The immediate response (0-8h) shows increased activation of hemostasis and inflammation along with excessive corticosteroid production. In the 8-24h period, there is an excessive catabolic state with energy mobilization from fatty and amino acids. At 24-48 hours, detoxification, immune regulation and metabolic adjustments are primarily active. In the 5-10 day period, energy requirements are still elevated but reduced compared to the previous time points.

Conclusion:
Severe trauma causes a major disruption in the metabolism. Immediately after trauma, the body activates life-saving pathways and begins to mobilize excessive energy resources by breaking down fats and amino acids for ATP production. Initial treatment and intensive care should take this excessive energy demand into account and assess the extent to which organ-protective treatment (e.g. liver) may be beneficial to the patient.

748

P. Goeller[2], V. Ihle[1], H. Seth-Smith[2], F. Imkamp[2], S. Mancini[2], M. Kälin[1], A. Egli[2], O. Nolte[2], V. Hinic[2]

A novel Nocardia species in disseminated nocardiosis: diagnostic challenges in a post-transplant patient with non-responsive pneumonia

Division of Infectious Diseases and Hospital Epidemiology, University Hospital Zurich[1], Institute of Medical Microbiology, University of Zurich[2]

Introduction:
Disseminated nocardiosis is a rare and difficult to diagnose infection. Its clinical and radiological presentation can resemble common respiratory infections, and the concurrent presence of other airway pathogens often delays the diagnosis of nocardiosis until after empirical pneumonia treatments have proven ineffective. This case highlights the importance of early consideration of nocardiosis in differential diagnoses for pneumonia in immunocompromised patients unresponsive to standard treatments and describes an infection with a new Nocardia spp..

Results:
A 60-year-old male patient presented with cough and dyspnoea three months post kidney transplantation. Laboratory results showed elevated C-reactive protein levels and an upper respiratory Influenza A infection. A CT scan revealed infiltrates in the right lower lobe, suggestive of bacterial superinfection, though other tests for respiratory pathogens were negative. The patient was treated with oseltamivir and piperacillin/tazobactam and discharged with amoxicillin/clavulanic acid. Despite treatment, the patient returned after fourteen days with persistent cough and progressive pulmonary consolidations. A transbronchial biopsy returned typical respiratory aerobic bacteria. Consecutive bronchoalveolar lavage cultures yielded Aspergillus fumigatus and repeatedly Mycobacterium chimaera. M. chimaera was interpreted as colonization, leading to the diagnosis of influenza-associated pulmonary aspergillosis. The patient was started on isavuconazole. Four weeks later, the patient was hospitalized again with worsening respiratory symptoms and a new focal seizure with facial palsy. Cranial MRI showed multiple cerebral abscesses. Cerebrospinal fluid analysis was negative, but a brain abscess puncture confirmed Nocardia spp. through both culture and partial 16S sequencing. Whole-genome sequencing (WGS) revealed a previously undescribed Nocardia species, most closely related to N. acididurans (TYGS.dsmz.de dDDH 39.2%; new species cutoff is <70%). The strain was susceptible to imipenem and cotrimoxazole. The patient eventually recovered following a complex therapeutic course.

Conclusion:
This case highlights the diagnostic complexity of disseminated nocardiosis. The prior isolation of other respiratory pathogens delayed the identification of Nocardia as the underlying causative agent, emphasizing the need for comprehensive diagnostics in patients unresponsive to standard therapies. WGS identified a new species, underscoring the value of molecular tools in detecting novel pathogens and managing rare infections.

749

S. Gruber[1], M. Cavusoglu[2], I. Sudano[4], C. Rossi[2], F. Beuschlein[1, 3]

Short-Term Effect on Tissue Sodium Distribution in Hypertensive Patients Following Sodium Loading Test: a Sodium MRI study

Department of Endocrinology, Diabetology and Clinical Nutrition, University Hospital Zurich and University of Zurich[1], Institute of Diagnostic and Interventional Radiology, University Hospital Zurich and University of Zurich[2], Medizinische Klinik und Poliklinik IV, Klinikum der Universität München, Munich, Germany[3], University Heart Center, Cardiology, University Hospital Zurich and University of Zurich[4]

Introduction:
Emerging research suggests that tissue Na+ accumulation plays a role in blood pressure control, yet the mechanisms underlying the regulation of sodium storage remain unclear to date.

Methods:
In 31 hypertensive patients with a mean age of 49 years, of whom 61% were women, a sodium infusion test (SIT) was conducted to confirm or exclude the diagnosis of primary aldosteronism (PA). For this purpose, 2000 ml of isotonic saline were intravenously infused over 4 hours. Both before and immediately after the sodium infusion, each patient underwent sodium magnetic resonance imaging (23NA-MRI), a specialized noninvasive imaging technique that focuses on visualizing the distribution and concentration of sodium ions within tissues.

Results:
The mean sodium content in skin and muscle tissue in the study cohort was 45±3.4 mmol/L and 17.9±2.8 mmol/L, respectively, prior to the intervention. Following salt loading, in both compartments a significant increase in salt accumulation (+18%, $p<0.001$; +4.4%, $p=0.004$) could be observed. Based on the SIT, PA was diagnosed in 17 cases (54.8%) and excluded in four cases (12.9%), while remaining inconclusive in ten cases (32.3%). Across diagnostic categories, the aldosterone-to-renin ratio (ARR) correlated positively with the level of baseline salt content in the skin ($p=0.03$[IS1]). While a similar trend was evident in muscle tissue, it did not reach statistical significance. Muscle salt accumulation was significantly less pronounced in patients with a post-SIT aldosterone level above the median of 135 ng/l compared to those with lower aldosterone values (Δ1.48% versus Δ7.23%, $p=0.016$).

Conclusion:
This study demonstrates a significant increase in sodium accumulation within skin and muscle tissues among hypertensive individuals following short-term sodium loading. In addition, we demonstrate a positive correlation between ARR and sodium stores in the skin prior to intervention. In muscle tissue, we observe a negative correlation between post-SIT aldosterone levels and the percentage of sodium accumulation. The data may provide an indication of a potential influence of aldosterone on sodium dynamics within body tissues. Increasing patient numbers and further investigation is required to assess whether differences in tissue sodium distribution before and after loading could serve as a discriminating factor between endocrine forms of hypertension and essential hypertension.

750

L. Di Venanzio[1], E. Gorica[1], M. Shafeeq[1], N. Atzemian[1], V. Masciovecchio[1], S. Costantino[1], F. Ruschitzka[1], F. Paneni[1]

Epigenetic editing of BET proteins restores autophagy and cardiac function in cardiometabolic heart failure with preserved ejection fraction

CTEC- Center for Translational and Experimental Cardiology[1]

Introduction:
Cardiometabolic heart failure with preserved ejection fraction (cHFpEF) is a prevalent disease whose underlying mechanisms are poorly understood. Autophagy appears to be involved in the pathophysiology of the disease. Epigenetic modulators, particularly BET (bromodomain and extraterminal) proteins, have emerged as transcriptional regulators in response to environmental stressors and potential therapeutic targets. This study investigates whether BET proteins modulate autophagy in cHFpEF and if their pharmacological inhibition by BET protein inhibitors can restore autophagic flux, rescuing cardiac damage.

Methods:
An established mouse model of cHFpEF combining metabolic and hemodynamic stress over 15 weeks was used. Mice were treated with either vehicle or the selective BET inhibitor RVX-208 for 14 days. Autophagic gene expression was assessed using a custom real-time PCR array and validated by immunoblotting. To examine chromatin changes, ChiP-seq assays was performed to study the enrichment of active chromatin marks and BET proteins gene loci in cardiac specimens from the different experimental groups.

Results:
Autophagy was impaired in cHFpEF mice, evidenced by upregulation of mTOR signaling and decreased expression of autophagosome genes such as Atg7 and Atg13. Gene profiling revealed deregulation of key autophagy-related genes, including Atg5, TMEM74, and PS6K (an mTOR target). ChiP-seq revealed strong enrichment of BET proteins and active chromatin marks at the mTOR promoter, suggesting a direct role of BET proteins in regulating autophagy. Treatment with RVX-208 restored autophagic gene expression and improved both diastolic dysfunction and exercise tolerance.

Conclusion:
Our study unveils a BET-driven epigenetic mechanism regulating autophagy in cHFpEF. Pharmacological inhibition of BET proteins restores autophagic flux while improving cardiac function in cHFpEF mice. Our results set the stage for preclinical studies testing FDA-approved BET inhibitors in the setting of HFpEF.

751

R. Erlebach[1], U. Pale[2], T. Beck[2], S. Markovic[2], M. Seric[2], S. David[1], E. Keller[2]

Limitations of SpO2 / FiO2 - Ratio for Classification and Monitoring of Acute Respiratory Distress Syndrome

Institute of Intensive Care Medicine, University Hospital Zurich and University of Zurich[1], Neurocritical Care Unit, Department of Neurosurgery and Institute of Intensive Care Medicine, University Hospital and University of Zurich[2]

Introduction:
Current and former definitions of acute respiratory distress syndrome (ARDS) include a hypoxemia criterion. Traditionally, this has been assessed by the ratio of partial pressure of oxygen in arterial blood (PaO2) divided by the fraction of inspired oxygen (FiO2). There is increasing interest of a continuous, non-invasive surrogate, such as the peripheral oxygen saturation (SpO2) divided by FiO2 (SpO2/FiO2) ratio. Recently, a new global definition of ARDS added the SpO2/FiO2-ratio as a surrogate for PaO2/FiO2 in an effort to provide an ARDS definition that is more suitable for resource-limited settings. To assess the limitations of the SpO2/FiO2-ratio in the classification of ARDS severity, we focused on classification accuracy and monitoring of disease progression using retrospective data from three high-resolution ICU databases. Additionally, we provide theoretical and technical explanations for classification discrepancies.

Methods:
In this retrospective observational cohort study we used data from three ICU databases: MIMIC-IV (USA), SICdb (Austria) and ICU-Cockpit from the USZ (Switzerland). The latter is a big data platform collecting high-resolution (up to 200 Hz for continuous signals) multimodal data since 2016 from over 2400 patients of the Neurocritical Care Unit and the medical ICU. Adult patients with ARDS were selected by applying the Berlin definition (ICU-Cockpit) or by ICD-10 codes (SICdb and MIMIC-IV). ARDS severity was calculated with the PaO2/FiO2-ratio and the SpO2/FiO2-ratio applying the thresholds of the new global definition of ARDS. We evaluated clinical performance using ARDS severity classification accuracy. Further the impact of FiO2 settings on ARDS severity and trending ability by correlating corresponding changes in FiO2, SpO2 and PaO2 were assessed. Limitations of SpO2 measurements were evaluated through comparison with arterial oxygen saturation (SaO2) from arterial blood gas analysis, and conversion between PaO2/FiO2 and SpO2/FiO2 was evaluated by comparing our data and published linear and log-linear imputations. The study was funded by Innosuisse.

Results:
Overall, 708 ARDS patients were included in the analysis. Based on the PaO2/FiO2-ratio, admissions were classified as no, mild, moderate, and severe ARDS in 7.9%, 7.2%, 47.0% and 37.9%. Alignment of ARDS severity categories was 69.1% (Fig. 1). The SpO2/FiO2-ratio overestimated the PaO2/FiO2-ratio category in 28.0% and underestimated it in 2.9% of admissions. The SpO2/FiO2-ratio was highly influenced by FiO2 setting, visualized by separation of ARDS severity categories by FiO2 (Fig. 2a). Classification accuracy also differed by FiO2 settings, ranging from an accuracy of 22% at FiO2 70% to an accuracy of 91% at FiO2 55% (Fig. 2b). Changes in PaO2/FiO2-ratios severity categories between two consecutive datapoints were correctly detected by the SpO2/FiO2-ratio in only 19.6% (Fig. 3a). During relatively stable respiratory conditions, proportional changes in FiO2 were strongly correlated with proportional changes in PaO2 (r = 0.88), indicating similar PaO2/FiO2-ratios, but they were not correlated with proportional changes in SpO2 (r = 0.44), indicating that FiO2 changes alter the SpO2/FiO2-ratio disproportionately (Fig. 3b and 3c).

Figure 1:

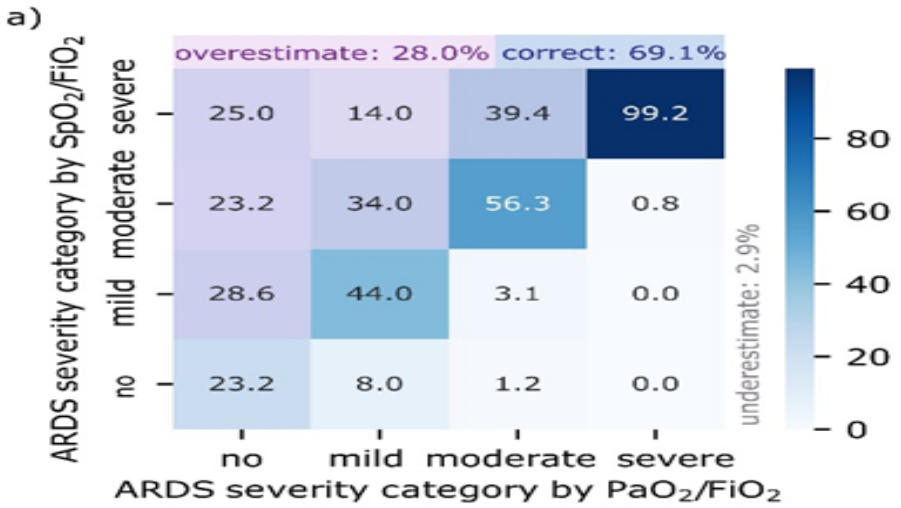

Figure 2:

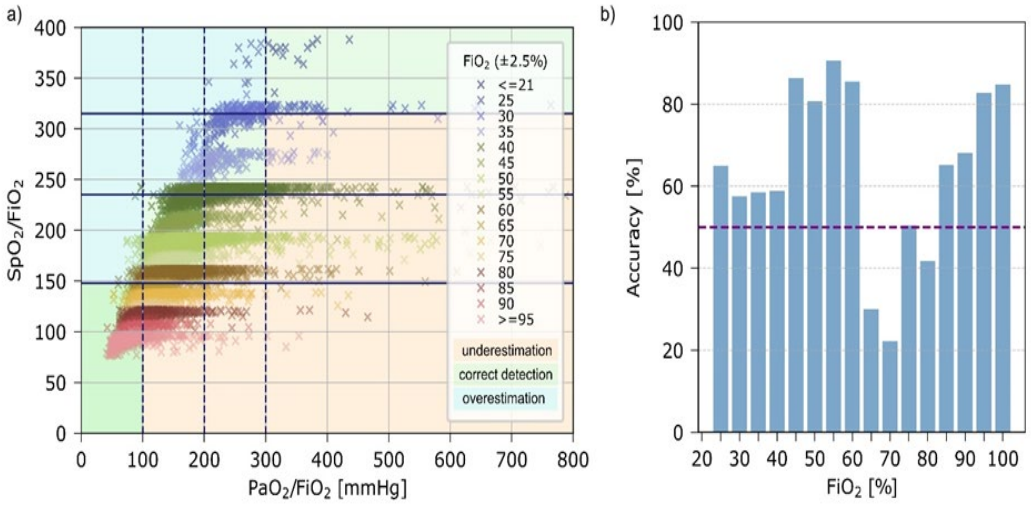

Figure 3:

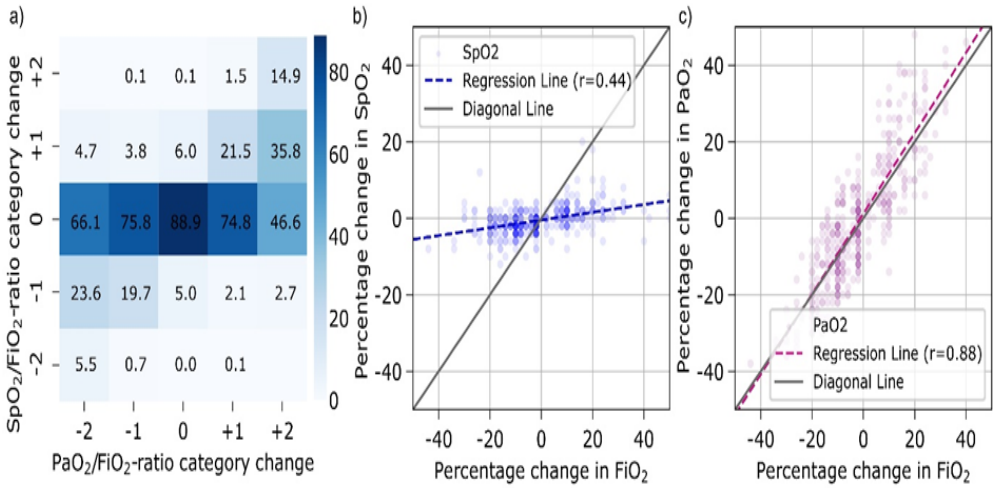

Conclusion:

The use of SpO2/FiO2 interchangeably with PaO2/FiO2 for severity classification and monitoring of disease progression is limited by its inadequate trending ability and high dependence on FiO2 settings. This discrepancy in severity classification may influence treatment decisions and patient selection in clinical trials. Better performance using non-invasive approaches to classify ARDS may be achieved through more complex machine learning models.

752

S. Mohammed[1], P. Enz[1], N. Atzemian[1], E. Gorica[1], M. Telesca[1], G. Panteloglou[2], F. Ruschitzka[1, 3], S. Costantino[1, 3], F. Paneni[1, 3]

The BET Protein Inhibitor Apabetalone rescues Doxorubicin-Induced Endothelial Senescence and Vascular Dysfunction

Centre for Translational and Experimental Cardiology (CTEC), Department of Cardiology, University Hospital of Zurich[1], Institute of Clinical Chemistry, University Hospital of Zurich[2], University Heart Center, Department of Cardiology, University Hospital of Zurich[3]

Introduction:
Caner survivors are a growing population which are more likely to die of cardiovascular disease (CVD). Anthracyclines (i.e. Doxorubicin, DOXO) are widely used anti-cancer drugs which exert cardiotoxic and vascular aging effects. It has been demonstrated that cells that evade apoptosis after DOXO treatment enter a state of senescence, leading to endothelial dysfunction and arterial stiffness – key predictors of future cardiovascular events. Furthermore, accumulation of senescent endothelial cells plays a pivotal role in cardiometabolic disorders and life span reduction. Yet, only a few senolytics are known to date, partly due to the poor grasp of the molecular mechanisms that control the senescence survival programme.Bromo and extraterminal domain (BET) proteins, known epigenetic reader proteins, recognize acetylated histone tails and regulate gene transcription. Apabetalone (RVX-208), an FDA-approved BET inhibitor, has been shown to modulate transcriptional programs involved in inflammation, cancer, and renal disease. Yet, its potential role in endothelial senescence and cardio-oncology remains elusive. Our study aims to investigate whether pharmacological modulation of BET proteins by RVX-208 can mitigateDoxorubicin-induced endothelial senescence.

Methods:
Human aortic endothelial cells (HAECs) were treated with doxorubicin (DOXO, 50–500 nM) for 48 hours to induce senescence, assessed by morphological changes, cell cycle arrest markers (p21, p16, p53), SASP release, SA-β-gal activity, and DNA damage (γH2AX). Conditioned media from DOXO-treated cells was collected for molecular analyses and treatment of non-senescent HAECs. To evaluate the senolytic or senomorphic effects of RVX-208, HAECs were co-treated with DOXO (100 nM) and RVX-208 (5–20 μM). RNA sequencing, proteomics, ATAC-seq, and ChIP-seq were performed to assess transcriptional and chromatin accessibility changes. In vivo, C57BL/6J mice received a single intraperitoneal injection of DOXO (10 mg/kg) with or without pre-treatment with apabetalone (150 mg/kg, oral gavage). Endothelial function was evaluated ex vivo via aortic ring relaxation assays.

Results:
DOXO-treated ECs showed a dose-dependent increase in senescence markers (p16, p21 and p53).Of interest, treatment with RVX-208 (15mM) prevented the upregulation of senescent markers (p16, p21 and p53) while rescuing alterationsin cell morphology and reducing the number of SA-b gal positive cells. RVX-208 prevented DOXO-induced upregulation of genes involved in inflammation, oxidative stress and mitochondrial dysfunction as shown by RNA-seq and proteomic analysis. Conditioned media from DOXO-treated ECs showed an enrichment of SASP-associated markers (IL6, CCL2, IL8, TIMP2 and PDGF-b) as shown by proteome analysis.Exposure of healthyECs to conditioned media from senescent ECsrecapitulated aging features. Notably, RVX-208 blunted the release of SASP markers (IL6, CCL2 and IL8) from DOXO-treated ECs. In DOXO-treated mice, an increase in the expression of cell cycle inhibitors was observed, which was mitigated by RVX-208 treatment. Furthermore, RVX-208 rescued DOXO-induced impairment of acetylcholine-dependent endothelial relaxation. Mechanistically, both ATAC-seq and ChIP-seq demonstrated that RVX-208 treatment reduces the enrichment of BET protein (BRD4) on the promoter regions of cell cycle inhibitors (P53 and P21), leading to their transcriptional repression. This reduction is associated with an increase in the expression of C-MYC, NANOG, and KLF4 proteins, which are involved in the rejuvenation of endothelial function.

Conclusion:
Targeting BET proteins with RVX-208 may offer a promising therapeutic strategy to prevent endothelial aging and vascular dysfunction in cancer patients undergoing cardiotoxic therapies.

753

Ll. Walter[1], V. Kana[1], M. Herwerth[1], S. Hösli[1], P. Roth[1]

Relapse activity in pregnancy and the postpartum year in women with multiple sclerosis

Universitätsspital Zürich[1]

Introduction:
Multiple sclerosis (MS) is the most common autoimmune disorder of the central nervous system and primarily affects women of childbearing age. Previous data suggest a protective effect during pregnancy with a rebound of disease activity after delivery. The underlying pathomechanisms and the impact of discontinuing disease-modifying therapies (DMT), especially given the contraindication of many potent DMT during pregnancy, are still incompletely understood.

Methods:
Pregnancies in women with MS were identified by screening longitudinal data sampled during clinical routine at the Department of Neurology, University Hospital Zurich, between 1.1.2010 and 31.10.2023. Data recorded during routine follow-up visits included clinical data, imaging data (MRI), biomaterial markers (blood, cerebrospinal fluid), as well as therapy-related data. Statistical analyses were performed with IBM SPSS Statistics with a two-sided significance level of alpha = 0.05.

Results:
A total of 112 pregnancies among 70 women resulted into 95 live births. Eleven women had 14 first-trimester-miscarriages, 2 women had an abortion and 1 new-born died due to birth at non-viable gestational age. Out of 96 pregnancies that reached the 22nd gestational week, at least one relapse during pregnancy or the postpartum year occurred in 33 cases. Most relapses occurred in the first trimester postpartum (14 out of 43 relapses, 32.6%), and most frequently presented with isolated sensory deficits (48.8%). Women with occurrence of a relapse during pregnancy or in the year thereafter were less frequently exposed to a DMT (66.7% vs. 87.3%, p=0.016). MRI at the time of diagnosis and conception showed more frequently spinal lesions in these patients. Disability progression within the first postpartum year was more frequent in the relapse group (25.8% vs. 5.5%, p<0.001), with sustained differences in EDSS at two years postpartum. Subgroup analysis of pregnant women treated with natalizumab indicated a lower relapse risk when natalizumab was continued into the third trimester. We did not observe an impact on pregnancy outcomes by relapse activity during pregnancy or the postpartum year.

Conclusion:
Relapses during pregnancy or the postpartum year occured in approximately one third of pregnant women leading to accelerated disability progression. Presence of spinal cord lesions before pregnancy onset and lack of or paused DMT before conception were associated with an increased risk of relapse during pregnancy and the first postpartum year. This study highlights the importance of actively addressing the subject of family planning in treatment decisions.

754

V. Masciovecchio[1], E. Gorica[1], J. Spezzini[1], M. Telesca[1], I. Papadopoulou[2], S. Mohammed[1], L. Di Venanzio[1], F. Paneni[1], B. Ludewig[2], F. Ruschitzka[1], S. Costantino[1]

Metabolic Stress in Alveolar Macrophages Enhanced Inflammation and Pyroptosis

Center for Translational and Experimental Cardiology (CTEC), Department of Cardiology, University Hospital Zurich and University of Zurich[1], Institute of Immunobiology, Kantonsspital St. Gallen[2]

Introduction:
Heart failure with preserved ejection fraction (HFpEF) is a global public health issue associated with pulmonary hypertension (PH). PH is characterized by increased pulmonary resistance followed by right ventricular hypertrophy and failure. HFpEF exacerbates PH through systemic inflammation, metabolic dysregulation, and inflammatory mediators. This altered immune landscape, particularly the activation of alveolar macrophages, contributes to endothelial damage in the lungs, intensifying vascular remodeling. However, the exact mechanisms underlying PH remain unclear. We investigated the impact of cardiometabolic HFpEF-induced distress on alveolar macrophages and their role in endothelial damage in experimental PH.

Methods:
Mice were fed with high-fat diet and L-NAME for 15 weeks in order to recapitulate PH. At the end of treatment, echography, treadmill exhaustion tests, and lung congestion were obtained. Single nucleus RNA-Sequencing (snRNA-seq) was used for alveolar macrophage profiling. In vitro assays featured murine macrophages exposed to metabolic stress caused via palmitic acid (PA) were used.

Results:
We demonstrated that murine HFpEF-induced PH (HFpEF-PH) leads to right ventricular remodeling and inflammation. SnRNA-seq identified upregulation of the Dusp1 gene in pulmonary macrophages of the HFpEF-PH group, emphasizing its regulatory role in modulating the alveolar macrophage response to metabolic and oxidative stress. In vitro metabolic stress in murine macrophages triggered oxidative stress, inflammation, and pyroptosis, with elevated markers such as IL-1β, TNF-α, and Caspase-1. Additionally, the autophagic machinery was disrupted, with genes like ATG14 and Beclin-1 upregulated and ATG7 downregulated. These changes promoted endothelial dysfunction through macrophage-derived secreted factors, linking metabolic stress to vascular pathology in HFpEF-PH.

Conclusion:
SnRNA-seq of a murine model of PH induced by 15 weeks of a high-fat diet and L-NAME treatment revealed the impact of metabolic stress on alveolar macrophages. Our findings highlight the significant role of alveolar macrophages in PH and suggest new targets for PH treatment.

756

R. Boulos[3], L. Rings[2, 3], P. Risteski[2, 3], F. Paneni[1], O. Dzemali[1, 2, 3], H. Rodriguez Cetina Biefer[1, 2, 3]

Platelet Dysfunction and Altered Immune Response in Acute Aortic Dissection Type A: Insights from RNA-Seq Analysis

Center for Translational and Experimental Cardiology (CTEC), Department of Cardiology, University Hospital Zurich[1], Department of Cardiac Surgery City Hospital of Zurich - Site Triemli[2], Department of Cardiac Surgery University Hospital Zurich[3]

Introduction:
Acute Aortic dissection type A (AADA) is a life-threatening cardiovascular disease characterized by aortic wall tearing. Patients diagnosed with AADA display a heightened propensity for bleeding, thereby rendering surgical intervention more intricate. Although the clinical and environmental factors contributing to aortic dissection are well established, the underlying genetics remain unclear. Here, we explored changes of the transcriptional landscape associated with AADA to identify key pathways implicated in disease development and progression. In particular, we focused on the relationship between platelet dysfunction and bleeding cascades.

Methods:
We conducted bioinformatic analyses of available bulk RNA-seq from AADA patients and control samples to identify differentially expressed genes. We used functional annotations and pathway analysis of these genes to uncover gene expression signatures. We further explored cell-specific signatures by leveraging single-cell RNA-seq datasets.

Results:
We observed 1655 differentially expressed genes in AADA vs controls. Functional annotations of these genes were marked by terms such as leukocyte migration and activation, plasma membrane, and blood circulation, suggesting alterations in several key processes related to hemostasis and vascular function. Moreover, pathway analysis showed that platelet degranulation, elevated platelet levels, and platelet activation pathways were dysregulated, supporting the involvement of platelet-related processes in disease progression. At the single-cell level, we observed changes in cell type proportions between the control and patient samples. An increase in helper T17 cells, macrophages, pericytes, and smooth muscle cells (SMCs) suggests an altered immune and vascular environment. Conversely, a lower number of mast cells, fibroblasts, and plasma cells can affect tissue repair and antibody production.

Conclusion:
This study provides a comprehensive overview of the transcriptional changes associated with AADA, and offer plausible mechanisms for the increased bleeding phenotype. Further investigation of vascular microenvirnment and cell-specific pathways could lead to new therapeutic targets for managing bleeding disorders in patients with AADA.

757

Y. Hu[1], L. Yang[2], J. Cai[2], X. Zhou[3], Y. Liu[3]

Plasma Proteomics Identify Molecular Features and Biomarkers of Fulminant Myocarditis

Department of Cardiology, University Heart Center, University Hospital Zurich[1], Global Institute of Future Technology, Shanghai Jiao Tong University[2], National Clinical Research Center for Cardiovascular Diseases, Fuwai Hospital, National Center for Cardiovascular Diseases, Chinese Academy of Medical Sciences and Peking Union Medical College[3]

Introduction:
Fulminant myocarditis (FM) is a specific and most severe subtype of myocarditis, characterized by acute onset, rapid progression, and high mortality. Limited data are available on potential non-invasive biomarkers for the differential diagnosis of diseases. We aim to investigate the plasma proteomic profile and identify biomarkers that can facilitate early diagnosis and treatment of FM.

Methods:
In this study, data-independent acquisition mass spectrometry (DIA-MS) proteomic sequencing was performed on plasma samples obtained from eight FM patients, eight ST-segment elevation myocardial infarction (STEMI) patients and eight healthy controls (HCs). Potential markers of FM were further identified through a machine-learning pipeline. A larger cohort included 15 FM, 16 STEMI and 15 HCs was used to validate the proteomic signatures by enzyme-linked immunosorbent assay (ELISA).

Results:
A total of 573 proteins were identified in all plasma samples. Functional enrichment analyses uncovered dysregulation of complement and coagulation-related pathways, inflammation, and immune cell degranulation, which were likely contribute to the pathogenesis of FM. We found that two processes, complement activation (classical pathway) and the complement and coagulation cascades, obtained the highest enrichment ratio scores in the Gene Ontology (GO) and Kyoto Encyclopedia of Genes and Genomes (KEGG) analyses, respectively. We also derived protein coexpression networks through weighted gene correlation network analysis (WGCNA), grouping proteins into five coexpression modules that were associated with clinical traits and enriched for complement activation (turquoise) and acute-phase proteins (blue) in FM. 51 proteins were confirmed able to distinguish FM and STEMI patients. Furthermore, a unique biomarker panel comprising GPX3, C7, PGLYRP2, BCHE and ANPEP was established to differentiate FM from STEMI with high accuracy (auROC = 1.000). Some of these biomarkers were further validated by ELISA by the larger cohort.

Conclusion:
Proteomic signatures developed in this study reflected the dysregulation of key hematological functions in FM patients, and show potential for developing a valuable biomarker panel in complementary to current clinical parameters to aid in the early diagnosis of FM via plasma proteome.

758

L. Leuenberger[2, 8], L. Isenegger[2, 8], Y. Chen[4, 8], M. Burri[2, 8], S. Kollar[4], L. Planas-Paz[4], P. Bode[4, 7], A. Wozniak[5], S. Bauer[3], P. Schöffski[1], C. Pauli[4, 8], C. Britschgi[2, 6, 8]

Identifying Novel Vulnerabilities in Clear Cell Sarcoma Through Functional and Genomic Screening

Department of General Medical Oncology, University Hospitals Leuven, Belgium[1], Department of Medical Oncology and Hematology, Comprehensive Cancer Center Zurich, University Hospital of Zurich, Switzerland[2], Department of Medical Oncology and Sarcoma Center, West German Cancer Center, University Hospital Essen, University Duisburg-Essen, Essen, Germany[3], Department of Pathology and Molecular Pathology, Comprehensive Cancer Center Zurich, University Hospital of Zurich, Switzerland[4], Laboratory of Experimental Oncology, Department of Oncology, KU Leuven, Leuven Cancer Institute, Leuven, Belgium[5], Medical Oncology and Hematology, Tumorzentrum Winterthur, Cantonal Hospital Winterthur, Switzerland[6], present address: Department of Pathology, Cantonal Hospital Winterthur, Switzerland[7], University of Zürich, Switzerland[8]

Introduction:
Clear Cell Sarcoma (CCSA) is a rare soft tissue sarcoma characterized by specific gene fusions *EWSR1::ATF1* or *EWSR1::CREB1*, leading to the expression of an oncogenic fusion protein. Metastasized CCSA is resistant to conventional chemotherapy, targeted therapy or immunotherapy. This study aims to uncover new therapeutic strategies for CCSA by utilizing a whole-genome CRISPR/Cas9 knock-out screen combined with functional drug screening.

Methods:
We performed a genome-wide knock-out screen in the CCSA cell line model KAS using the pooled Brunello sgRNA library (Addgene # 73178, ~4 guides/gene, 19'114 genes). In parallel, three CCSA patient samples and multiple CCSA cell lines (SU-CCS-1, DTC-1, KAS) were treated with a library of 84 solid tumor pan-cancer drugs, and a custom drug library tailored to the hits of the CRISPR screen (70 compounds). Genes identified as critical vulnerabilities in CCSA were validated through single-gene knockouts, and promising therapeutic targets were further mechanistically interrogated and evaluated in a CCSA xenograft model.

Results:
Results revealed 1'552 significantly depleted genes (log fold change <-1 and FDR < 0.01) after 21 days, with enriched pathways in proteasome activity, mismatch repair, DNA replication, and, mTORC1 signaling, revealing critical vulnerabilities. Notable highly ranked depleted genes include the transcription factor and CCSA marker *SOX10*, as well as *MDM2, MCL1, CHEK1, HSPA5, PSMA5* and mTOR. Through integration of genetic knock-out and pharmacological inhibition data identified in our dual screening, we were able to identify several overlapping vulnerabilities. Initial validation of the therapeutic potential of PI3K/mTOR inhibition in CCSA cell models *in vitro* revealed an induction of apoptosis upon treatment. We then corroborated those findings in a CCSA xenograft mouse model *in vivo*. Treatment with the two combined PI3K/mTOR inhibitors omipalisib and copanlisib both resulted in significantly improved survival ($P = 0.027$ and $P = 0.036$, respectively) of tumor bearing mice, and reduced tumor growth, each compared to vehicle treatment.

Conclusion:
These findings offer new insights into actionable vulnerabilities in CCSA, with PI3K/mTOR inhibitors showing potential for therapeutic development. Future studies will investigate synergistic combinations to further optimize treatment efficacy and validate further vulnerabilities identified by our dual screening approach.

759

T. Diteepeng[3], Y. Puspitasari[2], S. Ministrini[1, 2], M. Telesca[3], D. Vdovenko[7], A. Akhmedov[2], J. Beer[2, 5], S. Costantino[3, 4], F. Ruschitzka[3, 4], F. Paneni[3, 4], G. Camici[2, 6], M. Luciani[3, 4]

Unfolding the Link Between Protein Misfolding and Stroke-Heart Syndrome

Cardiology Department, Luzerner Kantonspital, Lucerne, Switzerland[1], Center for Molecular Cardiology, University of Zurich, Schlieren, Switzerland[2], Center for Translational and Experimental Cardiology, Department of Cardiology, University Hospital Zurich, University of Zurich, Schlieren, Switzerland[3], Department of Cardiology, University Heart Center, University Hospital Zurich, Zurich, Switzerland[4], Department of Internal Medicine, Cantonal Hospital of Baden, Baden, Switzerland[5], Department of Research and Education, University Hospital Zurich, Zurich, Switzerland[6], Immunology-Oncology Section, Maisonneuve-Rosemont Hospital Research Center, Department of Microbiology, Infectious disease and Immunology, University of Montreal, Montreal, Quebec, Canada[7]

Introduction:
The brain-heart axis plays a key role in the post-stroke cardiovascular complications termed the stroke-heart syndrome (SHS). Alongside inflammatory and neurohormonal signals, protein misfolding has emerged as a potential contributor into this organ crosstalk due to the presence of ischemia-related misfolded toxic proteins (oligomers) and their propagation. However, their biological relevance in SHS remains elusive. This study investigates the involvement of protein misfolding in SHS by evaluating oligomer presence in the myocardium following an acute ischemic stroke (AIS) and its effects on cardiac function and proteostasis.

Methods:
AIS was induced via 45-minute left transient middle cerebral artery occlusion (tMCAO) in 3-4 months old wild-type C57BL/6J male and female mice, followed by 48 hours of reperfusion. Cardiac function was assessed using electro- and echocardiography at pre- and post-operative assessment. Oligomer localization and biological responses in proteostasis were examined.

Results:
AIS induced cardiac dysfunction, including irregular heart rates consistent with supraventricular arrhythmias, reduced cardiac output and a tendency towards decreased stroke volume and fractional shortening. Elevated oligomer levels in the ipsilateral brain hemisphere was detected, confirming the localized ischemic insult. Notably, increased oligomers accumulation in the myocardium is correlated with disrupted cardiac proteostasis, evidenced by alterations in the chaperone (heat-shock protein 90) and the unfolded protein response marker (cleaved ATF6). Myocardial responses included activated autophagy and antioxidant defenses by protein kinase AKT dephosphorylation, increased expression of autophagosome protein LC3B-II and catalase, reflecting a complex systemic response.

Conclusion:
AIS-induced oligomers accumulate in both the murine brain and heart indicating their systemic presence and correlation with disrupted cardiac resistance to proteotoxicity. These findings suggest oligomers as additional components of SHS pathophysiology with ongoing studies aimed at investigating the biological and clinical relevance of proteotoxicity in this adverse condition.

760

E. Gorica[1, 3], S. Costantino[1, 3], S. Mohammed[1], M. Telesca[1], A. Mongelli[1], F. Ruschitzka[1, 3], N. Hamdani[2], F. Paneni[1, 3]

The BET inhibitor Apabetalone Protects Against Heart Failure with Preserved Ejection Fraction by Suppressing Myocardial Inflammation

Center for Translational and Experimental Cardiology (CTEC), Department of Cardiology, University Hospital Zurich and University of Zürich, Zurich, Switzerland[1], Institute of Physiology, Ruhr University, Bochum, Germany, Bochum, Germany[2], University Heart Center, University Hospital Zurich, Zurich, CH, Zurich, Switzerland[3]

Introduction:
Posttranslational histone modifications, play a major role in cardiac hypertrophy and dysfunction. Apabetalone (APA), a selective inhibitor of bromodomain and extraterminal containing protein family (BET) proteins, prevents bromodomain-containing protein 4 (BRD4) interactions with chromatin thus modulating transcriptional programs in different organs.

Methods:
Mice were subjected to high fat diet feeding and L-NAME treatment for 15 weeks to induce cHFpEF. Histology, mouse echocardiography (Vevo3100) and Treadmill exhaustion test were performed. Unbiased gene expression profiling by PCR array and proteomics analysis (Olink) was employed in left ventricular (LV) myocardial specimens from HFpEF mice and control animals. Cultured cardiomyocytes (CMs) treated with palmitic acid (PA) were used as an in vitro model of metabolic stress. cHFpEF mice were chronically treated with the BET inhibitor APA (150mg/kg/day) or vehicle (DMSO). In order to translate our findings to the human setting, passive stiffness of skinned CMs collected from cHFpEF patients was assessed before and after APA treatment.

Results:
HFpEF mice displayed LV hypertrophy, diastolic dysfunction, myocardial fibrosis, lung congestion and impaired exercise tolerance as compared to controls. Interestingly, diastolic dysfunction - assessed by E/A ratio and isovolumic relaxation time (IVRT) - and lung congestion were significantly reduced in HFpEF mice treated with APA, while exercise tolerance was improved. Transcriptomic analysis in PA-treated CMs and LV mouse specimens from cHFpEF mice showed a profound deregulation of genes controlling inflammation, namely IL-6, TNF-alpha, and IL-1beta. ChIP assays showed BRD4 occupancy on the promoter of several inflammatory genes, including IL6. Treatment with APA suppressed most of inflammatory genes, with a pronounced effect on IL6 expression. Moreover, APA reduced circulating levels of several inflammatory chemokines. The beneficial effects of APA were explained by modulation of IL-6/CaMKII/STAT3 pathway both in cHFpEF hearts and PA-treated CMs. In skinned CMs from cHFpEF patients, both APA and IL6 blockade were able to attenuate passive stiffness.

Conclusion:
Our findings set the stage for preclinical studies and exploratory clinical trials testing APA in patients with cHFpEF.

761

J. Rieber[2], G. Meier Bürgisser[2], P. Wolint[2], I. Miescher[2], JG. Snedeker[1], M. Calcagni[2], P. Giovanoli[2], J. Buschmann[2]

Synergistic Effect of IGF-1 and PDGF-BB in Tendon Healing

Institute for Biomechanics, ETH Zurich[1], Plastic Surgery and Hand Surgery, USZ[2]

Introduction:
Tendon injuries, particularly ruptures, are common musculoskeletal conditions that involve prolonged healing and risks such as adhesion formation and re-rupture. Despite advancements in repair strategies, achieving full functional recovery remains challenging. Growth factors (GFs), including insulin-like growth factor-1 (IGF-1) and platelet-derived growth factor-BB (PDGF-BB), are known to significantly influence tendon healing. Their combined application may enhance repair outcomes.

Methods:
A bioactive electrospun polymer tube composed of Degrapol® (DP) was developed for tendon repair. The tubes incorporated IGF-1, PDGF-BB, or a combination of both via water-in-oil emulsion electrospinning. Three treatment groups were established: IGF-1 only, PDGF-BB only, and a combination of IGF-1 and PDGF-BB. Scaffold fiber morphology and cellular growth were analyzed using scanning electron microscopy (SEM). ELISA was used to study the release kinetics of IGF-1 and PDGF-BB over time. Rabbit tenocytes were cultured on the scaffolds, and cell morphology was evaluated microscopically. Gene expression of Ki-67, tenomodulin, Col1, and mTORC1 was assessed via qPCR on days 3 and 7. Mitochondrial function and energy metabolism of rabbit Achilles tenocytes and rabbit adipose-derived stem cells (ASCs) were examined using Seahorse analysis. Angiogenesis was assessed with the CAM assay.

Results:
Scaffolds incorporating IGF-1 or PDGF-BB individually showed similar effects on cell morphology, with no significant differences in aspect ratios compared to controls. Fiber thickness, pore size, and water contact angles were consistent across all growth factor-containing scaffolds. Gene expression analysis showed that Col1 was elevated in the IGF-1 and PDGF-BB groups but lowest in the combination group, while Ki-67 was highest in the combination group. Expression levels of mTORC1 and tenomodulin were comparable across all groups, including controls. Seahorse analysis revealed that OCR and ECAR were significantly higher in the IGF-1 group than in other groups for tenocytes. However, for ASCs, controls exhibited the highest metabolic activity. Energy mapping showed that ASCs relied more on mitochondrial respiration, whereas tenocytes exhibited glycolysis. In basal and maximal respiration, the IGF-1 group showed the highest OCR, followed by the combination group, which outperformed the PDGF-BB group.

Conclusion:
All growth factor-containing scaffolds exhibited similar structural properties, as assessed by SEM. Hydrophilicity was measured using water contact angle measurements, which indicated increased hydrophilicity in growth factor-containing scaffolds compared to pristine DegraPol scaffolds. This enhanced hydrophilicity is attributed to the incorporation of an aqueous growth factor solution during scaffold production by emulsion electrospinning, suggesting that the fabrication process effectively integrates the growth factors while maintaining structural consistency. The combined application of IGF-1 and PDGF-BB showed trends of synergistic effects on tendon healing, particularly in Seahorse analyses, where enhanced OCR suggested improved mitochondrial function and metabolism. However, optimizing the concentration ratio of the two GFs may yield even better results. These findings highlight the potential of IGF-1 and PDGF-BB to enhance tendon repair by promoting cellular and molecular responses, making this approach a promising strategy for in vivo tendon regeneration.

762

E. Parietti[1], A. Gómez Mejia[1], CC. Chang[1], S. Mairpady Shambat[1], A. Zinkernagel[1]

Rifampicin impairs intracellular eradication of Staphylococcus aureus by human macrophages

Department of Infectious Diseases and Hospital Epidemiology, University Hospital Zurich, University of Zurich[1]

Introduction:
Staphylococcus aureus (SA) persisters are a subpopulation of dormant bacteria that can survive high concentrations of antibiotics resulting in recurrent infections. Biofilms and the intracellular milieu of innate immune cells, such as macrophages, provide a stressful environment that can induce persisters, Rifampicin (RIF) is an antibiotic commonly used to treat biofilms. However, RIF was found to have immunomodulatory properties by interacting with host immune cells and alter their immune functions. In this project, we aimed to study the effect of RIF on macrophage activation and effector response against SA and the effectiveness of RIF in eradicating intracellular persisters.

Methods:
We treated human monocyte-derived macrophages (hMDMs) with RIF 24h before SA infection. The infection was then treated with different combinations of antibiotics, including RIF and flucloxacillin. We determined SAuptake by macrophages, the kinetic of intracellular survival and the formation of antibiotic persisters. We measured the expression of surface markers and the production of intracellular reactive oxygen species (ROS) and reactive nitrogen species (RNS) by multi-parametric flow cytometry analysis and cytokine production (IL-6, TNFα, IL-1β, IL-10) by ELISA to determine the activation status of hMDMs. We investigated the metabolic profiling of both mitochondrial respiration and glycolysis in macrophages by Seahorse XF Analyzer. Finally, we evaluated the effect of RIF at the transcriptional level by bulk RNA sequencing.

Results:
RIF treatment of macrophages before infection impaired SA intracellular killing by macrophages but reduced intracellular persisters. Moreover, RIF treatment reduced the production of intracellular RNS and the secretion of pro-inflammatory cytokines (IL-6, TNFα, IL-1β) in response to SA infection. On the other hand, we did not observe a significant alteration of ROS production or surface marker expression compared to macrophages not treated with RIF before infection. We did not observe any significant difference in the mitochondrial function, while the basal glycolysis and the glycolytic capacity were lower in macrophages that received the pre-treatment with RIF. Finally, we found that pre-treatment of macrophages with RIF reduces the expression of signaling pathways that have a central role in the activation of macrophages, including the cytokine-cytokine receptor interaction, JAK-STAT and PI3K-Akt signaling pathways.

Conclusion:
Our results showed that rifampicin treatment alters the capacity of macrophages to respond to SA by impairing the activation of the pro-inflammatory response and the intercellular killing capacity. Moreover, we show that this change in macrophage phenotype is associated with an increased survival of bacteria inside macrophages, but with a decreased intracellular persister formation. The reduction of intracellular RNS could be one reason for the increased survival of bacteria and reduction of persisters inside macrophages. Nevertheless, further investigations are needed to understand in depth the molecular mechanism and to identify antibiotics that can efficiently target intracellular persisting bacteria.

763

R. Penna[1, 2], S. Pascolo[1, 2]

Ic-siRNA: Developing A Trifunctional Therapeutic Integrating RNA Interference, Chemotherapy, and Immunostimulation for Cancer Treatment

Universitätsspital Zürich[1], University of Zurich[2]

Introduction:
In our laboratory we developed the immuno-chemotherapeutic RNA (icRNA), a novel anti-cancer molecule that combines the immunostimulating benefits of RNA therapy with the chemotherapeutic activities of 5-fluorouracil (5FU). Our studies demonstrated that 5FU-icRNAs could curb growth of cancers in mice, though it has not been curative. Thymidylate synthase (TS) has been identified as a predictive biomarker for 5FU resistance, as its overexpression is often linked to reduced treatment efficacy. Building on this, we envisioned a potentially enhanced icRNA-based anti-cancer therapeutic: the ic-siRNA. This innovative molecule shall leverage RNA interference (RNAi) to reduce TS expression while also delivering 5FU. Additionally, ic-siRNA can activate the innate immune system by stimulating RNA sensors, potentially reversing the immunosuppressive tumor microenvironment.

Methods:
Our primary goal is to evaluate the effectiveness of this innovative strategy. To achieve this, we plan to adopt a multimodal approach, combining in vitro studies to investigate gene silencing, immunostimulation, and chemotherapeutic activities, with in vivo mouse models to assess pharmacokinetics, tumor growth inhibition, and overall survival. Currently, we have developed a prototype ic-siRNA. For its validation, we employed a co-transfection system using firefly luciferase (fLuc) siRNA and fLuc mRNA

Results:
Our data demonstrate that both unmodified and modified fLuc siRNA effectively reduce fLuc expression, confirming that the ic-siRNA retains its RNAi activity. Our future efforts will focus on validating ic-siRNA directed to oncogenes or chemotherapy resistance genes in vitro and in vivo as superlative trifunctional anti-cancer drugs.

Conclusion:
By integrating RNAi, chemotherapy, and immune stimulation in one molecule, this strategy holds promises as a safe and efficient therapy for cancer patients.

764

N. Atzemian[1], S. Mohammed[1], E. Gorica[1], L. Di Venanzio[1], S. Costantino[1], F. Ruschitzka[1, 2], F. Paneni[1, 2]

Epigenetic and transcriptional landscape of the kidney in heart failure with preserved ejection fraction

Center for Translational and Experimental Cardiology (CTEC), Department of Cardiology University Hospital Zurich, University of Zurich, Zurich[1], Department of Cardiology, University Hospital Zurich[2]

Introduction:
Heart failure with preserved ejection fraction (HFpEF) and chronic kidney disease (CKD) constitute a high-risk phenotype with significant morbidity and mortality and poor prognosis. Multiple proinflammatory comorbid conditions influence the pathogenesis of HFpEF and CKD. The understanding of the molecular mechanisms underpinning kidney damage cardio-renal interactions in HFpEF remains poorly understood. Unveiling new molecular targets could pave the way for new mechanism-based interventions to prevent HFpEF and CKD progression.

Methods:
A mouse model of HFpEF, characterized by the combination of high-fat diet (60 kcal% fat,) and L-NAME in the drinking water (0.5g/L) for 15 weeks was employed. Control mice received a control diet (10 kcal% fat,) and vehicle in the drinking water (Fig. A). Deep renal phenotyping in control and HFpEF mice was performed by: i) renal biomarker profiling; ii) histological analysis; iii) RNA-Sequencing; iv) proteomics; v) CUT&RUN assay to investigate chromatin accessibility (Fig. B).

Results:
HFpEF mice displayed renal dysfunction as assessed by increased creatinine, cystatin C and galectin-3 levels (Fig. C), as well as alterations of tissue architecture as shown by Collagen 1A1 and Periodic acid-Schiff (PAS) staining (Fig. D). Bulk RNA-seq, validated by mass-spectrometry proteomics unveiled three top-ranking signals in HFpEF vs control kidneys, namely Kynureninase (KYNU), Receptor Accessory Protein 6 (REEP6), and Retinol Dehydrogenase 16 family member 2 (RDH16F2) (Fig. E). Analysis of the chromatin landscape by CUT&RUN assay identified increased accessible loci in HFpEF vs control kidneys, with a prominent role of epigenetic readers (BET proteins) in regulating the transcription of target genes. Of interest, enhanced BET protein enrichment was associated with kidney inflammation and fibrosis in HFpEF mice.

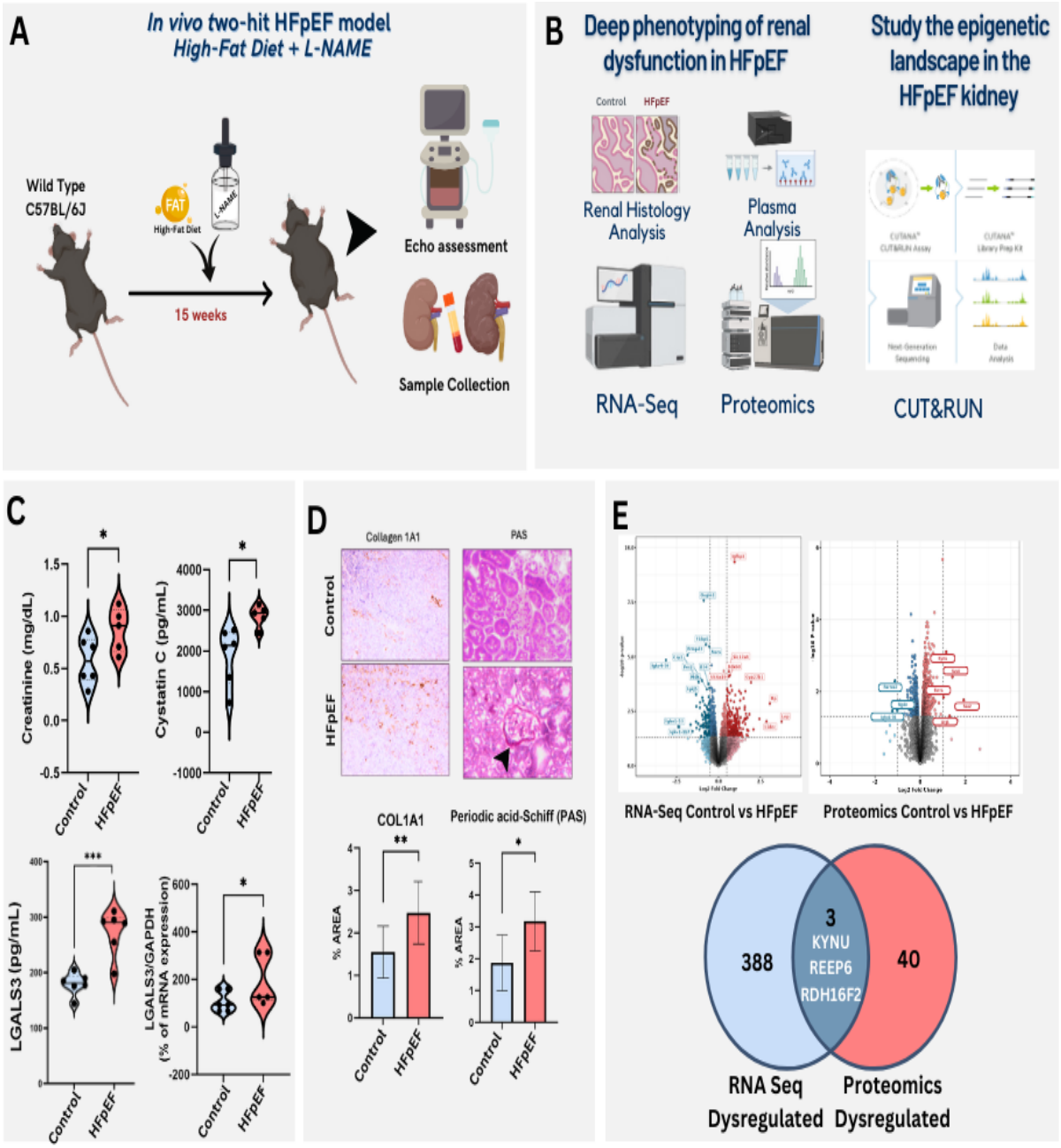

A) Schematic showing the mouse model of HFpEF; **B)** Multi-omic approach for deep phenotyping of the HFpEF kidney, incorporating plasma and histology renal function analyses, transcriptomics, proteomics and epigenomics; **C)** Markers of renal function; **D)** Periodic acid- Schiff and Collagen 1A1 stainings and quantification; **E)** Integration of RNA-seq and proteomic analysis showing convergence on 3 molecular targets, namely Kynureninase (KYNU), Receptor Accessory Protein 6 (REEP6), and Retinol Dehydrogenase 16 family member 2 (RDH16F2)

Conclusion:
HFpEF is associated with relevant epigenetic and transcriptional alterations in the kidney, eventually promoting organ dysfunction and structural remodeling. Our study sheds light on epigenome-environment interactions and new molecular targets potentially implicated in the progression of cardio-renal damage in HFpEF.

765

A. Mongelli[1], I. Papadopoulou[5], A. Mengozzi[4], E. Gorica Hoxha[1], S. Mohammed[1], H. Rodriguez Cetina Biefer[2], O. Dzemali[2], S. Costantino[1], L. Burkhard[5], F. Ruschitzka[3], F. Paneni[1, 3]

Role of paracardial fat in heart failure with preserved ejection fraction

Center for Translational and Experimental Cardiology (CTEC), Department of Cardiology, University Hospital Zurich, University of Zurich, Zürich , Switzerland[1], Department of Cardiac surgery, University Hospital Zurich, Zürich, Switzerland[2], Department of Cardiology, University Hospital Zurich, Zürich, Switzerland.[3], Department of Clinical and Experimental Medicine, University of Pisa, Italy[4], Medical Research Center, Kantonsspital St. Gallen, Switzerland[5]

Introduction:
Nowadays most of cardiovascular studies focused on epicardial adipose tissue (EAT) due to its direct contact to myocardium. However, another adipose tissue, the paracardial (pCF) has also found to correlate with high level of systolic blood pressure, high fasting glucose, elevated triglycerides, and an increased amount of C-reactive protein as well with coronary artery calcification. Interesting, the molecular pathways in which pCF modulate heart function and structure are poorly understood and no information are available on pCF molecular mechanism in hearth failure with preserved ejection fraction (HFpEF). HFpEF is characterized by the remodeling of left ventricle (LV) leading to diastolic dysfunction, atrial fibrillation, hypertension, mostly affects women and accounts for almost 50% of the HF cases. Despite HFpEF high incidence, the treatment options are limited and not specific.

Methods:
A mouse model of cHFpEF, characterized by the combination of high-fat diet (60 kcal% fat,) and L-NAME in the drinking water (0.5 g/L) for 15 weeks. Control mice received a control diet (10 kcal% fat,) and vehicle in the drinking water. Single-cell nuclei RNA sequencing (snRNAseq) was performed by using the 10x Chromium analyzer. Cell-cell communication analysis was performed by using CellChat Software. The function of top-ranked genes was investigated in vitro, in human adipocyte cell line in which the targets were up-regulated and down-regulated by lipid tranfection of target-carring plasmid and siRNA silencing respectively. Molecular and cellular analysis, such as qPCR, westernblot, FACS analysis, and co-culture with other cell types were performed to identify the pathways involved in pCF dysregulation.

Results:
The transcriptional and cellular landscape of pCF was performed by high-resolution snRNAseq analysis and 20’397 cells from control and cHFpEF mice were captured. Several clusters were identified. At clustering resolution, the analysis revealed two different adipocyte groups: adipocyte1 (defined by Pparg/Nrg4 markers) and adipocyte2 (Ncam1/Itga7 markers). The adipocyte2 cluster was highly enriched in cells from cHFpEF mice and showed a significant dysregulation of several genes on top of them neuronatin (NNAT, up-regulated) and Acetyl-CoA Carboxylase Alpha (ACACA, down-regulated). Pathway analysis confirmed the activation immuno-metabolic signaling, integrin-mediated signaling, adipocyte catabolic processes and inflammation in pCF cHFpEF. Interactome analysis unveiled a strong link between adipocytes and immune cell activation; while molecules for endothelial and smooth muscle cells develop and homeostasis are depleted in HFpEF vs control pCF specimens. In vitro analysis revealed the dysregulation of ROS production, Lipid peroxidation upon the modulation of selected targets. The secretome derived from treaded adipocytes was observed to activate the immune cells.

Conclusion:
Almost 50% of HF case presents the preserved ejection fraction and nowadays no specific treatments are developed for those patients. The transcriptome and secretome changes of HFpEF-pCF as well the secretome of treated dipocytes were able to activate immune cells suggesting the pCF as an active fat depot that could contribute to myocardial inflammation.

766

A. Mongelli[1], A. Farsetti[5], N. Hamdani[3], F. Ruschitzka[2], C. Gaetano[4], F. Paneni[1, 2]

Epigenetic Age of the Male and Female Heart: Insights into Cardiovascular Risk Assessment across Sexes

Center for Translational and Experimental Cardiology (CTEC), Department of Cardiology, University Hospital Zurich, University of Zurich, Zürich , Switzerland[1], Department of Cardiology, University Hospital Zurich, Zürich, Switzerland.[2], Department of cellular and translational Physiology, University of Bochum, Bochum, Germany[3], Laboratory of Epigenetics, Istituti Clinici Scientifici (ICS) Maugeri IRCCS, Pavia, Italy[4], National Research Council (CNR)-IASI, Rome, Italy[5]

Introduction:
Men and women show notable differences in symptoms/course and treatment of cardiovascular disease, suggesting the need for sex-specific biomarkers of cardiovascular damage. Chronological age is an established cardiovascular risk factor. However, people age differently, which matured the concept of “epi-genetic age determined by DNA metilation (DNAmAge)”. The DNAmAge of a tissue provides information on its biological age and it can differ from the chronological age. Gathering information on the biological age of the heart could provide hints on premature cardiac aging and risk stratification. The discrepancy between chronological age and DNAmAge is defined as DeltaAge (= chronological years – DNAmAge years) and it has shown to predict mortality in humans. In this study, we assess sex-related differences in cardiac epigenetic age.

Methods:
DNA was isolated from whole blood and heart specimens from women (N=92) and men (N=272) who underwent elective cardiac surgery for valve replacement or coronary artery bypass. After isolation, DNA was processed to convert the un-methylated cytosines to uracile. PCR reaction was used to amplify the target sequences followed by pyrosequencing to determine the methylation level of age-related CpGs.

Results:
Women were chronologically older than men (69.9±7 vs 64.6±9 years, $p<0.05$), while the 2 groups were comparable for cardiovascular risk factors. DeltaAge assessed in whole blood samples showed comparable values of chronological and epigenetic age in women and men. By contrast, DeltaAge assessed in cardiac specimens showed that 15.1% of women were biologically older (as compared to their chronological age) while a much higher rate (34.5%) was observed for men.

Conclusion:
We show that men’s heart is older than the female heart. Our study could set the stage for larger studies leveraging the epigenetic clock as a molecular marker of premature aging and clinical outcome in men and women.

767

A. Mongelli[1], A. Mengozzi[3], E. Gorica Hoxha[1], S. Mohammed[1], M. Telesca[1], C. Matter[1], F. Ruschitzka[2], F. Paneni[1, 2], S. Costantino[1]

Long non-coding RNA PANDA promotes endothelial senescence and oxidative damage through the interaction with NRF2

Center for Translational and Experimental Cardiology (CTEC), Department of Cardiology, University Hospital Zurich, University of Zurich, Zürich , Switzerland[1], Department of Cardiology, University Hospital Zurich, Zürich, Switzerland.[2], Department of Clinical and Experimental Medicine, University of Pisa, Italy[3]

Introduction:
Accumulation of reactive oxygen species and inflammation are major features of diabetic vasculopathy, yet the underlying mechanisms remain elusive. Long non-coding RNAs (lncRNAs) are emerging as important players in the pathogenesis of cardiovascular disease. Recent work has shown that PANDA, a newly identified lncRNA, is a key regulator of cellular senescence, apoptosis and oxidative stress.

Methods:
RNAseq was performed to aorta specimen from diabetic and no diabetic patients as well to Human aortic endothelial cells (HAECs) exposed to normal (NG, 5 mM) and high glucose concentrations (HG, 25 mM). PANDA depletion in HG-treated HAECs was obtained by siRNA transfection while a scrambled RNA was used as a negative control. RNAs sequencing (RNA-seq) and bioinformatic analysis (network perturbation amplitude, NPA) of treated HAECs unveiled transcriptional changes upon PANDA depletion. in NG condition PANDA was overexpressed by plasmid trasfection and a empty vector as control. Expression of PANDA was assessed by real time PCR. PANDA RNA immuno-precipitation (RIP) was performed to check its binding to relevant transcriptional factor (such as NRF2) as well Chromatin immunoprecipitation (ChIP) was performed to check the NRF2 binding on oxidative gene promoters. Cellular localization of NRF2 was investigated by Immunofluorescence. Beta-galactosidase and superoxide staining was used to detect endothelial senescence and ROS formation; while, migration and tube formation were employed to evaluate angiogenic properties of HAECs.

Results:
PANDA expression was significantly increased in diabetic human aorta as well in HAECs exposed to HG. Transcriptomic analysis revealed dysregulation of several genes upon PANDA silencing with the antioxidant gene heme oxygenase-1 (HMOX1) as the top-ranking transcript in HG-treated cells. Western blot analysis reveals the restored level of HMOX1 and TFRC1 upon PANDA depletion. NPA analysis showed a strong involvement of PANDA in senescence, DNA damage, NRF2 signaling, hypoxic stress response and proliferation. In HG, NFR2 is downregulated and PANDA silencing restores its level. Under HG condition, PANDA binds the transcription factor NRF2 and blocks its nuclear translocation of NRF2 where it binds HMOX1 and TFRC promoters. Silencing of PANDA in HG-treated HAECs reduced genes and cellular features of senescence, restored the expression of anti-apoptotic genes and decreases caspase 3 activity, improved endothelial migration and tube formation , and ROS formation were reduced.

Conclusion:
Hyperglycemia-induced upregulation of PANDA drives endothelial senescence while impairing angiogenic properties. PANDA depletion in HG-treated HAECs rescues maladaptive transcriptional changes through the interaction of NRF2 that in turn translocate into the nucleus enhancing the expression of the antioxidant gene HMOX1. Of note, targeting PANDA in the diabetic vasculature was able to rescue endothelial dysfunction. Our results indicate PANDA as a novel molecular target in the setting of diabetic vascular disease.

768

J. Jang[3], S. Guerra[3], D. Bochicchio[3], E. Breuer[3], A. Charlton[4], P. Dutkowski[2], P. Clavien[1], B. Humar[3]

Histological scoring and non-invasive assessment of ischemic injury in pretransplant uterus grafts

Privatklink Bethanien[1], University Hospital Basel[2], University Hospital Zürich[3], University of Auckland[4]

Introduction:
Uterus transplantation (UTX) serves as a viable alternative to surrogacy and adoption for individuals aspiring to motherhood but facing uterine infertility. UTX grafts usually come from live and also donation after brain death, but the increasing demand has put donation from cardiac death (DCD) into focus. DCD grafts are hampered by warm ischemia, however how ischemia impacts uterus quality is ill-studied. To this end, we characterized histological injury in uteri post ischemia and explored potential markers to assess pretransplant graft quality.

Methods:
Tissue samples from uteri exposed to defined periods of warm ischemia (WI; 30, 60, 90, 120, and 180 minutes) followed by cold ischemia (CI; 4 hours) were investigated. Artificial intelligence (AI)-assisted histology analysis was applied to HE- and EVG- (extracellular matrix, ECM) stained histology sections. RNA from uterine tissue was analyzed for transcripts that correlate to injury levels, code for secretory proteins, have human homologues, and react towards protective effects. Storage solution was used to validate the activity of potential injury marker candidates.

Results:
Histological AI analyses identified specific types of injury (cellular-type and ECM loss) correlating with ischemic exposure. Notably, 30 minutes WI had preconditioning-like protective effects. Transcriptomics correlated overall injury with inflammatory pathways, and collagen loss with proteolytic pathways, respectively. The latter was reflected in matrix metalloproteinase activities detected in the organ storage solution. Preliminary findings suggest the promotion of PPARgamma-regulated genes may exert protection from ischemia.

Conclusion:
Tissue collagen loss, proteolytic gene expression, and associated extrinsic proteolytic activity may serve to assess graft quality for the promotion of UTX in DCD settings.

769

TG. Donati[2], F. Ortelli[2], A. Protonotarios[3], Q. Chen[2], M. Hebeisen[1, 2], NE. Winkler[2], G. Montrasio[3], K. Savvatis[3], PAS. Olsen[4], C. Brunckhorst[2], F. Duru[2], AM. Saguner[2], PM. Elliott[3], KH. Haugaa[4], FC. Tanner[2]

Right ventricular outflow tract diameter for diagnosis of arrhythmogenic right ventricular cardiomyopathy

Department of Biostatistics, Epidemiology, Biostatistics and Prevention Institute, University of Zurich, Zurich, Switzerland[1], Department of Cardiology, University Heart Center, University Hospital Zurich and University of Zurich, Zurich, Switzerland[2], Inherited Cardiovascular Disease Unit, St Bartholomew's Hospital, London, UK[3], ProCardio Centre for Innovation, Department of Cardiology, Oslo University Hospital, Rikshospitalet, Oslo, Norway[4]

Introduction:
Enlargement of the right ventricular outflow tract (RVOT) is a key phenotypic feature of arrhythmogenic right ventricular cardiomyopathy (ARVC). Nevertheless, it is uncertain a) whether ARVC can cause isolated RVOT dilatation in general or in certain genotypes, b) which RVOT diameter shows the best properties for diagnosis of ARVC, and c) whether RVOT diameters exhibit added diagnostic value over the generally recommended basal right ventricular end-diastolic diameter (RVEDD).

Methods:
This study included patients with genetic testing and fulfilling the revised 2010 Task Force Criteria for definite ARVC. Participants were recruited from three prospective ARVC registries. Healthy asymptomatic subjects served as controls. Four RVOT diameters (Figure 1), RVEDD, and right ventricular end diastolic area (RVEDA) were measured offline and indexed to body surface area (BSA). Isolated RVOT dilatation was defined as RVOT diameter above the upper reference limit without concurrent RVEDA enlargement. Receiver operating characteristic (ROC) curves were used to compare the diagnostic properties of each diameter.

Results:
A total of 370 ARVC patients and 100 healthy subjects were enrolled. All RVOT diameters were larger in ARVC patients compared to controls (mean (SD) RVOT2/BSA: 19.6 (4.0) mm/m2; control: 16.5 (2.4) mm/m2). A dilated RVOT occurred in 189 (51%) and an isolated dilatation in 66 (18%) of patients. The percentages of isolated dilatation within specific genotypes were as follows: 13% PKP2, 23% DSP, 12% DSG2, 26% others, and 20% gene-elusive. All RVOT diameters showed similar diagnostic performance [RVOT2/BSA: Area under the curve (AUC) 0.75 (95% CI: 0.7–0.8)] and were comparable to RVEDD/BSA [AUC 0.70 (95% CI: 0.65 – 0.75)], although RVEDD/BSA exhibited the lowest point estimate (Figure 2).

Conclusion:
An isolated RVOT dilatation is observed in almost 20% of patients regardless of the genotype. All RVOT diameters showed similar diagnostic properties and were at least as useful as RVEDD.

770

TG. Donati[2], F. Ortelli[2], A. Protonotarios[2], Q. Chen[2], M. Hebeisen[1, 2], NE. Winkler[2], D. Cener[2], G. Montrasio[3], K. Savvatis[3], PAS. Olsen[4], C. Brunckhorst[2], F. Duru[2], AM. Saguner[2], PM. Elliott[3], KH. Haugaa[4], FC. Tanner[2]

Prognostic proprieties of echocardiographic right ventricular outflow tract diameter in arrhythmogenic right ventricular cardiomyopathy

Department of Biostatistics, Epidemiology, Biostatistics and Prevention Institute, University of Zurich, Zurich, Switzerland[1], Department of Cardiology, University Heart Center, University Hospital Zurich and University of Zurich, Zurich, Switzerland[2], Inherited Cardiovascular Disease Unit, St Bartholomew's Hospital, London, UK[3], ProCardio Centre for Innovation, Department of Cardiology, Oslo University Hospital, Rikshospitalet, Oslo, Norway[4]

Introduction:
Right ventricular outflow tract (RVOT) dilatation is a key phenotypic feature of arrhythmogenic right ventricular cardiomyopathy (ARVC). It is not known whether the echocardiographic RVOT diameter predicts adverse cardiovascular events.

Methods:
This study included patients with genetic testing and fulfilling the revised 2010 Task Force Criteria for definite ARVC. Participants were recruited from three prospective ARVC registries and categorized according to a primary or secondary prevention situation. The outcome was defined as the first occurrence of sustained ventricular arrhythmia (VA) or death. The RVOT diameter was indexed to body surface area (BSA) and Cox regression models were used to evaluate its association with outcome.

Results:
331 ARVC patients with mean age 47 (16.2) years, 73% in primary prevention, and median follow-up of 6.8 [3.9-10.5] years were included. Mean RVOT/BSA diameter was 19.6 (4.1) mm/m2. Univariable regression revealed a strong association between RVOT/BSA and increased risk of VA (hazard ratio (HR) 1.07 [1.02-1.13], p-value 0.003) or death (HR 1.33 [1.24-1.42], p-value <0.001). Multivariable models demonstrated that the association with VA was independent of LVEF (HR 1.08 [1.03-1.14], p-value 0.003), but not RV fractional area change (FAC) (HR 1.02 [0.96-1.08], p-value 0.506) or RV basal end-diastolic diameter (EDD) (HR 1.03 [0.97-1.10], p-value 0.355), while the association with death was independent of LVEF, RVFAC, and RVEDD (all p-values <0.001). In primary prevention, RVOT/BSA was marginally associated with VA (HR 1.07 [1.00-1.16], p-value 0.050), but strongly with death (HR 1.34 [1.22-1.47], p-value <0.001). In secondary prevention, RVOT/BSA was not associated with VA (HR 1.00 [0.93-1.07], p-value 0.968) but with death (HR 1.29 [1.13-1.48], p-value <0.001).

Conclusion:
Patients with definite ARVC and larger RVOT/BSA diameter are at increased risk of adverse events during follow-up. In patients with definite ARVC, RVOT/BSA diameter is useful for event prediction in both primary and secondary prevention.

771

E. Parietti[2], D. Bivona[1], A. Tarnutzer[2], D. Bongiorno[1], N. Musso[1], S. Stefani[1], S. Mairpady Shambat[2], S. Zinkernagel[2]

Assessment of Staphylococcus aureus phenotypic heterogeneity mediated by small colony variant formation

Department of Biomedical and Biotechnological Sciences (BIOMETEC), Section of Microbiology, University of Catania, Catania, Italy[1], Department of Infectious Diseases and Hospital Epidemiology, University Hospital Zurich, University of Zurich, Zurich, Switzerland[2]

Introduction:
S. aureus small colony variants (SCVs) represent a subpopulation of bacteria, which acquired mutations in genes involved in metabolism, leading to an extended generation time compared to their parental strain. SCVs are able to persist intracellularly in nonprofessional phagocytes and are often difficult to eradicate with antibiotics alone resulting in recurrent infections. The aim of this project was to investigate the capacity of S. aureus SCV to adapt to the stressful environment in the host and antibiotics. To this end, we compared three clinical S. aureus strains isolated from a patient with chronic ankle osteomyelitis: the wild-type (WT) IS1, its naturally occurring counterpart SCV-IS2, and the normal colony size-IS3 isolated after four months of antibiotic treatment.

Methods:
All S. aureus strains were genotypically characterized by whole genome sequencing with short and long reads. For the phenotypical characterization, colony size on blood agar plates and growth in liquid culture were analyzed. To characterize the stress response, survival of bacteria and antibiotic tolerance capacity was measured after 3 days of pH5.5 stress or after extended nutrient deprivation (1, 3, 6 days).

Results:
The three strains were identified as MSSA-ST1. A point mutation with deletion in a gene encoding for a cysteine hydrolase was found in SCV-IS2 and IS3 strains. A comparable growth rate of the three strains were observed, but an extended lag-phase for SCV-IS2 compared to WT-IS1 and IS3 was identified. After 3 days of pH-stress, the survival rate of the three strains was comparable, but a higher antibiotic tolerance was measured in SCV-IS2 and IS3 as compared to WT-IS1. A higher antibiotic tolerance in SCV-IS2 and IS3 was observed also after extended nutrient deprivation.

Conclusion:
The SCV-IS2 and IS3 showed a higher capacity to adapt to environmental stress leading to an increased antibiotic tolerance. The genetic mutation in the cysteine hydrolase resulting in a truncated protein might be responsible for the observed phenotype. Nevertheless, further studies are needed to better assess the role of this mutation in SCV formation and persistence.

772

IM. Bugueno[6], V. Platania[5, 6], G. Alastra[4, 6], F. Machla[3, 6], N. Tavernaraki[5, 6], S. Svanberg[1], K. Kodonas[2, 6], P. Dittrich[1], TA. Mitsiadis[5, 6]

Development of tooth-on-chip models for simulating human dental tissues

Department of Biosystems Science and Engineering, ETH Zürich, Mattenstrasse 26, 4058 Basel, Switzerland[1], Department of Endodontology, School of Dentistry, Aristotle University of Thessaloniki, Thessaloniki, Greece[2], Department of Prosthodontics, Tissue Engineering Core Unit, School of Dentistry, Faculty of Health Sciences, Aristotle University of Thessaloniki, Thessaloniki, Greece[3], Department of Veterinary Medical Sciences, University of Bologna, 40126 Bologna, Italy[4], Foundation for Research and Technology—Hellas (FORTH), University of Crete, 700 13 Heraklion, Greece[5], Orofacial Development and Regeneration, Institute of Oral Biology, Faculty of Medicine, Centre of Dental Medicine, University of Zurich, 8032 Zurich, Switzerland[6]

Introduction:
Tooth pathologies, including genetic conditions, trauma, caries, periodontal diseases, and oral cancer, affect a large portion of the global population and place a significant burden on healthcare systems. Current treatments primarily replace damaged dental tissues with inert materials, leading to the loss of tooth vitality and reduced functionality. Preserving tooth vitality is crucial. Dental mesenchymal stem cells (DMSCs), particularly dental pulp stem cells (DPSCs), have been extensively studied for their regenerative potential. However, DPSCs show limited ability to regenerate dentin, especially after damage from caries or trauma. Efforts are ongoing to harness DPSCs for regenerating the dentin-pulp complex and restoring tooth function. Despite progress, dental regenerative therapies remain far from clinical use due to a lack of understanding of pulp biology and the absence of platforms to model human dental pulp. This gap limits the development of effective treatments for dental diseases. *In vitro* tools that mimic human dental tissues would be invaluable for regenerative dentistry, drug testing, and pre-clinical studies. Organs-on-chips are microfluidic devices that allow us to culture living cells in perfused chambers, and can mimic tissue microenvironments by regulating factors like fluid flow, cell patterns, and mechanical forces, in a controlled setting.

Methods:
We aimed to develop an innovative tool for generating and regenerating human dental pulps using advanced organ-on-a-chip technology. Our “pulp-on-a-chip” model incorporates human dental pulp stem cells (hDPSCs) along with vascularization, provided by human endothelial cells (HUVEC and HUAEC), and innervation, provided by primary mouse sensory trigeminal ganglia cells. We studied the crosstalk between hDPSCs, vascularization, and innervation using immunostaining, qPCR, various confocal microscopy techniques, and we performed single-cell RNA sequencing to dissect the cellular composition and heterogeneity within the pulps-on-chips. We also integrated human trigeminal sensory neurons (hTGNs), derived from induced pluripotent stem cells (iPSCs) generated from hDPSCs, and immortalized human dental-pulp-specific endothelial cells (hDPECs).

Results:
These microfluidic devices provide the optimal conditions for the formation and analysis of extensive vascular and neural networks, mimicking the physiology of the dental pulp. Furthermore, it allowed the comparative analysis of gene expression at single cell resolution, with the studies carried out on human dental pulps. Our multicellular models in the microfluidic devices showed a similar heterogeneity and cellular composition to the dental pulps from extracted human teeth.

Conclusion:
In addition, this work provides a cornerstone for more complex and specialised microfluidic dental models, which are needed to unravel complex oral diseases, and to evaluate potential new molecules in regenerative dentistry. This model closely mimics the physiology of the dentin-pulp complex and will be validated by studying human tooth responses to pharmacological treatments and microbial infection.

773

C. Meisel[3], R. Destefani[3], I. Valookkaran[3], A. Batavia[1], F. Catto[2], N. Rupp[1], T. Mitsiadis[3], C. Porcheri[3]

The Notch1/Delta-like-4 axis is crucial for the initiation and progression of Oral Squamous Cell Carcinoma

Department of Pathology and Molecular Pathology[1], IMAI MedTech[2], Institute of Oral Biology[3]

Introduction:
Head and neck squamous cell carcinoma (HNSCC) is the sixth most common type of cancer, annually affecting 850.000 people worldwide. Among the different types of HNSCC, oral squamous cell carcinoma (OSCC) is the most common malignant neoplasm affecting the oral cavity. Although modern multimodal therapy has improved clinical management of this disease, tumor recurrence and distal metastasis correlate with poor prognosis, with a median overall survival of ten months. Screenings via exome sequencing identified the Notch pathway as a major mutation hotspot, with mutations leading to truncation, insertion-deletion and missense. Although frequently mutated in OSCC, the precise role of Notch in the initiation and development of OSCC remains largely unknown, with contrasting results that are supportive of either an oncogenic or a tumor-suppressive role

Methods:
We utilized transgenic animal models in combination with advanced confocal, light-sheet, live imaging microscopy and Next-Generation Sequencing to investigate Notch-dependent changes during OSCC progression. Ad-hoc Notch interference was additionally assessed in mice and patient-derived cells to elucidate the functional impact of pathway inhibition.

Results:
In this study we demonstrated that the Notch signalling pathway plays a crucial role in the development and progression of OSCC. Specifically, we found that during disease progression, the Notch1 receptor establishes a preferential interaction with the Delta-like-4 ligand, while the Jagged1 ligand is lost in the malignant overgrowth. This ligand selection begins in the early hyperplastic stage and persists through the most advanced, invasive stages. Mechanistically, Delta-like-4 induces the downregulation of Notch effectors within the Hey family, ultimately promoting cell undifferentiation and mobility.

Conclusion:
Our findings highlight the significance of the Notch1/Delta-like-4 signalling axis as oncogenic driver in OSCC. Specific components of this pathway, implicated since the onset of the disease, show great promise as early diagnostic markers. Moreover, targeted inhibition of the pathway has demonstrated potential in suppressing tumor growth and cancer cell migration. These results mark a significant advancement in our understanding of OSCC and provide a solid basis for developing future diagnostic and therapeutic strategies against oral cancer.

774

C. Dollé[1], T. Tutumlu[1], J. Nemeth[1]

Multiomic Analysis of Bacille Calmette-Guérin (BCG)'s Immunomodulatory Effects in People with HIV

Department of Infectious Diseases and Hospital Epidemiology[1]

Introduction:
Despite the success of antiretroviral therapy (ART) in controlling HIV-1 infection, a definitive cure remains elusive due to the persistence of the latent HIV-1 reservoir. Evidence suggests that coinfection with Mycobacterium tuberculosis (Mtb) and HIV-1 is associated with reduced opportunistic infections and a lower setpoint viral load, highlighting a complex interaction between the immune system and these pathogens. To deepen our understanding of the interplay between the immune system, mycobacterial infection, and HIV-1 persistence, the BELIEVE trial, a phase 2 randomized, double-blind, placebo-controlled study, investigates the potential of Bacille Calmette-Guérin (BCG) vaccination to modulate immune responses in people with HIV (PWH).

Methods:
The trial involves 55 participants from the Swiss HIV Cohort Study (SHCS) and systematically assesses the effects of BCG vaccination on virological and immunological parameters, including the latent HIV-1 reservoir. Our approach incorporates comprehensive systems methodologies - high-dimensional flow cytometry, proteomics, transcriptomics, and systems serology - combined with advanced computational analyses, such as Bayesian networks and machine learning, to assess the immune system's response to BCG vaccination.

This integrative analysis aims to uncover immune correlates and molecular signatures that illuminate BCG's role as a potential immunomodulatory agent in PWH. By leveraging diverse datasets, including immune cell populations, antibody responses, latent reservoir dynamics, and clinical data, we seek to evaluate the broader impacts of BCG vaccination on HIV-1 latency and immunity.

Results:
tba

Conclusion:
tba

775

W. Barcik[1], M. Soyka[1], W. Staiger[1], S. Brugger[1]

The role of bacteria-derived histamine in allergy associated airway diseases

University Hospital Zurich[1]

Introduction:
The prevalence of allergic diseases is rising dramatically and affects up to 40% of the population worldwide, with respiratory allergies being among the most common ones. Chronic rhinosinusitis (CRS) is an inflammatory disease of the upper respiratory tract (URT), characterized by ciliary dysfunction, mucus overproduction, and mucosal edema resulting. The inflammatory process can induce tissue remodeling such as nasal polyp formation. Type 2-CRS and other respiratory conditions associated with allergic reactions are complex diseases presenting with common etiologies of inflammation and/or infections. Histamine that is secrete by host cells during allergic reactions is well recognized for its effects in the immediate type (type I) hypersensitivity response, however, the relevance of altered histamine levels in disease conditions such as type 2 chronic rhinosinusitis is less well understood. The presence of histamine-secreting bacteria has been well documented in foods, but their presence and mechanisms of action within the host has just started to be investigated. I have previously discovered that bacteria capable of secreting histamine are present in the human gastrointestinal tract indicating that mast cells and basophils should not be considered as the only sources of histamine in the human body. Surprisingly, there is still a lack of data on the mechanisms by which the bacterial microbiota of the URT influence respiratory allergic diseases.

Methods:
To identify and characterize the URT bacterial microbiota composition in the context of histamine producers we collected nasal swabs from healthy volunteers and nasal secretions taken from patients with type 2 CRS and control subjects. To check the amount of secreted bacterial histamine we determined the level of histamine secreted to the supernatant by inoculating the samples in BHI media supplemented with 10% FCS and 1% histidine and incubating the culture for 72 h in 37°C. The culture supernatant was filter sterilized and the measurement of secreted histamine was done by the UPLC-DAD method.

Results:
Initially, to optimize the methodology, a small cohort from healthy volunteers was screened. Bacteria isolated from nose swabs belonged to Lactobacillales, Mycobacteriales, Bacillales, Pseudomonadales, Streptomycetales, Micrococcales and Propionibacteriales order. Out of 30 strains, we identified one strain of Staphyloccocus capitis that in in-vitro conditions secreted more histamine to the supernatant than positive controls. Afterwards, using nose secretion cohort, we have inoculated whole mucus samples in rich liquid media, incubated for 72h 37°C to allow whole bacteria consortiums from each sample to grow. In screened nasal samples from CRS patients and control subjects by UPLC-DAD, we have observed that the amount of histamine secreted by bacteria was lower in the CRS type 2 patients compare with control subjects.

Conclusion:
Bacteria that are able to produce and secrete histamine are present in URT. Even though it might seem surprising that bacterial histamine level is lower in CRS type 2 patients compared to control subjects, the outcome is in line with my previous finding. During my earlier research, I have observed a significant decrease in the number of inflammatory cells in bronchoalveolar lavage in animals' gavaged with bacteria that secrete histamine, compared to positive control. The histamine secretion from bacteria most probably have influence on allergic responses and can have immunological consequences, however the effects required detailed further studies.

776

S. Hertegonne[1], A. Gomez-Mejia[1], A. Tarnutzer[1], CC. Chang[1], A. Kempchinksy[1], E. Parietti[1], S. Mairpady Shambat[1], A. Zinkernagel[1]

Stress adapted Staphylococcus aureus modulates neutrophil effector response for its survival during infection

Department of Infectious Diseases and Hospital Epidemiology, University Hospital Zurich, University of Zurich, Zurich, Switzerland[1]

Introduction:
Staphylococcus aureus is a pathobiont that intermittently colonizes and causes mild to severe invasive infections in humans. *S. aureus* infections are often difficult-to-treat as a result of emergence of antibiotic resistance and tolerance mechanisms. Antibiotic tolerance is a transient phenomenon where the bacterial population can withstand high antibiotic concentrations which are otherwise lethal. Under certain conditions during infection due to host mediated or antibiotic mediated stress, a subpopulation enter the dormant phase able to survive and tolerate high concentrations of antibiotics due to the formation of so-called persister cells. The inability to clear persistent bacteria leads to chronic and relapsing infections, characterized by recurring abscess formation. To treat abscesses, surgical debridement is needed, which can be a challenge and adds to the overall health care associated costs. *S. aureus* abscesses are characterized by high infiltration of polymorphonuclear neutrophils (PMNs). PMNs are arguably the most important primary cellular defence against bacterial infections. PMNs combat invading pathogens via a plethora of effector functions, including phagocytosis, production and release of reactive oxygen species, and degranulation. Patients with hereditary or acquired disorders leading to abnormal PMN functions or numbers, have been shown to suffer from recurrent and severe *S. aureus* infections. While there are a vast number of staphylococcal virulence factors directly and indirectly targeting PMN recognition and function, the interplay between PMNs and *S. aureus* inside abscesses is still not well understood.

Methods:
We investigated how acid stress adapted *S. aureus* modulates the PMN response towards better bacterial survival inside the abscess milieu. To achieve this, we used PMN *ex vivo* co-culture model. Multi-parametric flow cytometry and confocal microscopy were used to quantify kinetics and dynamics of PMN functional responses, such as phagocytosis, degranulation, and regulated cell death. Cytokine levels were measured to characterize the immune response. Our *ex vivo* results were confirmed using an *in vivo* mouse abscess model.

Results:
We observed that PMNs showed reduced phagocytosis of stress adapted *S. aureus*, resulting in overall decreased bacterial killing. Moreover, PMNs became more activated and showed rapid release of the contents from primary granules, both *ex vivo* and *in vivo*. Simultaneously, higher surface expression of phosphatidylserine was observed, indicating that the cells were apoptotic. However, we observed no differences in caspase 3/7 activity, nor did we see changes in the production of pro-inflammatory or pro-apoptotic chemokines and cytokines. Furthermore, we observed this PMN response only in reaction to the actual bacteria and not the secreted virulence factors. Our preliminary results suggest that this reaction is triggered by changes in the cell wall and/membrane of stress adapted *S. aureus*.

Conclusion:
Taking these results together, we hypothesize that acid stress adapted *S. aureus* induces rapid and extreme degranulation, after which the PMNs enter an inert state and are unable to perform their other effector functions or undergo apoptosis. These findings provide unique insights into differential functional responses of PMNs in an abscess interacting with stress adapted *S. aureus*. Further understanding of the interplay will allow to develop more effective therapeutic strategies to tackle pyogenic *S. aureus* infections and may in the future allow to avoid surgical interventions resulting in increased morbidity and mortality.

777

P. Laphanuwat[1], E. Camarillo-Retamosa[1], C. Seiler[1, 2, 3], C. Ospelt[1]

Unveiling Synovial Fibroblast Morphology Using Cell Painting Imaging for Drug Screening

Center of Experimental Rheumatology, Department of Rheumatology, University Hospital Zurich, University of Zurich[1], Department of Advanced Computing Sciences, Maastricht University, Maastricht, The Netherlands[2], Mathematics Centre Maastricht, Maastricht University, Maastricht, The Netherlands[3]

Introduction:
Synovial fibroblasts are recognized as major players in the pathogenesis of rheumatoid arthritis (RA). Their interactions within the joint microenvironment trigger various immune responses and lead to joint deterioration. Thus, targeting synovial fibroblasts is a potential new therapeutic option for RA. Currently, no preclinical high-throughput screening test exists to evaluate how drug candidates affect the activated phenotype of synovial fibroblasts. High-content imaging (HCI) provides a powerful solution by enabling comprehensive assessment of drug-induced phenotypic and functional changes.

Methods:
Age- and gender-matched synovial fibroblasts from shoulder joints (OA n=8, RA n=8) were analyzed using a modified Cell Painting protocol (Bray et al., 2016) to visualize key cellular structures. Images were acquired with the CellInsight™ CX7 (Thermo Fisher) system, extracting ~1,200 cellular features via CellProfiler. To validate the model, senescence was induced in fibroblasts using x-ray irradiation (10 Gy) and inflammatory stimulation with IFNα, IL1, TNF, LPS, or PIC. Fibroblasts were treated with structure-targeting drugs (CHX, MG132, PAB, CPT, PTX) with or without IL1 for 24 hours, using DMSO as a control. All doses were non-toxic. Data were split into gender- and joint-matched training and test sets, and a random forest classifier was used for feature-based classification. Receiver operating characteristic (ROC) curves assessed model performance.

Results:
The validation experiment showed accurate prediction of senescence in healthy and systemic sclerosis skin fibroblasts as well as OA synovial fibroblast based on morphological changes. Synovial fibroblasts were then stimulated with inflammatory cytokines, and our classifier also successfully detected morphological differences between stimulated and unstimulated control synovial fibroblasts. IL1 and PIC were found to induce the most pronounced alterations in cell morphology. IL1 was co-administered with the drug treatments individually to amplify morphological alterations. Compared to the DMSO control, the cytoskeleton-interfering drug PTX enhanced our ability to distinguish between resting and active states of cells based on morphological differences. DNA topoisomerase inhibition (CPT), protein translation inhibition (CHX) or proteasome inhibition (MG), significantly impaired the ability of the model. This indicated that our model might predict changes based on DNA/RNA content and proteasome activity under IL1 stimulation. We also evaluated the model's ability to distinguish between resting stage RA and OA synovial fibroblasts. However, the model's performance in this context was no better than random chance.

Conclusion:
We developed a valid classifier pipeline in synovial fibroblasts that sensitively detected morphological changes in different activation states of synovial fibroblasts. Although the classifier was unable to differentiate RA from OA synovial fibroblasts, morphological changes induced under inflammatory conditions were sufficient for reliable prediction of an activated cell state. We propose our HCI approach as a tool to assess the functional states of synovial fibroblast that can be used as a reference for future high-throughput, drug-screening applications.

778

TB. Beck[1], E. Keller[1]

ICUCockpit: IT infrastructure for the collection of multi-modal, high-resolution patient data and online validation of predictive algorithms in a live data stream

Institut für Intensivmedizin[1]

Introduction:
The introduction of AI models trained on ever-growing datasets is set to revolutionize healthcare by enabling more precise diagnostics and personalized treatment plans within hospitals. This evolution will enhance patient outcomes and streamline clinical workflows, effectively bridging the gap between model development and practical implementation. However, most of the predictive models developed for critical care settings are not implemented in practice. A major reason is that offline validation of models is often not indicative of successful clinical deployment. However, regulatory requirements make it difficult to obtain rapid feedback on clinical performance.

Methods:
To this end, we present the ICUCockpit, a self-hosted IT infrastructure developed at the Neurosurgical Critical Care Unit at the University Hospital Zurich. It supports the integration and collection of multi-modal patient data from heterogeneous data sources, such as medical devices, electronic health records, and lab results. Uniquely, the ICUCockpit allows for the collection of high-resolution waveform data, such as from electrocardiography (ECG), electroencephalography (EEG), artificial ventilation, and multiple biosensors. The patented innovative data streaming platform supports a seamless integration of ML-based predictive algorithms into the live data stream to enable online validation and produce clinical decision-support. Additionally, an integrated dashboard enables point-of-care as well as remote monitoring of patient condition, by using data visualizations and a privacy-preserving webcam feed from the bedside.

Results:
Currently, we collect data from two critical care units at the University Hospital of Zurich and an extension to account for pediatric cases is planned. As of end of 2024, data from over 2,700 patients with more than 300,000 monitoring hours has been collected. We continuously extend the set of available patient signals and develop methods to extract additional information from unstructured data, such as clinical notes or video streams. Our database has been used for the development of various algorithms for use in a critical care setting, such as neurologic prognostication, detection of epileptic seizures, or false alarm reduction. Based on the live data stream of ICUCockpit, we conduct online validation of developed ML-based algorithms, such as probability prediction of delayed cerebral ischemia (DCI) and incidental SARS-CoV-2 infection, without affecting clinical decision-making (“silent validation”). Initial silent validation results for DCI prediction showed that while the number of true positives and false negatives was almost equal with and without algorithm, the number of false positives was reduced by 164 in decision making with algorithm support ($p<0.01$). Further, combining the total number of additional diagnostics were reduced by more than 15%.

Conclusion:
ICUCockpit can offer services for various stakeholders. It allows for offline and online evaluation of ML-based algorithms to fulfil regulatory compliance and follow guideline principles outlined for medical AI development, such as continuous monitoring of model performance after deployment. Further, our IT infrastructure can be locally deployed and customized to allow for secure and ethically sound data collection for clinical research, with a unique focus on high-resolution data (i.e., waveforms). Finally, our interdisciplinary approach ensures both clinical effectiveness and meaningful integration into clinical workflows for any predictive algorithm. ICUCockpit is supported by two SNF projects, one within NFP 75.

779

M. Labarile[5, 10], M. Huber[10], K. Leuzinger[1], M. Perreau[3], A. Ramette[9], S. Yerly[11], M. Cavassini[7], M. Stöckle[4], A. Rauch[2], A. Calmy[11], J. Notter[6], E. Bernasconi[8], HF. Günthard[5, 10], C. Pasin[5, 10], RD. Kouyos[5, 10]

HIV Transmission Dynamics in the Swiss HIV Cohort Study

Clinical Virology, University Hospital Basel, Basel, Switzerland[1], Department of Infectious Diseases, Bern University Hospital, University of Bern, Bern, Switzerland[2], Division of Immunology and Allergy, Lausanne University Hospital, University of Lausanne, Lausanne, Switzerland[3], Division of Infectious Diseases and Hospital Epidemiology, University Hospital Basel, University Basel, Basel, Switzerland[4], Division of Infectious Diseases and Hospital Epidemiology, University Hospital Zurich, Zurich, Switzerland[5], Division of Infectious Diseases, Cantonal Hospital St Gallen, St Gallen, Switzerland[6], Division of Infectious Diseases, Lausanne University Hospital, Lausanne, Switzerland[7], Ente Ospedaliero Cantonale Lugano, University of Geneva and University of Southern Switzerland, Lugano, Switzerland[8], Institute for Infectious Diseases, University of Bern, Bern, Switzerland[9], Institute of Medical Virology, University of Zurich, Zurich, Switzerland[10], Laboratory of Virology and Division of Infectious Diseases, Geneva University Hospital, University of Geneva, Geneva, Switzerland[11]

Introduction:
HIV incidence in Switzerland has declined significantly since the 1990s but has remained stable for the last years. To further lower transmission, it is essential to understand the epidemiological context within which these transmissions happen on a fine-grained level. To this end, we used the Resistance Database of the Swiss HIV Cohort Study (SHCS) and applied a distance-based clustering approach to identify and characterize HIV transmission clusters in Switzerland.

Methods:
We collected 28,746 HIV-pol sequences from 14,229 people with HIV (PWH) in the SHCS, which contain all resistance tests and retrospective sequences obtained for the whole cohort. We created a network of sequences with HIV-TRACE and a genetic distance threshold of 0.01 (masking known drug resistance mutations). We report trends in the way the overall network grows over time and describe qualitative patterns on the level of individual clusters.

Results:
We found 1,052 distinct extant clusters as of 2024, made up of 6,849 individuals (48.1%). The remaining 7,380 individuals (51.9%) had no recorded sequence that was within a genetic distance of 0.01 of someone else's sequence. The growth of clusters over time was very heterogeneously distributed across clusters, with 45 (5.3%) clusters accounting for half of all cluster growth from 2014 to 2019 (Figure 1A). Similarly, 25 (2.5%) clusters accounted for half of all cluster growth since 2019 (10 of which were also in the previous 45). Of these 60 fast-growing clusters, 47 contained mostly MSM. For one cluster, no plausible narrative of transmission could be established, as it was a continuously growing cluster of almost exclusively males reporting heterosexual route of transmission, who were spread out over different regions of the country. We investigated whether the individuals that entered the network over time were connected to people with detectable viral load, i.e., had a recent viral load measurement ≥1000 copies/µl (Figure 1B). This proportion dropped over time from 56.6% in 2010 to 20.5% in 2020 but stayed far above the cohort-wide proportion of RNA measurements ≥1000 copies/µl (12.6% and 1.8%, respectively), showing that diagnosed, SHCS-enroled PWH with viremia contribute to HIV transmission. However, 776 (25.1%) of cluster growth events happened with all the connected individuals having undetectable viral load, indicating that the source of the transmission might either be an undiagnosed PWH or not enrolled in the SHCS.

Conclusion:
Half of the growth of HIV clusters in Switzerland is concentrated in 45 (4.5%, 2014-2019) or 25 clusters (2.4%, since 2019). The significant amount of new cluster members that, at the time of their diagnosis, did not cluster with people with detectable viral load indicates that these transmission events might

come from outside the network. Though the proportion of newly enrolled PWH that cluster with people with recent viremia has dropped over time, it still plays a role in ongoing transmission. Together, this approach enables the surveillance and near real-time analysis of HIV transmission patterns in Switzerland to inform public health interventions at the community-level and emphasizes the importance of continued enrolment of PWH into longitudinal studies.

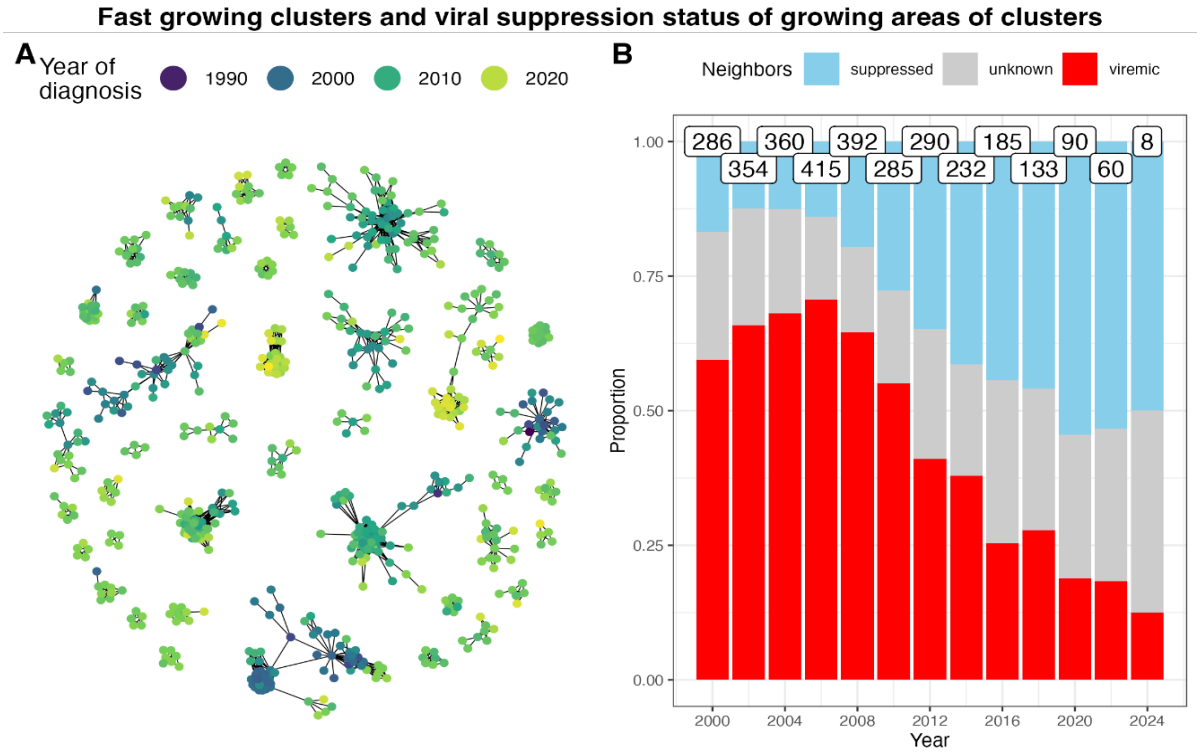

Figure 1: (A) Clusters that accounted for half of all cluster growth between 2014 and 2019, except the largest cluster, which is not shown due to space limitations. Nodes are individuals, colored by the year of their HIV diagnosis. Two nodes are connected by an edge if there is at least one pair of HIV-pol sequences, one from each individual, such that the two sequences are within a genetic distance of 0.01 according to the TN93 model. (B) Status of neighboring individuals when a new person enters the HIV network and clusters with at least one other individual.

780

J. Feiereisen[3], R. Boulos[3], Y. Kalbas[4], H-C. Pape[4], O. Dzemali[1, 2, 3], H. Rodriguez Cetina Biefer[1, 2, 3]

Traumatic Intracranial Hemorrhage in Mechanical Heart Valve Patients: A Retrospective Analysis of Incidence and Outcomes

Center for Experimental and Translational Cardiology (CTEC), University of Zurich, Zürich, Switzerland[1], Clinic for Cardiac Surgery, City Hospital Zurich—Triemli, Zürich, Switzerland[2], Clinic for Cardiac Surgery, University Heart Center, Zurich, Switzerland[3], University Traumatology Center, Zurich, Switzerland[4]

Introduction:
The current ESC, EACTS, and ACC/AHA guidelines recommend mechanical heart valve (MHV) implantation for aortic valve replacement and mitral valve replacement for patients younger than 60 years. While MHVs offer durable solutions, they require lifelong anticoagulation with warfarin, thereby increasing the risk of bleeding complications such as intracranial hemorrhage. This study aimed to evaluate the incidence and outcomes of traumatic intracranial hemorrhage in patients with MHV and to investigate the influence of long-term anticoagulation on post-traumatic events.

Methods:
We conducted a retrospective study at the University Hospital Zurich, analyzing all MHV interventions performed between 1988 and 2022. We included patients who experienced traumatic events, including isolated and combined procedures (e.g., double valve interventions, concurrent coronary artery bypass grafting). We recorded the incidence of traumatic brain injury (TBI), cerebral hemorrhage, and the need for surgical intervention. After 30 days, we evaluated the therapeutic anticoagulation status and associated outcomes.

Results:
A total of 64 MHV recipients who had experienced traumatic events were identified (mean age 53.98 years; 67% male). Most patients (70%) presented with a single traumatic event, whereas 11% experienced three or more events. Of the 42 patients (66%) with TBI, 28 (44%) had cerebral hemorrhage. Neurosurgical intervention was required in nine individuals, with only one case of poor neurological outcome. Postoperative bleeding occurred in seven patients (14%), with only one requiring vitamin K administration. Overall, 94% of patients achieved favorable outcomes after conservative management.

Conclusion:
Our findings revealed a low incidence of intracranial hemorrhage related to anticoagulation in MHV patients following trauma. Conservative treatment strategies were effective in most cases. These results underscore the importance of individualized patient selection and risk assessment to optimize the bleeding and thromboembolic outcomes in this population.

781

M. Graure[1], N. Nierobisch[1], A. De Vere-Tyndall[1], V. Kana[1], P. Roth[1], M. Herwerth[1, 2, 3]

Clinical Profile and Treatment Outcome in Chronic Relapsing Inflammatory Optic Neuropathy: a Longitudinal Retrospective Study

Klinik für Neurologie, Universitätsspital Zürich[1], Klinikum rechts der Isar der TU München - Klinik und Poliklinik für Neurologie, München, Germany[2], University of Zurich - Neuroscience Center, Zürich, Switzerland[3]

Introduction:
Chronic relapsing inflammatory optic neuropathy (CRION) is a rare form of optic neuritis characterized by multiple relapses and steroid dependence. Despite its definition as a diagnosis of exclusion, recent studies have suggested that CRION is associated with myelin oligodendrocyte glycoprotein antibodies (MOG Ab). Acute treatment involves corticosteroids followed by oral tapering. Steroid-sparing maintenance immunotherapy regimens remain uncertain due to the rarity of the condition. This study aims to investigate the etiology and disease course of CRION, as well as evaluate the long-term visual outcomes associated with different therapeutic regimens.

Methods:
In this retrospective, longitudinal study, patients with recurrent optic neuritis were screened from 4179 individuals from the outpatient Neuroimmunology Clinic at the University Hospital of Zurich over the course of 11 years. Fulfilment of clinical and paraclinical diagnostic criteria for CRION were reviewed retrospectively.

Results:
Twenty-five patients were included. 64% of individuals presenting with CRION exhibited MOG Ab positivity. Cerebrospinal fluid (CSF) analysis revealed pleocytosis in 20.8% of cases, with elevated Interleukin 6 (IL-6) levels predominantly observed in MOG Ab-positive patients. Extensive optic nerve involvement was present in all MOG Ab-positive individuals and in 62.5% of seronegative individuals. Of 24 patients with final visual acuity (VA) data, 8.8% of affected eyes had VA < 0.1, and 10.8% of affected eyes had VA >0.1-<0.5. Higher numbers of optic neuritis episodes correlated with poor VA outcomes. MOG Ab-positive cases showed worse outcomes than seronegative cases. Male sex individuals had poorer outcomes compared to female individuals. Maintenance immunotherapy was administered in 15 individuals during follow-up. 5 Patients subsequently or concomitantly received more than one therapy. Rituximab was used in 10 cases (41.7%), tocilizumab in 8 cases (33.3%), azathioprine in 3 cases (12.5%), mycophenolate mofetil in 2 cases (8.3%), and cyclophosphamide and natalizumab were each used in one case (4.2%). Disease stability was most frequently observed in patients receiving therapy with tocilizumab.

Conclusion:
Patients with a CRION phenotype are in most cases MOG-Ab-positive and differ in their clinical presentation and disease course from MOG-Ab-negative CRION patients. This limits the applicability of current diagnostic criteria for treatment decisions. Early efficient therapy is important to prevent relapse associated unfavorable visual outcome. Tocilizumab emerges as a promising therapeutic option in CRION, especially in case of elevated CSF IL-6 levels.

782

A.L. Leblond[8, 12], B. Helmchen[8], M. Ankavay[6, 11], D. Lenggenhager[8, 12], J. Jetzer[8, 12], F. Helmchen[2, 12], H. Yurtsever[3], R. Parrotta[8, 12], M. Healy[8, 12], A. Pöschel[5, 12], E. Markkanen[5, 12], N. Semmo[1, 10], M. Ferrie[4], L. Cocquerel[4], H. Seeger[8], H. Hopfer[7, 9], M. Beat[8], J. Gouttenoire[6, 11], D. Moradpour[6, 11], A. Gaspert[8], A. Weber[8, 12]

HEV ORF2 protein-antibody complex deposits are associated with glomerulonephritis in hepatitis E with reduced immune status

Bern University Hospital[1], Brain Research Institute[2], Cantonal Hospital Aarau[3], Institut Pasteur de Lille[4], Institute of Veterinary Pharmacology and Toxicology[5], Lausanne University Hospital[6], University Hospital Basel[7], University Hospital Zurich[8], University of Basel[9], University of Bern[10], University of Lausanne[11], University of Zurich[12]

Introduction:
Hepatitis E virus (HEV) infection, one of the most common forms of hepatitis worldwide, is often associated with extrahepatic, particularly renal, manifestations. Extrahepatic manifestations are expected to develop either directly, by HEV infection of the respective organs or indirectly, by immunologic reactions. However, the underlying pathomechanisms are incompletely understood. Here, we report the development of a de novo immune complex-mediated glomerulonephritis (GN) in a kidney transplant recipient with chronic hepatitis E.

Methods:
We performed immunostaining, electron microscopy, and mass spectrometry after laser-capture microdissection using liver and kidney samples. Western blots and deglycosylation assays were also conducted to further characterise the HEV ORF2 capsid protein.

Results:
The HEV ORF2 capsid protein produced in excess was detected not only in the liver but also in the kidneys, especially in the glomeruli. The retrospective examination of kidney biopsies revealed a dynamic with increasing glomerular deposition of the HEV ORF2 capsid protein in the course of chronic HEV infection and in parallel with the deterioration of kidney function. Within glomeruli, HEV ORF2 capsid protein co-localised with immunoglobulin G (IgG), forming glomerular HEV ORF2 protein-IgG immune complexes. Interestingly, the glomerular HEV ORF2 capsid protein corresponds to a truncated, non-infectious, genome-free and non-glycosylated HEV ORF2 capsid protein. No productive HEV infection of kidney cells was detected. Patients with acute hepatitis E display similar but less pronounced deposits of HEV ORF2 capsid protein.

Conclusion:
Our results establish a link between the production of HEV ORF2 capsid protein and the development of hepatitis E-associated GN in the immunocompromised state. The formation of glomerular HEV ORF2 protein-IgG immune complexes discovered here provides a potential mechanistic explanation of how the hepatotropic HEV can cause variable renal manifestations. These findings directly provide a tool for etiology-based diagnosis of hepatitis E-associated GN as a distinct entity and suggest therapeutic implications.

785

D. Balun[1], S. Drack[1], S. Kling[1], H. Walt[1], H. Essig[1]

Validation of a trifold methodology for the diagnosis of oral squamous cell carcinoma in comparison to the conventional histopathological examination.

Universitätsspital Zürich[1]

Introduction:
Head and neck squamous cell carcinoma (HNSCC) is among the most common malignant tumors worldwide, accounting for 450,000 deaths in 2018. Its incidence is projected to increase by 30% by 2030. The most common subtype, oral squamous cell carcinoma (OSCC), is currently diagnosed through histopathological assessment following an invasive biopsy, which remains the gold standard. The decision to perform a biopsy is primarily based on clinical examination and the clinician's expertise. Numerous alternative methods for diagnosis such as autofluorescence, chemiluminescence, etc. have been proposed. However, the existing literature remains largely inconclusive and fails to provide significant evidence of the superiority of these methodologies. The need for new non-invasive methods of diagnosis is of interest to clinicians and patients alike. We propose such a new method in this study.

Methods:
Optical Coherence Elastography (OCE) is a novel, non-invasive imaging technique that leverages the altered physical properties of cancerous tissue to provide precise information about lesions. Complementary to this, Optical Coherence Tomography (OCT) enables the evaluation of lesion depth, which is critical for staging and treatment planning. Additionally, 5-Aminolevulinic Acid (5-ALA) administration induces the accumulation of Protoporphyrin IX (PpIX) within cancerous tissues, allowing for photodynamic detection. We propose integrating these three techniques - OCE, OCT, and photodynamic diagnostics - could serve as a less invasive alternative for OSCC diagnosis. Twenty OSCC tissue specimens routinely obtained from tumor resection surgeries will be sequentially analyzed using the three modalities. Additionally, tumor-derived organoids (n = 5) will be cultured from these specimens and subjected to the same diagnostic procedures to serve as positive controls. Histopathological analysis of both the tumor samples and organoids will reveal the extent of tumor infiltration into healthy tissue. Statistical analysis will be performed upon completion of data collection.

Results:
At the time of writing, the study is in the process of acquiring the required tissue specimens and establishing organoid cultures for further analysis. The first preliminary findings from this study are expected in early spring of 2025. Approval has been granted by the cantonal ethics committee of Zurich (BASEC-Nr. 2024-00883).

Conclusion:
This trifold, non-invasive diagnostic approach could potentially revolutionize cancer detection in a clinical setting.By reducing the need for invasive biopsies, this method could lower patient discomfort and the risk of complications such as infections and permanent tissue damage. Furthermore, this study will contribute to the existing knowledge of OSCC-derived organoid cultivation and provide new insights into the clinical applicability of OCE, OCT, and photodynamic diagnostics using 5-ALA and Hypericin.

786

Q. Chen[2], T. Donati[2], M. Hebeisen[1, 2], N. Winkler[2], J. Michel[2], B. Stähli[2], A. Kasel[2], F. Tanner[2]

A Prospective Cohort Based Preprocedural Prediction Model for One-year Survival After Transcatheter Aortic Valve Implantation

Department of Biostatistics, Epidemiology, Biostatistics and Prevention Institute, University of Zurich, Zurich, Switzerland[1], Department of Cardiology, University Heart Center, University Hospital Zurich and University of Zurich, Zurich, Switzerland[2]

Introduction:
In patients with severe aortic stenosis who are not candidates for surgery, transcatheter aortic valve implantation (TAVI) reduces all-cause mortality. However, registry data have reported a one-year mortality rate after TAVI ranging from 10% to 25%. Accurate prediction models are needed to identify patients at high mortality risk after TAVI to prevent futile interventions. This study aimed to develop and validate a pre-procedural prediction model to assess the risk of early death after TAVI.

Methods:
Patients undergoing TAVI due to severe aortic stenosis were prospectively recruited into a cohort. Eligible patients were divided into derivation and validation cohorts in a temporal manner. Four experienced cardiologists selected potential clinical and echocardiographic predictors from the baseline characteristics. A prediction model was developed using multiple logistic regression after imputing missing data. The performance of prediction model was assessed through receiver operating characteristic (ROC) curve and calibration plots to evaluate discrimination and calibration.

Results:
A total of 1,702 patients were enrolled in the study, with 1,278 patients used to develop the prediction model and 424 patients assigned to the validation cohort (Figure 1). Twelve potential predictors were incorporated into the final model. The area under the ROC curve was 0.74 (95%CI 0.70-0.78) for the derivation cohort and 0.72 (95%CI 0.64-0.81) for the validation cohort (Figure 2). Using a threshold of 0.2 to define high risk, 30% of patients classified as high risk in the validation cohort died within one year following TAVI.

Figure 1: The flowchart of patient determation

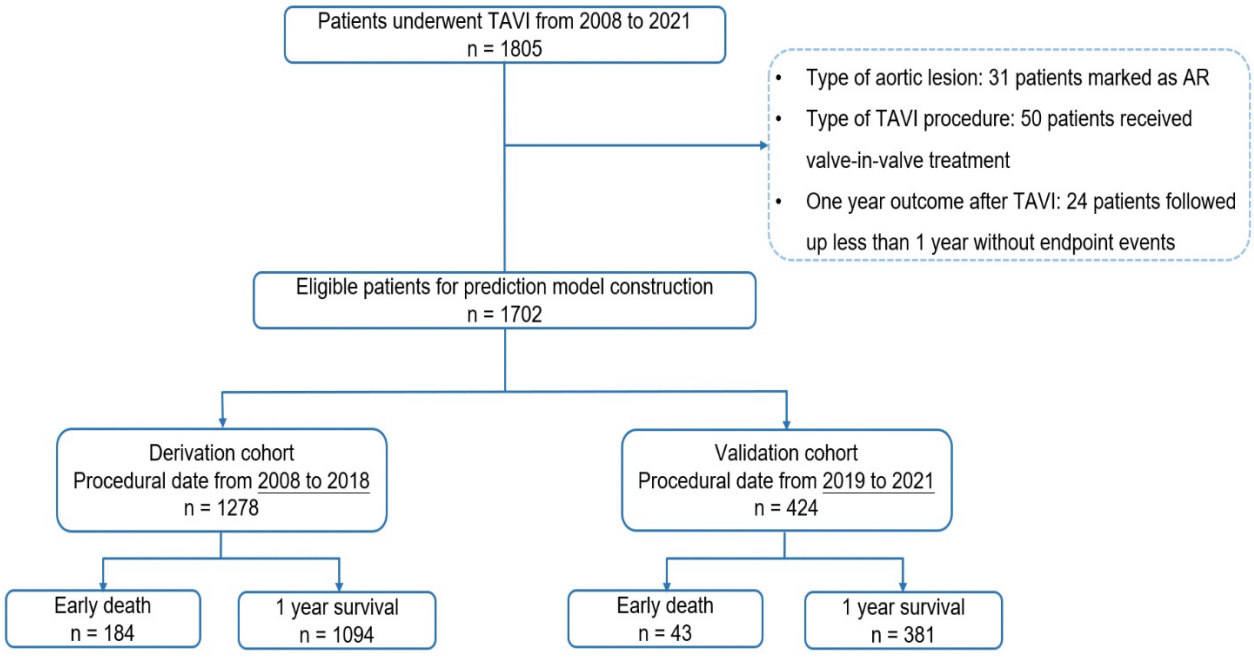

Figure 2: Discrimination and calibration of the prediction model among validation population

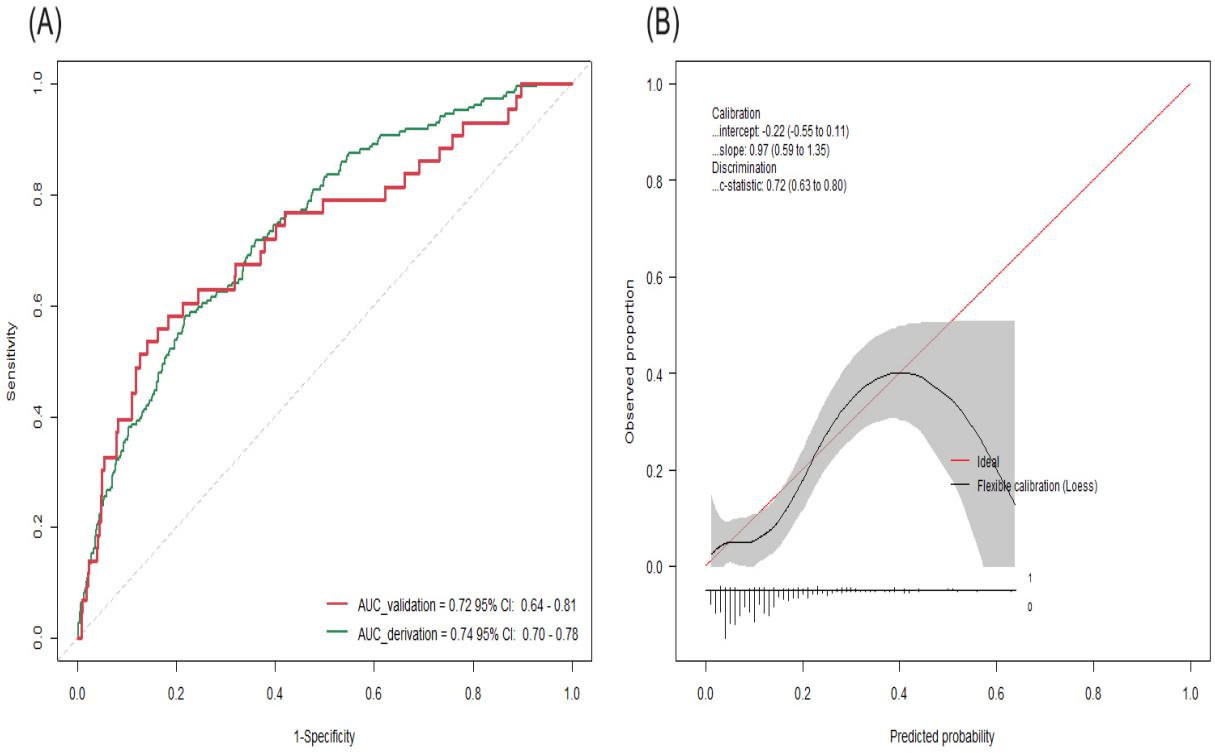

Conclusion:
Our prediction model demonstrated acceptable performance in predicting one-year mortality after TAVI in a real world European modern cohort, highlighting its potential for integration in routine clinical practice. Specifically, it may help evaluate the necessity of TAVI when anticipated benefits are uncertain.

787

B. Ohm[2], K. Kurowski[1], V. Veal[2], J. Heyer[1], P. Bronsert[1], W. Jungraithmayr[2]

CD26 as a target for combination therapy with immune checkpoint inhibition in thymic epithelial tumors

Department of Clinicopathology, University Medical Center Freiburg, Germany[1], Department of Thoracic Surgery, University Medical Center Freiburg, Germany[2]

Introduction:
Therapeutic options for the treatment of thymic epithelial tumors (TET) in advanced stages are limited. The use of immune checkpoint inhibitors (ICI) in thymomas is controversial due to their hazardous immune-mediated toxicity. Combination therapies would lower the toxicity while increasing the therapeutic effect. We here analysed CD26, a transmembrane protein expressed in various malignancies, as a potential target receptor for treatment in combination with ICI.

Methods:
Epithelial cells and lymphocytes in tissue microarrays (TMA) of TET from 112 patients operated in our institution between 2006 and 2022 were analysed for CD26, PD-L1, CTLA-4, PD-1, LAG3, TIM3 and TIGIT using HALO Image Analysis Platform.

Results:
Among all analytes, CD26 and PD-L1 were the receptors most abundantly expressed. CD26 expression was highest in AB and B1 thymomas. CD26 expression on epithelial cells was low in type A, B3 thymomas and in thymic carcinoma. A high epithelial CD26 expression correlated significantly with Masaoka Koga stage I in B thymomas. CD26-expression was high on lymphocytes in AB and B1 thymomas, but scarce in type A, B3 and in thymic carcinoma. PD-L1 – expression was high on epithelial cells from B thymoma.

Conclusion:
We show for the first time that CD26 is expressed in advanced type AB and B1 thymomas along with the IC receptor PDL-1. These expression patterns potentially qualify as targets for a combination treatment.

788

V. Reber[1, 3], S. Lengsfeld[1, 3], N. Varghese[4], Y. Emara[1, 3], L. Probst[1, 3], C. Bathelt[1, 3], L. Werlen[1], A. Eckert[4], B. Winzeler[1, 2, 3]

Effects of dulaglutide on oxytocin plasma levels in healthy men: a secondary analysis of a randomized, double-blind, placebo-controlled crossover study

Department of Clinical Research, University Hospital Basel, University of Basel[1], Department of Endocrinology, Diabetology and Clinical Nutrition, University Hospital Zurich[2], Department of Endocrinology, Diabetology and Metabolism, University Hospital Basel[3], Neurobiology Laboratory for Brain Aging and Mental Health, University Psychiatric Clinics Basel[4]

Introduction:
In animal studies, systemic and central injections of GLP-1 were found to increase plasma oxytocin concentrations. Additionally, recent rodent research revealed that 70% of GLP-1 receptor-positive neurons in the paraventricular nucleus also expressed oxytocin receptors. When oxytocin and GLP-1 were co-administered systemically, there was a significant increase in action potential firing in oxytocin-receptor-positive neurons in the paraventricular nucleus. Based on these findings, considering the functional and anatomical proximity as well as the synergistic effects, we hypothesized that dulaglutide may modulate and increase oxytocin plasma levels in humans.

Methods:
This is a secondary analysis of a randomized, double-blind, placebo-controlled crossover trial of healthy eugonadal men, age 18-50 years with active and satisfactory sex lives that examined the effect of the GLP-1 RA dulaglutide on sexual desire as a primary endpoint. Participants were randomly assigned (1:1) to receive either dulaglutide or placebo for four weeks. Oxytocin plasma levels were measured repetitively in a standardized manner, with three samples taken every 15 minutes at baseline and at the evaluation visit. We used the mean of these three measurements for our analysis. Changes within individuals were then compared after four weeks of treatment with the GLP-1 receptor agonist dulaglutide versus placebo using paired *t*-tests.

Results:
The median [IQR] age of participants at inclusion was 24.5 [21.0, 29.0] years, and the median BMI was 23.85 [22.15, 25.00]. Mean (SD) oxytocin baseline levels were comparable between groups: 50.6 pq/ml (17.0) in the treatment group and 50.5 pq/ml (18.2) in the placebo group. After 4 weeks of treatment with dulaglutide and placebo oxytocin concentrations remained stable and were 53.2 pq/ml (12.7) and 50.5 pq/ml (17.8), respectively. Mean (SD) change from baseline in oxytocin concentrations was + 2.6 pq/ml (21) in the treatment group and 0.0 pq/ml (19.4) in the placebo group. The estimated difference between the two treatment was: 2.58 [95% CI −12.9, 18.4].

Conclusion:
Our study found no significant change in oxytocin plasma levels following a four-week treatment with dulaglutide versus placebo. Differences in results compared to animal data may be due to lower dosing, central versus peripheral administration, choice of GLP-1 RA, or acute versus chronic use. In addition, whether the results would be different in women or in people with obesity/diabetes mellitus, where altered GLP-1 metabolism is expected, needs to be investigated in future studies.

789

B. Beyersdorf[1], S. Voglis[1], Z. Guoming[2], J. Sarnthein[1], L. Regli[1], M. Germans[1]

Treatment Outcomes and the Role of the DES scheme in the Appropriate Treatment Selection for High Grade Dural Arteriovenous Fistulas

Department of Neurosurgery, Clinical Neuroscience Center, University Hospital Zurich, Zurich, Switzerland[1], Department of Neurosurgery, Lanzhou University Second Hospital, Lanzhou, China[2]

Introduction:
Endovascular and microsurgical treatment are viable options for the majority of Borden Type III dural arteriovenous fistulas (dAVF). This study examines treatment outcomes in a comparative analysis of endovascular and surgical treatment modalities for Borden Type III fistulas and explores clinical implications of the DES scheme in selecting ideal candidates for surgical therapy.

Methods:
Patients diagnosed with dAVF with leptomeningeal venous drainage admitted to the departments of Neurosurgery or Neuroradiology of the University Hospital Zurich between January 2014 and October 2021 were included in this study. Comprehensive patient data including demographics, clinical presentation and dAVF characteristics including established classifications were collected. Treatment outcomes were assessed based on post-interventional angiographic imaging. In addition, treatment-related complications were assessed based on the Clavien-Dindo classification.

Results:
Among all Borden Type III dAVFs, 15 were initially treated with endovascular treatment (60% complete occlusion rate) and 10 with microsurgical disconnection (90% complete occlusion rate) (p=0.18). Subgroup analysis of dAVFs meeting the criteria for directness and exclusivity based on the DES scheme showed a 100% complete occlusion rate after microsurgical disconnection, whereas embolization achieved a complete occlusion rate of 60% (p=0.06). There was no significant difference in the rate or severity of treatment-related complications between treatment modalities.

Conclusion:
This study suggests microsurgical disconnection as a viable primary treatment modality for Borden Type III dAVFs, particularly in dAVF that meet the criteria of directness and exclusivity according to the DES scheme. The DES scheme demonstrates its relevance in selecting the most appropriate treatment strategy for affected patients.

791

J. Baum[1], C. Boggon[2], N. Ranzoni[1], D. Megias Ramos[1], L. Isa[2], S. Brugger[1]

Microbiota engineering for the eradication of Staphylococcus aureus

Department of Infectious Diseases and Hospital Epidemiology, University Hospital Zurich, University of Zurich[1], Department of Materials, ETH Zurich[2]

Introduction:
Staphylococcus aureus is a common human pathobiont that is associated with high morbidity and mortality infection and a high antibiotic resistance burden. S. aureus primarily colonizes the upper respiratory tract and colonized individuals are known to carry a higher risk of developing infections. Dolosigranulum pigrum and Corynebacterium pseudodiphtheriticum are commensal bacteria from the upper respiratory tract that are negatively associated with S. aureus colonization from 16S rRNA amplicon sequencing screens, yet the mechanisms underpinning this observation remain unclear. Here we investigate interactions between these two commensal organisms with the pathobiont S. aureus using both macroscopic in vitro techniques together with a novel, single-cell characterisation technique called bio-sCAPA.

Methods:
We use co-culture assays to investigate pair-wise interactions between the commensals and S. aureus. The inhibition is assessed after 24h and quantified using custom code. To investigate the nature of the inhibition bacteria are extracted from the inhibition zone and plated for enumeration. To look at the three-way interaction model we pre-condition the agar with C. pseudodiphtheriticum before performing the co-culture assay. Over a period of 72h both the growth of D. pigrum as well as the inhibition of S. aureus are assessed. Additionally, we use bio-sCAPA to deposit bacteria and evaluate the inhibition on a single cell level. After S. aureus is deposited on a PDMS template we place a nutrient containing agar pad, that has been pre-conditioned with the commensal bacteria, on top of the template. The template is then placed under a microscope where we can take time lapse images of the S. aureus cells. From the time-lapse images parameters such as deposition yield, lag time as well as growth rate of single bacteria can be extracted and compared.

Results:
We demonstrate that all primary isolates of D. pigrum that we tested lead to robust pathobiont inhibition. The inhibition is of a bactericidal nature and S. aureus does not easily develop resistance even with repeated exposure. We show that C. pseudodiphtheriticum interactions with S. aureus are strongly dependent on culturing conditions with only nutrient poor environments leading to complete growth inhibition indicating competition for scarce nutrients. Combining what we learn from pairwise interaction studies, we use a three-way interaction model to demonstrate how C. pseudodiphtheriticum promotes D. pigrum growth which directly leads to earlier onset of inhibition of S. aureus.

Conclusion:
This work demonstrates complex, combinatorial interactions taking place within a 3-member community in the human nose and presents evidence supporting the potential use of D. pigrum and C. pseudodiphtheriticum to robustly prevent S. aureus colonisation.

792

E. Voloviceva[3, 4], S. Bernhard[3], S. Goetze[1], A. Othman[2], A. von Eckardstein[3, 4], J. Robert[3, 4]

Brain apoE particle composition defines its functions

ETH Zurich[1], Functional Genomics Center Zurich[2], University Hospital Zurich[3], University of Zurich[4]

Introduction:
Alzheimer's disease (AD) is the leading cause of dementia in elderly adults, with 55 million cases recorded worldwide in 2019. This number is expected to almost triple by 2050. It is known that genetic variations of apolipoprotein E (*APOE*) affect the risk of AD development and the age of onset, with the *APOE4* allele being detrimental, *APOE3* neutral, and *APOE2* protective. However, the link between the *APOE* genotypes, isoforms of the apoE protein, the composition of apoE particles, and their function in AD remains poorly characterized. Previous studies indicated that various cell types, including astrocytes, pericytes, and microglia, produce apoE in the central nervous system; moreover, they suggest that the role of apoE in the brain depends on the cell type of origin. Notably, the composition of apoE particles appears to be linked to the cell type of origin, with pericyte-secreted apoE containing more cholesterol than astrocyte-secreted apoE. This creates a challenge for studying the roles of different apoE isoforms in AD pathogenesis. In the current project, we propose a cell-type and genotype-specific approach to investigate the composition and functions of apoE particles. We hypothesize that the protein and lipid compositions of apoE particles are influenced by the APOE genotype and the cell type of origin. These unique lipidome and proteome signatures, in turn, affect the functions of apoE particles in AD pathogenesis.

Methods:
To test our hypothesis, we are differentiating the apoE-secreting cells of the central nervous system: astrocytes, pericytes, and microglia from human induced pluripotent stem cells (iPSCs). By including apoE-secreting cells with different *APOE* genotypes (derived from isogenic iPSCs) in our study, we will investigate the influence of genetic variants on apoE particle composition in a cell-type-specific manner. We will investigate the protein and lipid compositions of apoE particles secreted by each differently genotyped cell type using liquid chromatography-mass spectrometry (LC-MS). Next, we will assess the role of these particles in AD by characterizing their effect on amyloid beta and tau accumulation in neurons.

Results:
We have differentiated and characterized human brain pericytes, astrocytes, and microglia from iPSC. We confirmed that each cell type secretes apoE, which can be harvested from culture media. In addition, undifferentiated, human iPSCs also secrete apoE, although they do not express ATP-binding cassette transporter (*ABCA1*) mRNA. Due to the lack of *ABCA1*, which is involved in the lipidation of apoE particles, we hypothesize that iPSC-secreted apoE will have distinct lipidation patterns compared to mature human cells. We have tested the LC-MS methods using human cerebrospinal fluid (CSF) and confirmed that both proteins and lipids associated with apoE particles are detectable.

Conclusion:
By the end of our project, we aim to answer key questions: how the composition of apoE particles is linked to the cell type of origin and *APOE* genotype, and how these particles affect cerebrovascular health in the context of AD. These findings will significantly advance our understanding of the role of apoE in AD and open the possibility of developing more targeted and effective treatments.

793

Y. Gütlin[1], A. Egli[1]

Toward sustainable and reproducible MALDI-TOF MS: Impact of target selection and hardware maintenance on mass spectral quality

Institute of Medical Microbiology, University of Zurich, Zurich, Switzerland[1]

Introduction:
Matrix-assisted laser desorption ionization-time of flight mass spectrometry (MALDI-TOF MS) has revolutionized microbial identification in routine diagnostics, offering cost-effectiveness, speed, and accuracy. However, reproducibility remains a key limitation, with mass spectral quality (MSQ) being critical for accurate species identification. To address this, we investigated technical and hardware factors influencing MSQ. Technical factors included a comparison of reusable steel vs. disposable targets, considering associated environmental and cost implications. For hardware factors, we analysed over 900 weekly measurements of five reference strains to assess the influence of long-term instrument performance on MSQ.

Methods:
A collection of 47 isolates from 39 species, previously selected for their identification challenges with MALDI-TOF MS were expanded by two *Candida* spp. isolates. Each isolate was analysed in duplicate, with three biological replicates per target type. Five established MSQ markers were calculated to compare steel and disposable targets. Additionally, over 900 weekly measurements of five reference strains were analysed to assess MSQ variation over time.

Results:
Disposable targets exhibited higher proportions of ribosomal peaks detected per isolates, higher total signal intensity and lower measurement error, while steel targets produced stronger ribosomal peak signal intensity (Figure 1). Taxa-specific differences in MSQ markers, such as median ribosomal peak intensity for *Listeria monocytogenes*, were observed. While disposable targets offer workflow convenience, reusable steel targets may present advantages in terms of long-term cost and sustainability, pending further evaluation.

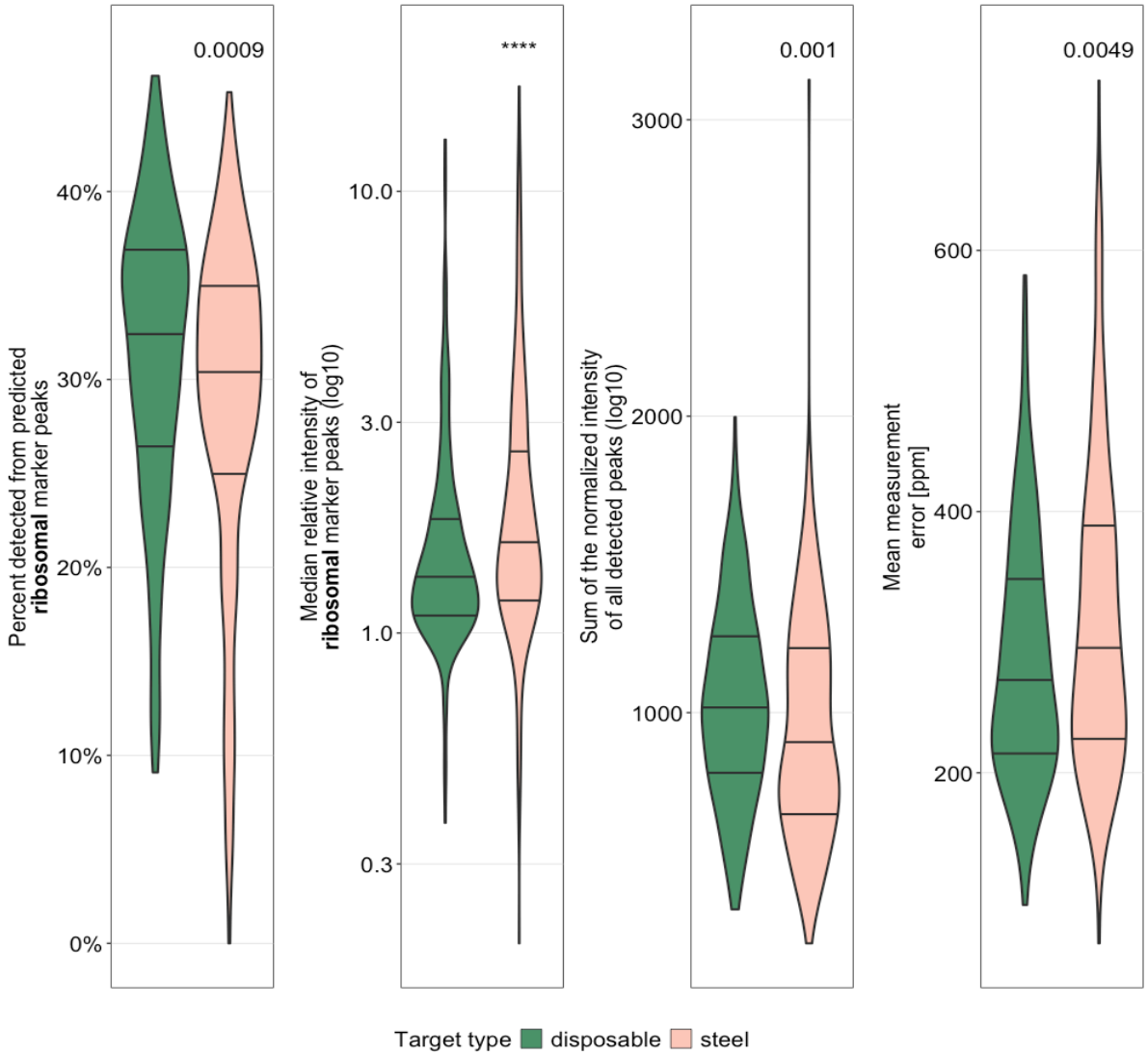

Conclusion:
Exploring technical factors such as target selection alongside hardware factors like long-term instrument performance may help to optimize reproducibility in MALDI-TOF MS. There is no clear disadvantage in terms of MSQ for using steel targets. Future analyses incorporating environmental, cost, and workflow considerations will further guide sustainable and reliable practices.

794

B. Siedentop[6], M. Papadimitriou-Olivgeris[7, 8], J. Epprecht[6], P. Monney[4], G. Tzimas[4], M. Frank[5], P. Tozzi[2], M. Kirsch[2], M. van Hemelrijck[3], O. Dzemali[1, 3], R. Kouyos[6, 9], B. Hasse[6]

Using machine learning to create a new diagnostic algorithm for infective endocarditis

Center for Translational and Experimental Cardiology (CTEC), Department of Cardiology, University Hospital of Zurich, University of Zurich, Zurich[1], Department of Cardiac Surgery, Lausanne University Hospital and University of Lausanne, Lausanne[2], Department of Cardiac Surgery, University Hospital Zurich and University of Zurich, Zurich[3], Department of Cardiology, Lausanne University Hospital and University of Lausanne, Lausanne[4], Department of Cardiology, University Hospital Zurich and University of Zurich, Zurich[5], Department of Infectious Diseases and Hospital Epidemiology, University Hospital Zurich and University of Zurich, Zurich[6], Infectious Diseases Service, Cantonal Hospital of Sion and Institut Central des Hôpitaux (ICH), Sion[7], Infectious Diseases Service, Lausanne University Hospital and University of Lausanne, Lausanne[8], Institute of Medical Virology, University of Zurich, Zurich[9]

Introduction:
Diagnosing infective endocarditis (IE) remains a significant challenge, even today. IE is a rare but severe disease with rising incidence rates. The DUKE criteria, widely recognized diagnostic criteria for IE, have been published and subsequently revised. However, these criteria often lead to inconclusive results with approximately one-third of patients being classified as having “possible IE”. Moreover, their sensitivity and specificity in clinical practice are limited, with reported values of around 80%. To date, research in IE diagnosis has heavily relied on the invaluable insights from clinical experts. However, it remains unclear whether integrating expert knowledge with statistical and machine learning approaches could enhance diagnostic accuracy and yield a reliable diagnostic score for clinical practice.

Methods:
To develop an improved diagnostic score for IE we leverage retrospective and prospective data collected from two Swiss University hospitals over a ten-year period (2014-2024). We apply statistical and machine learning methods, including lasso regression and decision tree-based models to predict IE. The predictor variables for these models are informed by current IE diagnostic guidelines, relevant literature, and input of clinical experts. Our models are trained using data from the Lausanne University Hospital (CHUV), which includes a well-documented control group. Only cases clearly classified by the Endocarditis team are included to ensure data reliability. To evaluate the generalizability of our models, we validate their performance using the data from the University hospital Zurich. To benchmark our approach, we compare the performance of the newly developed diagnostic score against existing IE diagnosis guidelines.

Results:
Our preliminary findings highlight the potential for improving current IE diagnosis guidelines. After splitting the CHUV dataset, which includes 479 IE cases and 949 control cases, into training and test subsets, we trained a Lasso regression model and evaluated its performance. The model achieved for binary classification a sensitivity of 90%, a specificity of 95%, an accuracy of 93% and an AUC of 97% in ROC-analysis. In comparison, for the CHUV data, the recently revised DUKE criteria by the International Society for Cardiovascular Infectious Diseases show a sensitivity of 76%, a specificity of 96%, an accuracy of 90% and an AUC of 86 %, counting all “possible IE” (28%) cases according to the criteria as rejected IE cases. Hence, these exploratory results suggest that incorporating expert knowledge with statistical and machine learning approaches could enhance IE diagnosis by improving the ability to differentiate between non-IE patients and IE patients while providing each patient with a quantifiable risk of IE. However, further validation is needed to determine the generalizability of our trained models across different hospital settings and larger independent datasets.

Conclusion:
Our preliminary results demonstrate the potential for enhancing IE diagnosis by integrating expert knowledge with statistical and machine learning methods. The developed models show high accuracy and robustness, with an increased discriminatory ability in comparison to current guidelines. Further validation with external datasets is needed to confirm their generalizability and clinical applicability.

795

M. Sun[2], A. Mohammed[3], D. Villars[2], K. Portmann[4], M. Mastall[2], M. Bouzereau[2], A. Köpp[2], T. Look[2], P. Westarp[2], P. Roth[2], K. Eyer[4], S. Pascolo[1], M. Weller[2], K. Joesph[3], V. Ravi[3], T. Weiss[2]

Rapid generation of multitargeting CAR-PBMCs: a novel immunotherapeutic strategy against glioblastoma

Department of Dermatology, University Hospital Zurich and University of Zurich, Zurich, Switzerland[1], Department of Neurology and Clinical Neuroscience Center, University Hospital and University of Zurich, Switzerland[2], Department of Neurosurgery, Medical Center and Faculty of Medicine, University of Freiburg, Freiburg, Germany[3], Laboratory for Functional Immune Repertoire Analysis, Institute of Pharmaceutical Sciences, Department of Chemistry and Applied Biosciences, ETH Zürich, Zürich, Switzerland[4]

Introduction:
Glioblastoma is the most common and aggressive primary brain tumor in adults with an urgent need for more effective treatment strategies. Cellular immunotherapies with engineered immune cells expressing synthetic chimeric antigen receptors (CAR) to recognize and attack cancer cells have great therapeutic potential. However, significant barriers impede the breakthrough and wide implementation of CAR immune cells against solid tumors, such as glioblastoma. These include limited immune cell activation within the immunosuppressive tumor microenvironment, heterogeneously expressed antigens and long and costly manufacturing strategies requiring weeks, during which many patients experience disease progression, making them ineligible for the treatment. To address these challenges, we developed a novel mRNA-based CAR-engineered peripheral blood mononuclear cell (CAR-PBMC) platform and explored the therapeutic activity against glioblastoma. This approach leverages the rapid production of multitargeting CAR-PBMCs from non-activated, non-expanded peripheral blood cells, offering a potentially effective and scalable treatment for glioblastoma.

Methods:
CAR-PBMCs were generated using mRNA electroporation to transiently express various CAR constructs. Flow cytometry and viability assays were utilized to investigate the transfection efficiency and the distribution of CAR expression across PBMC subpopulations. In vitro cytotoxicity assays were performed to evaluate the anti-tumor activity. Antigen specificity was validated using target antigen knockout (KO) target cells. In vivo efficacy was investigated using orthotopic glioma mouse models, where tumor progression was monitored through MRI imaging and survival analysis. Additionally, an ex vivo human brain slice model were utilized to assess the safety and tumor-specific activity of CAR-PBMCs against glioma cells.

Results:
Flow cytometry analysis showed robust transfection efficiency and viability, with effective CAR expression across PBMC subpopulations. *In vitro* cytotoxicity analysis showed that CAR-PBMCs exhibited significant tumor-killing activity against glioma cells, particularly when combined with cytokines. Antigen specificity was confirmed through specific killing of antigen positive target cells and absence of activity against target antigen knockout cells. In orthotopic glioma mouse models, CAR-PBMC therapy showed reduced tumor volumes and prolonged survival, with no toxicity based on body weight monitoring and MRI imaging. *Ex vivo* human brain slices analysis further confirmed selective anti-glioma activity without damaging healthy neurons, microglia, or astrocytes. Immunophenotyping revealed enhanced activation and infiltration of CAR-PBMCs within the tumor microenvironment.

Conclusion:
This study highlights the potential of CAR-PBMCs as a novel adoptive cell therapy for glioblastoma, offering a simplified and clinically applicable manufacturing process through rapid generation without prior activation or expansion. The demonstrated safety and efficacy provide a strong foundation for clinical translation. Further optimization of cytokine support and antigen targeting could enhance therapeutic outcomes, advancing CAR-PBMCs as a promising immunotherapeutic strategy.

796

S. Traxel[1], F. Schmidt[1], C. Beerli[1], D. Vuong[1], R. Speck[1], S. Bredl[1]

Turning tumors hot: Reprogramming the tumor microenvironment using engineered macrophages expressing a chimeric cytokine receptor

Department of Infectious Diseases and Hospital Epidemiology, University Hospital Zurich[1]

Introduction:
Triple-negative breast cancer (TNBC) is a highly aggressive subtype of breast cancer that lacks hormone receptors and HER2 amplification, making it unresponsive to standard hormone or HER2-targeted therapies. Immune checkpoint inhibitors (ICIs) have shown promise in “hot” tumors with high T cell infiltration. In contrast, ICI efficacy remains limited in “cold” tumors with low T cell infiltration. Tumor associated macrophages (TAMs) are critically influencing this immunophenotype of the tumor microenvironment (TME). Depending on the microenvironment, macrophages have different phenotypes: TAMs usually have an immunosuppressive phenotype, which is induced by cytokines like IL-10 and TGFβ. In contrast, macrophages with an inflammatory phenotype are induced by signals like IFNγ. They have anti-tumoral activity by enhancing T cell infiltration, generating an anti-tumor immune response and by directly affecting tumor cell viability. Thus, they are associated with good prognosis and a hot TME. Here, we describe genetically engineered macrophages with the aim to develop an adoptive cell therapy that reprograms the TME from cold to hot and enhances the outcome in TNBC.

Methods:
To generate inflammatory macrophages in an immunosuppressive TME, we engineer macrophages to express a chimeric cytokine receptor (ChCR). We designed two ChCR variants that induce an IFNγ-like signaling (STAT1) upon binding of either IL-10 or TGFβ, cytokines prevalent in the TME. To engineer the macrophages, we transduced monocytes with lentiviruses to express the ChCR. We assessed changes in their phenotype, secretome, and transcriptome analyzed following stimulation with IL-10 or TGFβ. Finally, we assessed the anti-tumoral activity of these reprogrammed macrophages in co-culture assays with 3D TNBC spheroids.

Results:
ChCR-expressing macrophages showed robust STAT1 activation in response to IL-10 or TGFβ stimulation, resulting in an inflammatory phenotype similar to IFNγ activation, as confirmed by phenotypic markers, and transcriptomic profiling. Moreover, ChCR stimulation led to the upregulation of CXCL9 and CXCL10, chemokines essential for lymphocyte recruitment, and other genes associated with good response to ICIs. Importantly, ChCR-stimulated macrophages showed significant anti-tumoral effects in 3D TNBC spheroids.

Conclusion:
We successfully engineered macrophages with ChCRs that reprogramms them within an IL-10- and TGFβ-rich environment, inducing an inflammatory phenotype and anti-tumoral activity. The expression of CXCL9 and CXCL10 suggests that ChCR macrophages could potentially induce lymphocyte infiltration and disruption of the cold TME. Thus, adoptive cell therapy using ChCR enginerred macrophages could be a promising strategy to improve outcomes in TNBC patients, particularly those with low immune cell infiltration, thereby addressing a critical unmet clinical need.

798

D. Moysidis[1], DB. Benz[1], M. Gajic[1], A. Pazhenkottil[1], P. Kaufmann[1], R. Buechel[1], AG. Giannopoulos[1]

Rationale and Development of the Computed Tomography Simulated Pressure Loss Index (CTSPLI)

Coronary Atherosclerosis Biomechanics Lab, Department of Nuclear Medicine, University Hospital Zurich, Zurich, Switzerland[1]

Introduction:
Combining coronary CT angiography (CCTA) and computational fluid dynamics offers promising non-invasive alternatives for functional assessment of coronary artery disease (CAD). We describe the rationale and development of the Computer Tomography Simulated Pressure Loss Index (CTSPLI), a non-invasive computational metric based on CTFFR that can objectively phenotype CAD at the coronary artery level

Methods:
CTSPLI was developed in 15 healthy individuals who underwent CCTA and PET-myocardial perfusion imaging and were characterized by lack of atherosclerotic plaques, normal endothelium-dependent-(cold pressor test-induced hyperemia), and endothelium independent-(adenosine-induced hyperemia) vasodilatation and hence normal epicardial coronaries and microvasculature. In these individuals, CTFFR analysis identified functional disease as regions with FFR drop of ≥0.0015/mm. CTSPLI was then calculated by combining the length of functional disease with the magnitude of pressure loss along the artery. CTSPLI provides a quantitative assessment of the flow resistance distribution in epicardial coronaries, where lower values (approaching 0) indicate diffuse CAD and higher values (approaching 1) focal CAD. A second cohort of 29 patients undergoing CCTA and CTFFR due to suspected obstructive CAD was retrospectively enrolled for the clinical investigation of CTSPLI. Coronaries were phenotyped as having focal, diffuse of mixed CAD patterns based on a. visual assessment of the distribution of plaques and CT-FFR pullback patterns and b. using CTSPLI.

Results:
A total of 76 arteries (LAD: 36, LCX: 19, RCA: 21) from 29 patients were analyzed. Expert visual assessment based on anatomy and CT-FFR classified 21 arteries as focally diseased, 46 as diffusely diseased and 9 with mixed pattern. CTSPLI-derived physiology led to reclassification of a total of 46 arteries (57.8%) with 42% of focal disease reclassified to a diffuse or mixed pattern, whereas 24% of diffuse disease was reclassified as functional focal CAD.

Conclusion:
CTSPLI can effectively and objectively phenotype CAD patterns, potentially enabling non-invasive personalization of management and revascularization strategies.

799

C. Arnaud-Boissel[1], K. Zielinska[1], LC. Hinte[2], C. Nombela-Arrieta[1], F. von Meyenn[2]

Trained immunity and inflammatory memory in the bone marrow

Department of Medical Oncology and Hematology, University Hospital and University of Zurich[1], Institute of Food, Nutrition and Health, Department of Health Sciences and Technology, ETH Zurich[2]

Introduction:
Trained immunity is a form of adaptation that enhances the reactivity and response of innate immune cells to secondary challenges. This mechanism is antigen-independent, and instead depends on the transmission of epigenetic signatures from hematopoietic stem cells (HSPCs) exposed to certain inflammatory stimuli to their progeny of innate immune cells. HSPCs reside in bone marrow (BM) tissues, which support the reprogramming of hematopoietic progenitors upon infections or malignancies. Apart from hematopoietic cells, the BM contains a large and heterogenous population of mesenchymal - mainly CXCL12-abundant reticular cells (CARc) - as well as arterioral and sinusoidal endothelial cells (AECs and SECs), all together termed 'stroma'. These stromal cells closely regulate HSPC activity to control hematopoiesis and are very sensitive to inflammatory signals. It is not known whether BM stroma, akin to HSPCs can remember prior inflammatory episodes, which may potentially impact their response to subsequent challenge. But interestingly, recent studies have revealed the ability of structural cells across multiple organs – e.g. skin, gut, lungs – to record information about prior inflammation by altering their epigenetic state. This feature is intriguingly reminiscent of the mechanism responsible for maintaining memory in trained immunity. In light of this recent evidence, our work focuses on testing the existence of inflammatory memory in BM stroma as well as its relevance in the control of immune responses upon insults.

Methods:
We aim to address this question by (1) investigating the potential existence and duration of inflammatory memory in BM stromal cells – CARc, AECs and SECs; (2) determining to what extent BM stromal cells participate to the reprogramming of HSPCs to achieve trained immunity. We use a validated trained immunity mouse model (injection with the polysaccharide beta-glucan as a first inflammatory challenge, followed by bacterial infection as a secondary challenge) and combine it with flow cytometry, 3D-organ-wide microscopy, transcriptomics and epigenetic analyses (notably Cleavage Under Targets and Tagmentation or CUT&Tag).

Results:
For the BM hematopoietic compartment, our results largely recapitulate with those published by other groups: we report a small expansion of MPP3 and downstream progeny up to 7 days after beta-glucan exposure and a decrease in MPP4. The majority of hematopoietic cells are back to normal frequencies by 28 days.
For the BM stromal compartment, our data indicates no changes in architecture or cell frequency after beta-glucan exposure. However, we find that CARc, AECs and SECs undergo progressive and distinct changes in their transcriptomic states after exposure, and are able to return to a basal state by 28 days. We have also been working on refining CUT&Tag to adapt the protocol to rare FACS-isolated BM stromal cells in order to investigate their epigenetic state.

Conclusion:
Overall, our results indicate BM stromal cells are able to sense the inflammatory cues necessary to reprogram HPSCs during trained immunity. We hope our future findings help identify the cellular sources for the cytokines initiating trained immunity in the BM, as well as inform on the durability, strength and quality of HSPC training. Notable applications include vaccination refinement, anti-cancer immunotherapies and treatment against certain cardiovascular diseases, which have been linked to abnormal or dysfunctional HSPC reprogramming, a process termed maladaptive trained immunity.

800

L. Ilcheva[2], A. Janenko[1], A. Tobias[2], O. Dragan[1], P. Nestor[2], H. Rodriguez Cetina Biefer[2], O. Dzemali[2]

Efficacy of a Novel Protocol for Eliminating Mycobacterium chimaera in Heater-Cooler Units: Single Center Clinical Study

Department of Cardiac Surgery, City Hospital Zurich[1], Department of Cardiac Surgery, University Hospital of Zurich[2]

Introduction:
Mycobacterium chimaera, a non-tuberculous mycobacterium, has become a significant concern in cardiothoracic surgery, particularly open-heart procedures. This slow-growing pathogen causes severe disseminated infections through bioaerosols from contaminated heater-cooler units (HCUs) during cardiopulmonary bypass. Since the first documented outbreak in 2013, M. chimera infection has been recognized as a global health issue. Current disinfection methods have proven to be largely ineffective. This study evaluated a novel protocol using a stable hypochlorous acid solution (Hydroliq) to eliminate M. chimera from infected HCUs and maintain M. chimera-free devices.

Methods:
This study was conducted from March 2023 to August 2024 in two phases. Phase I explored different amounts of Hydroliq and water change intervals in three HCUs using redox potential (ORP ≥500 mV), pH, chloride ion levels, and mycobacterial cultures as outcome measures. Phase II implemented the optimized protocol during cardiopulmonary bypass surgery, with regular M. chimera microbiological testing, redox potential, chloride ion levels, and pH values.

Results:
In the first phase, different concentrations and frequencies of water changes were tested, leading to an optimal decontamination regime by adding 200 ml Hydroliq with twice-weekly water changes. In the second phase, 337 cardiac surgeries were performed over 7 months using treated HCUs. This achieved optimal results, maintaining a redox potential above 500 mV (median 598 mV) (Figure 1), median pH value of 7.39 (Figure 2), and median chloride anion concentration of 1.33. No M. chimera infections were detected during this period, demonstrating the effectiveness of this protocol in clinical practice.

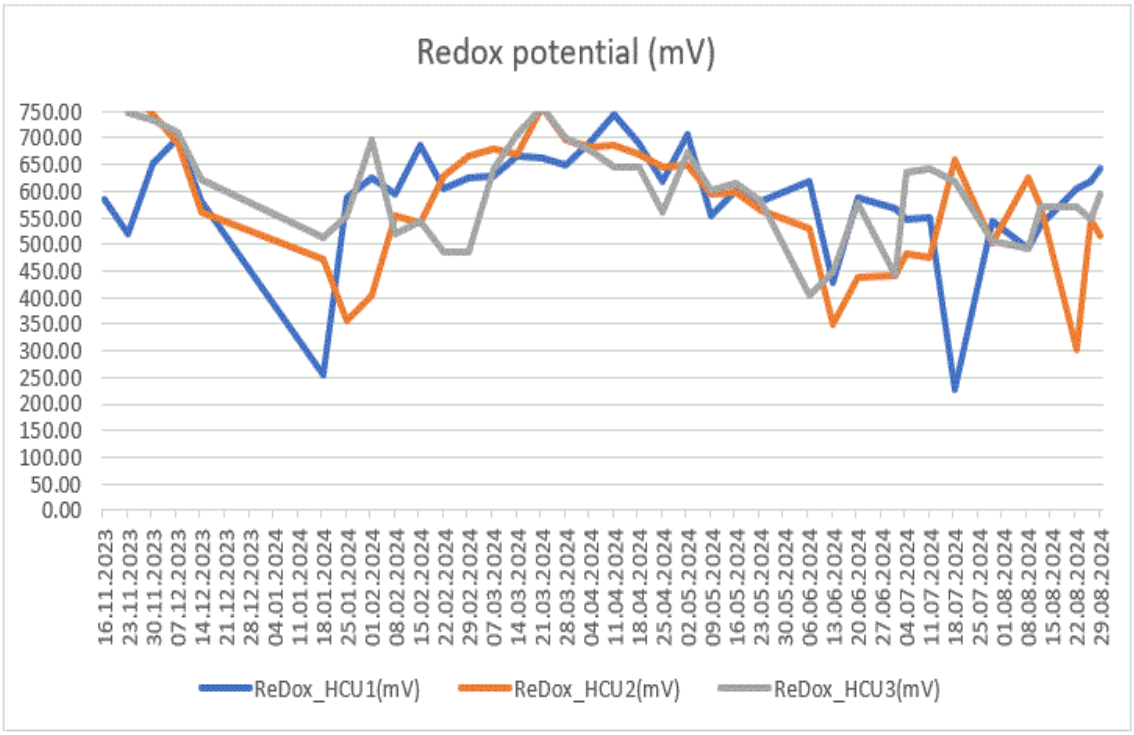

Figure 1. Redox potential (ORP) in mV during second phase of the study

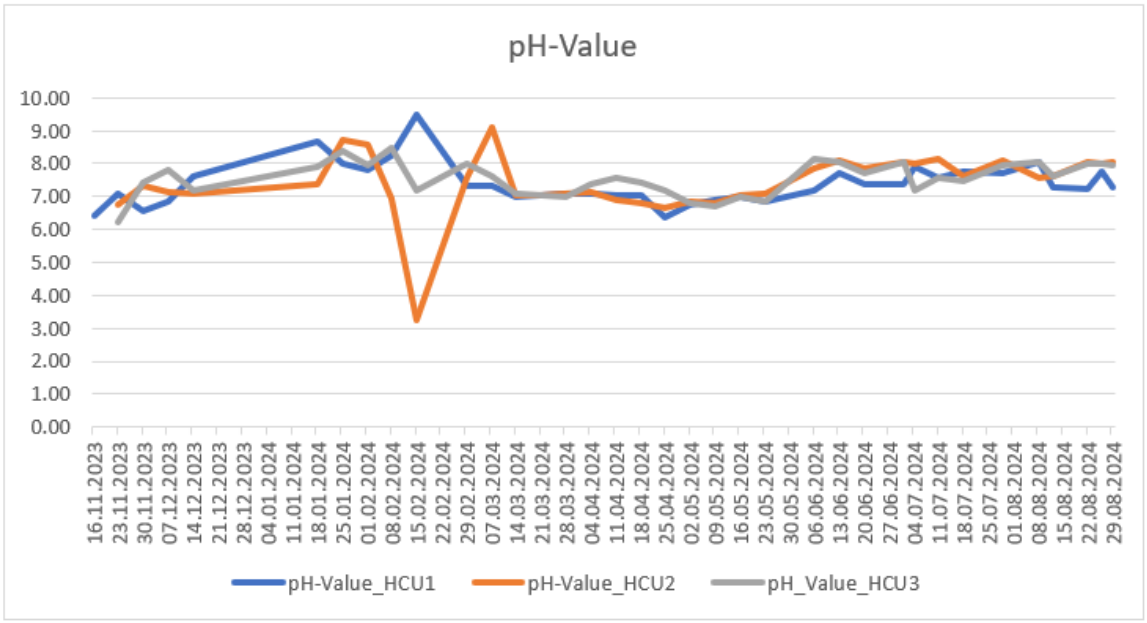

Figure 2. pH values during second phase of the study

Conclusion:
This novel decontamination protocol effectively eliminated M. chimera from HCUs and reduced postoperative infections in patients undergoing cardiac surgery. These findings support the implementation of this method as a safe and effective strategy to prevent HCU-related infections. Further investigation with a larger dataset is required to prove or reject this approach.

801

M. Soballa[1], M. Mastall[1], D. Villars[1], L. Hänsch[1], M. Mayoux[2], S. Tugues[2], M. Weller[1], P. Roth[1]

ICAM-1 CAR T cells enhance survival and remodel the tumor microenvironment in glioma mouse models

Department of Neurology and Brain Tumor Center, University Hospital Zurich and University of Zurich[1], Institute of Experimental Immunology, University of Zurich[2]

Introduction:
Chimeric antigen receptor (CAR) T-cell therapy, while effective against hematological malignancies, has faced significant hurdles in its application to solid tumors. Challenges in CAR T-cell therapy for glioblastoma include the immunosuppressive tumor microenvironment, the limited infiltration of CAR T-cells into the tumor, heterogeneous target expression and antigen escape. In this study, we focused on targeting Intracellular adhesion molecule-1 (ICAM-1), a protein expressed on both glioma cells and tumor-associated cells like macrophages and endothelial cells.

Methods:
Glioblastoma and normal brain tissue microarray sections (TMA) were immunohistochemically analyzed for ICAM-1 expression. Second-generation human and murine ICAM-1-targeting CAR T cells were generated by lentiviral or retroviral transduction of T cells from healthy human donors or murine splenocytes. Their efficacy was evaluated in co-culture assays with human and murine glioma and endothelial cell lines. Syngeneic and xenograft orthotopic glioma mouse models were used to assess the in vivo activity of CAR T cells. Ex vivo analysis of these tumors included examination of changes in the tumor microenvironment using high-dimensional flow cytometry.

Results:
Immunohistochemical staining of TMA revealed a significant upregulation of ICAM-1 in human glioblastoma tissue compared to normal brain tissue. Single-cell RNA sequencing data from glioblastoma specimens showed a high level of ICAM-1 expression in tumor-associated macrophages. Human and murine ICAM-1-targeting CAR T cells displayed strong lysis of ICAM-1-expressing glioma and endothelial cells in vitro. Intratumoral application of CAR T cells resulted in a survival benefit in both syngeneic and xenograft glioma mouse models. Ex vivo analysis of the tumor microenvironment revealed treatment-induced changes from our CAR T cell therapy and indicates potential for further enhancements.

Conclusion:
Our study demonstrates that ICAM-1-targeting CAR T cells improve survival in human and murine glioma mouse models. Flow cytometry of the tumor microenvironment reveals therapy-induced changes, for future improvements of the CAR T cell therapy.

802

N. Ziak[1], A. Abidi Ostorero[2], M. Generali[2], T. Hornemann[1], M. A. Lone[1]

Understanding the selective neurotoxicity of Serine-palmitoyltransferase mutations towards motor and sensory neurons

University Hospital Zurich[1], UZH[2]

Introduction:
Sphingolipids (SLs) are a diverse class of lipids that play crucial roles in various cellular functions, including cell structure and signaling. Dysregulation in their metabolism contributes to various neurological disorders such as Amyotrophic Lateral Sclerosis (ALS). Notably, ALS manifests as specific degradation of motor neurons while sparing sensory neurons. Certain mutations in the serine-palmitoyltransferase (SPT), the first and rate-limiting enzyme in the de novo SL synthesis, are linked to ALS. Interestingly, another group of mutations in the same enzyme leads to an opposing clinical phenotype, namely Hereditary Sensory and Autonomous Neuropathy type 1 (HSAN1). It manifests as sensory loss, including pain, pressure, temperature and vibration. HSAN1 mutations result in the pathological formation of atypical and neurotoxic 1-deoxysphingolipids (1-deoxySL) by altering the substrate specificity of the enzyme from serine to alanine. Whereas SPT-ALS mutations impair the homeostatic control of the enzyme, which results in an uncontrolled and overshooting formation of SL species. This PhD project aims to unravel the mechanisms causing selective neurotoxicity of the SPT-ALS and SPT-HSAN1 mutations toward sensory and motor neurons, by studying the differentiation of mutant cells into the respective neuron types.

Methods:
In Vitro Models for Neuronal Differentiation
We use an in vitro model where neuronal differentiation is induced through transcription factor overexpression. Cells are transfected with a plasmid carrying at least the master transcription factor Neurogenin-2 (NGN2), leading to iCortical neurons upon differentiation. iSensory neurons additionally express the transcription factor BRN3A, while iMotor neurons express ISL1 and LHX3. Upon doxycycline induction, neuronal differentiation begins, generating induced neurons (iNeurons). Our research focuses on analyzing sphingolipid profiles in mature motor and sensory iNeurons and tracking changes during differentiation. In a second step, we will compare the profiles of "healthy" neurons to patient-derived iPSCs suffering from ALS and HSAN1. Assessment of Neuronal Differentiation and Functionality Neuronal differentiation will be monitored by assessing specific developmental markers through immunohistochemistry and quantitative PCR. Sphingolipid profiles will be analyzed via mass spectrometry to determine lipid composition and potential metabolic alterations. Additionally, we investigate the impact of perturbing sphingolipid metabolism. ALS-like conditions can be mimicked by ceramide supplementation, while HSAN1 is modeled by adding 1-deoxysphinganine and increasing the alanine-to-serine ratio. We will also assess pharmacological inhibitors such as Myriocin, which blocks serine palmitoyltransferase (SPT).

Identification of Biomarkers in Lipid Profiles
We will analyze sphingolipid profiles in patients with genetic ALS—including both previously published and newly identified variants—as well as sporadic ALS, using mass spectrometry. This study aims to identify biomarkers linked to disease phenotypes and lipid dysregulation in ALS and HSAN1.

Results:
Preliminary results indicate that there are differences in differentiation between the differentiation of healthy control cell lines compared to the patient-derived iPSCs.

Conclusion:
The in vitro models models allow us to study and manipulate pathomechanisms underlying selective neurotoxicity in sensory neurons and motor neurons, potentially revealing novel therapeutic targets. Additionally, the characterization of ALS-associated SPT variants versus sporadic will be carried out. Potential biomarkers, which we find in this analysis, could assist in the diagnosis for sporadic patients, but might also play a role in idiopathic ALS cases.

803

K. Hofer[2], N. Sievi[3], F. Schmidt[3], A. Egli[1], J. Deuel[2]

Real-time breath analysis for the detection of invasive fungal infections in neutropenic high-risk patients (REDEFINE)

Institute of Medical Microbiology, University of Zurich[1], University Hospital Zurich, Department of Medical Oncology and Hematology[2], University Hospital Zurich, Department of Pulmonology[3]

Introduction:
Patients with hematologic malignancies and concomitant neutropenia are at high risk of developing invasive fungal infections (IFI) that are associated with high morbidity and mortality. As these patients typically have severe thrombocytopenia, direct diagnostic sampling with invasive procedures is often not possible due to the high peri-interventional risk. Therefore, the presumptive diagnosis of IFI is primarily based on compatible lung findings on computed tomography and serologic detection of the fungal cell wall components galactomannan and ß-d-glucan, which, however, have limited sensitivity and specificity. These diagnostic difficulties contribute to inappropriate and delayed treatment of IFI, leading to rapid progression, angioinvasion, and dissemination in the neutropenic host. On the other hand, patients without clear evidence of IFI are often subjected to prophylactic and empiric antifungal treatments with potentially toxic side effects. Hence, a more effective yet rapid, reliable diagnostic tool to identify fungal pathogens causing IFI is urgently needed. Since fungi are known to produce a wide range of specific volatile metabolites, breath analysis has the potential to fill this diagnostic gap using secondary electrospray ionization high-resolution mass spectrometry (SESI-HRMS), a state-of-the- art breath analysis method that enables high-resolution identification of detected molecules through a non-invasive approach with a rapid turnaround time.

Methods:
The REDEFINE study is designed to screen for IFI with weekly breath analysis using SESI-HRMS in all participating patients treated for acute myeloid leukemia at the Department of Medical Oncology and Hematology at the University Hospital Zurich. At the same time, we will measure established serum biomarkers (galactomannan/ß-d-glucan and Aspergillus-/Mucorales-specific PCR) and perform low-dose computed chest tomography to ensure accurate EORTC/MSG (European Organization for Research and Treatment of Cancer/Mycoses Study Group) group assignment at different time points in each individual patient. This will allow to determine a set of specific volatile biomarkers in patients with proven or probable IFI, enabling a more rapid and reliable detection of IFI with the ultimate goal of redefining its diagnostic criteria.

804

G. Wick[3, 4], T. Loosli[3, 4], N. Han[3, 4], S.E. Chaudron[3, 4], L. Johnson[1], H. Günthard[3, 4], M. Egger[1, 5, 7], R. Lessells[2, 6], R. Kouyos[3, 4]

HIV superinfections and dolutegravir resistance in South Africa: a modelling study

Centre for Infectious Disease Epidemiology and Research, University of Cape Town, Cape Town, South Africa[1], Centre for the AIDS Programme of Research in South Africa, Durban, South Africa[2], Department of Infectious Diseases and Hospital Epidemiology, University Hospital Zurich, Zurich, Switzerland[3], Institute of Medical Virology, University of Zurich, Zurich, Switzerland[4], Institute of Social and Preventive Medicine (ISPM), University of Bern, Bern, Switzerland[5], KwaZulu-Natal Research Innovation and Sequencing Platform (KRISP), University of KwaZulu-Natal, Durban, South Africa[6], Population Health Sciences, Bristol Medical School, University of Bristol, Bristol, United Kingdom[7]

Introduction:
HIV superinfections are rarely documented and not well understood, and their impact on the epidemiology of HIV is unclear. Reports of superinfection incidences are highly variable across studies, ranging from 0% to 7.7% per year. As individuals may be superinfected with HIV strains carrying drug resistance mutations, superinfections may represent a potential driver of emergent drug resistance and thus increase the risk of resistance-related treatment failure. This may be particularly relevant in settings with a high HIV prevalence, programmatic antiretroviral therapy (ART), and limited resources for viral load monitoring with individuals remaining viremic for extended durations.

Methods:
MARISA (Modelling Antiretroviral drug Resistance in South Africa) is a compartmental model calibrated to the HIV epidemic in South Africa, including four layers: i) care cascade, ii) sex, iii) disease progression, iv) drug resistance. We extended the model to include superinfections among people living with HIV in South Africa from 2005 to 2040. In our model, superinfection rates depended on sex, treatment stage, drug combination, and the viral resistance genotype. We assumed that superinfections of individuals on ART requires the transmitted virus to have resistance to nucleoside reverse transcriptase inhibitors, and NNRTI or dolutegravir, depending on the regimen. Superinfections in individuals not on ART are not conditional on drug resistance. We further assumed that superinfection results in virological replication, hence superinfection of an individual on suppressive treatment leads to a treatment failure.
We evaluated our model for a broad range of parameter values related to superinfection (e.g. superinfection transmission rate and required resistance level) to account for the large uncertainty of superinfection dynamics. Outcomes were superinfection incidence, superinfection-related transmission of intermediate or high level dolutegravir resistance, and treatment failures due to superinfections.

Results:
In our model, superinfections are rare compared to new infections, with only one out of 44 (2.3%, range: 0.9%-3.7%) HIV infections being a superinfection of HIV positive individuals in 2035. However, more than four out of five superinfections result in the transmission of intermediate or high resistance to dolutegravir (Figure 1 A, 87.7%, range: 81.3%-90.2%). In 2035, 1170 (range: 450-1790) treatment failures are estimated to be a consequence of a superinfection with a dolutegravir resistant HIV strain (Figure 1 B). These represent 1.5% (range: 0.6%-2.2%) of all incident treatment failure with dolutegravir resistance on dolutegravir-based ART.

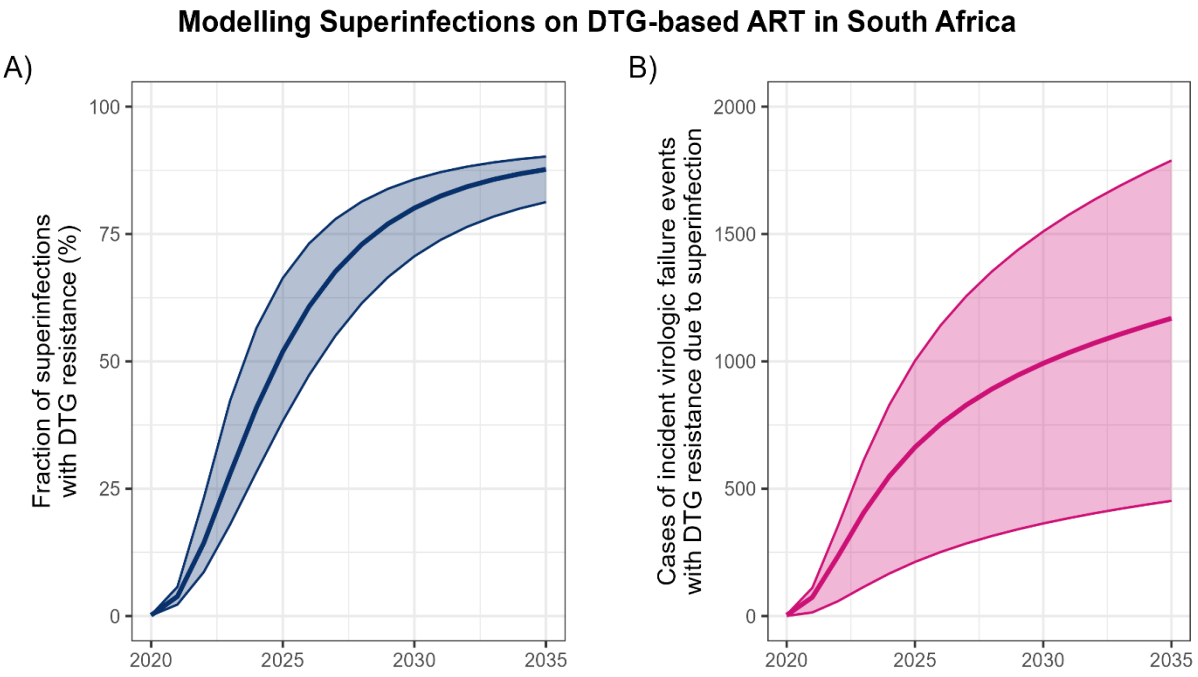

Figure 1: Modelled resistance and viral failure on dolutegravir-based treatment linked to superinfections. Lines correspond to best informed parameter assumptions; shaded areas show model outcomes representing different simulated scenarios, covering a range of superinfection parameter values from more to less likely superinfections to account for the parameter uncertainty. A) The proportion of superinfections with dolutegravir (DTG) resistance among all superinfections. B) The number of viral failures per year with dolutegravir resistance due to superinfections are shown.

Conclusion:

Our findings suggest that superinfections may represent a source of emergent drug resistance and affect HIV treatment outcomes at an individual level but will have only a minor impact on the prevalence of resistance and failure at the population level. While superinfections are rare, most cases are expected to result in emergent drug resistance, which could pose a challenge for the sustainability of current HIV treatment.

805

NE. Winkler[2], G. Tsiourantani[2], Q. Chen[2], TG. Donati[2], M. Hebeisen[1, 2], J. Michel[2], B. Stähli[2], AM. Kasel[2], FC. Tanner[2]

Clinical Significance of Dilated Left Ventricular Outflow Tract in patients undergoing Transcatheter Aortic Valve Implantation

Department of Biostatistics, Epidemiology, Biostatistics and Prevention Institute, University of Zurich[1], Department of Cardiology, University Heart Center, University Hospital Zurich and University of Zurich[2]

Introduction:
A dilated left ventricular outflow tract (LVOT) can lead to inaccurate stroke volume (SV) calculation and aortic stenosis (AS) grading (1). This study aimed to define a normal LVOT diameter and identify potential problems with SV calculation in patients with severe AS undergoing transcatheter aortic valve implantation (TAVI).

Methods:
This retrospective analysis included 744 AS patients undergoing TAVI. LVOT diameter was assessed by two-dimensional echocardiography and compared with normal values from the NORRE study (2). Differences in SV calculation between LVOT and Simpson method were evaluated.

Results:
Median age was 81 [77–85] years with 44% females. Median LVOT diameter was 21.0 [IQR 20.0–23.0] mm (females: 20.0 [19.0–22.0]; males: 22.0 [21.0–24.0]; p-value <0.001). Median LVOT diameter indexed to body surface area (BSA) was 11.7 [IQR 10.9–12.5] mm/m2 (females: 11.8 [11.1–12.7]; males: 11.5 [10.7–12.5]; p-value 0.003). LVOT dilatation was defined as exceeding two standard deviations of the mean resulting in upper reference limits (URL) of 25 mm and 14 mm/m2, respectively. LVOT dilatation occurred in 3% (0.3% females and 2.6% males, respectively) and LVOTI dilatation in 6% of patients (3.4% females and 2.4% males, respectively). Median velocity time integral (VTI) was 19.5 cm [16.0–23.0]. SV calculation resulted in larger values with LVOT compared to Simpson method. Among the 513 patients (69.0%) with a ≥10% difference between LVOT and Simpson method, only 14 (2.7%) exhibited a dilated LVOT.

Conclusion:
The URL for a normal LVOT is 25 mm (14 mm/m2) in severe AS patients eligible for TAVI. LVOT diameter differs between females and males, even when indexed to BSA. LVOT dilatation occurs in 6% of patients. The impact of LVOT dilatation on SV calculation appears to be modulated by high variability of LVOT VTI.

806

A. Buck[2, 6], S. Lee[6], R. Wegmann[6], I. Sakic[2], J. Mena[6], F. Vasella[3], J. Friesen[2], E. Le Rhun[3], A. Zeitlberger[4], N. Tatari[1], L. Regli[3], G. Hutter[1, 5], M. Neidert[4], M. Weller[2], B. Snijder[6], T. Weiss[2]

Spatially resolved functional profiling for glioblastoma

Brain Tumor Immunotherapy Lab, Department of Biomedicine, University of Basel[1], Department of Neurology, Clinical Neuroscience Center, University Hospital and University of Zurich[2], Department of Neurosurgery, Clinical Neuroscience Center, University Hospital and University of Zurich[3], Department of Neurosurgery, Kantonsspital St. Gallen, St. Gallen[4], Department of Neurosurgery, University Hospital Basel[5], Institute of Molecular Systems Biology, Department of Biology, ETH Zurich[6]

Introduction:
Glioblastoma is the most common and aggressive primary brain tumor in adults, with a median overall survival of less than 20 months due to limited treatment efficacy and inevitable tumor recurrence. Standard therapies, including surgery, radiotherapy, and chemotherapy, provide only transient benefits, largely due to glioblastoma's extensive heterogeneity. This heterogeneity is evident on magnetic resonance imaging (MRI), where distinct tumor regions can be delineated into a necrotic center, a contrast-enhancing tumor core, and a non-contrast-enhancing infiltration zone, which contains both normal and infiltrating tumor cells and appears hyperintense on T2/FLAIR imaging. The diffuse infiltration of tumor cells into surrounding brain tissue impedes complete surgical resection, leading to relapse from residual cancer cells. While genomic and transcriptomic differences between the tumor core and infiltration zone are well characterized, their functional implications, particularly in drug sensitivity and therapeutic response, remain poorly understood.

Methods:
To address this gap, we implemented MRI-guided sampling to obtain region-specific tissue from the contrast-enhancing tumor core and the 5-aminolevulinic acid (5-ALA)-fluorescent infiltration zone in glioblastoma patients. We then performed single-cell functional drug response profiling using pharmacoscopy to assess differential drug sensitivities across tumor regions, patients, and tumor cell subpopulations, characterized by the expression of either Nestin, marking cancer cells with a more stem-like phenotype, or S100B, identifying more differentiated cancer cells.

Results:
Our analysis revealed substantial heterogeneity in treatment response at multiple levels: between tumor regions, among patients, and across tumor subpopulations. These findings suggest that a single-agent therapy is unlikely to be universally effective. To overcome this challenge, we developed a drug complementarity score, integrating region-specific drug response data from 23 patients treated with a 59-drug panel. We selected 20 promising drug combinations and validated them in a cohort of nine patients, where combination therapy resulted in a significantly higher fraction of on-target drug responses compared to single agents. Notably, combinations comprising one oncology and one neuroactive drug exhibited enhanced synergy and greater drug responses compared to combinations within the same drug class (oncology + oncology or neuroactive + neuroactive), highlighting the potential of cross-class therapeutic strategies in glioblastoma treatment. The drug combinations demonstrated robust activity across tumor regions, cell subpopulations, and patients.

Conclusion:
Given the extensive intra- and intertumoral heterogeneity in glioblastoma, a one-size-fits-all treatment approach is unlikely to succeed. Instead, our findings support the rationale for combination therapies that account for glioblastoma's complexity, offering a more effective strategy to prevent tumor recurrence in clinical settings.

807

I. Sakic[1], E. Uijttewaal[2], R. De Luca[3], E. Puca[3], M. Weller[1], D. Neri[4], U. Elling[2], T. Weiss[1]

CRISPR-guided optimization of tumor-targeted cytokine therapy against glioblastoma

Department of Neurology, Clinical Neuroscience Center, University Hospital Zurich and University of Zurich, CH-8091 Zurich, Switzerland[1], Institute of Molecular Biotechnology of the Austrian Academy of Science (IMBA), Vienna Biocenter (VBC), Dr. Bohr Gasse 3, 1030, Vienna, Austria[2], Philochem AG, Libernstrasse 3, 8112 Otelfingen, Switzerland[3], Philogen Spa, Piazza La Lizza 7, 53100 Siena, Italy[4]

Introduction:
Glioblastoma is a deadly brain tumor with a poor overall survival, remaining one of the most challenging neoplasms to treat. Despite decades of research, substantial progress in the standard of care has been limited due to the immunosuppressive tumor microenvironment, highly invasive tumor nature, heterogeneity among patients, and resistance to conventional therapies. While immunotherapy has transformed treatment paradigms in other cancers, its success in glioblastoma has been limited. To address this unmet need, we explored the potential of L19-TNF, an antibody-cytokine fusion protein targeting the tumor-specific extracellular domain B (EDB) of fibronectin, to deliver TNF-alpha specifically to the tumor site and enhance antitumor immunity. Early clinical trials of L19-TNF in combination with the chemotherapy Lomustine for recurrent glioblastoma showed promise; however, toxicity associated with Lomustine limits its broader therapeutic utility, demanding alternative and synergistic treatment strategies.

Methods:
We employed a nove *in vivo* CRISPR screening approach to systematically identify tumor vulnerabilities and druggable target genes that potentially also act in synergy with L19-TNF immunotherapy. This platform overcomes limitations of previous CRISPR screening strategies such as off-target effects and uncertainties with tumor engraftments *in vivo* and also enables a temporal control of the genetic perturbations. Using genome-wide and targeted CRISPR screens in immunocompetent, orthotopic glioma models with and without L19-TNF selection pressure, we identified key glioblastoma drivers and uncovered novel vulnerabilities.

Results:
We successfully conducted a genome-wide *in vivo* CRISPR screen that identified critical regulators of RNA processing, PI3K signaling, angiogenesis, and tumor proliferation. The top hits could be validated in a separate targeted *in vivo* CRISPR screen. *In vitro* studies revealed that small-molecule inhibitors targeting our top three candidate genes led to significant glioma cell killing. Preliminary *in vivo* studies demonstrated extended survival in syngeneic mouse models when combined with L19-TNF therapy.

Conclusion:
We could establish this innovative *in vivo* CRISPR screen in Zurich that overcomes limitations in the field and discover promising novel vulnerabilities of glioblastoma when studied in a complex environment of fully immunocompetent hosts. Ongoing studies will focus on validating the expression and therapeutic relevance of these candidate genes in human glioblastoma tissues across newly diagnosed and recurrent cohorts.

808

F. Westphal[1], D. Harmacek[1], R. Elena[1], L. Weidmann[1], K. Castrezana Lopez[1], B. George[1], S. von Moos[1], T. Schachtner[1]

Correlation of activity, and chronicity indices derived from Banff lesion scores with injury dimension scores from biopsy-based transcript diagnostics

University Hospital Zurich[1]

Introduction:
The histological results of kidney allograft biopsies are classified according to Banff and enable medical professionals to estimate the prognosis and make treatment decisions. Recently, indices for activity and chronicity based on the Banff classification (Haas et al., Vaulet et al.) have gained attention. Biopsy-based transcript diagnostics offer a novel approach to classify and quantify rejection and injury of kidney allograft biopsies. Roufosse et al. recently raised the question if transcript diagnostics offer similar or additional information to activity and chronicity indices based on light microscopy.

Methods:
465 kidney allograft biopsies from the University Hospital Zurich were included. All biopsies were analyzed histologically according to Banff 2022 and by the Molecular Microscope Diagnostics System (MMDx). The activity and chronicity indices were calculated as linear combinations of Banff lesion scores according to the authors Haas et al. and Vaulet et al. The molecular injury dimension scores of global disturbance, acute kidney injury, and atrophy-fibrosis were obtained from the MMDx report. Data were analyzed with Python 3.9.

Results:
The activity indices of Haas and Vaulet had mean values (standard deviation) of 2.12 (1.98) and 0.28 (0.18), respectively. The correlation of the normalized two activity scores was 0.81. The correlation increased to 0.89 by using the modified activity index provided by Vaulet, which excludes thrombotic microangiopathy and donor-specific antibodies (DSA) from the linear combination. The chronicity indices of Haas and Vaulet had mean values (standard deviation) of 5.41 (4.39) and 0.39 (0.24), respectively, and achieved a correlation of 0.93. The molecular injury dimension scores of global disturbance, acute kidney injury, and atrophy-fibrosis had mean values (standard deviation) of -0.21 (3.0), 0.17 (0.67), 0.41 (0.29). The molecular injury dimensions of global disturbance and acute kidney injury showed a moderate and low correlation with the histological activity indices (0.21 to 0.44). Notably, the correlation of the global disturbance score with the modified activity index from Vaulet was highest (0.54). The molecular atrophy-fibrosis score showed a moderate correlation with the histological chronicity indices (0.47 (Haas et al.) and 0.54 (Vaulet et al.)).

Conclusion:
Our results demonstrate that indices, which are designed to predict similar target conditions, correlate best. The addition of DSA to the activity index of Vaulet leads to a less strong correlation with the Haas activity index. The different molecular injury dimensions assessed by the MMDx correlate only moderately with the indices derived from the Banff lesions. Therefore, the different techniques applied to kidney allograft biopsies generate at least partially different information. If a more in-depth analysis of this information could lead to an improvement in prognostication needs to be studied.

810

M. Mastall[1], G. Dunkel[3], N. Okada[2], T. Weiss[1], B. Weigelin[3], M. Weller[1], P. Roth[1]

Dual-CAR T cells against NKG2D ligands and VEGFR2 accumulate in orthotopically implanted glioma and prolong survival of immunocompetent glioma-bearing mice

Department of Neurology, University and University Hospital Zurich, Switzerland[1], Project for Vaccine and Immune Regulation, Graduate School of Pharmaceutical Sciences, Osaka University, Osaka, Japan[2], Werner Siemens Imaging Center, Department of Preclinical Imaging and Radiopharmacy, Eberhard Karls University, Tuebingen, Germany[3]

Introduction:
Glioblastoma is the most common malignant brain tumor with a devastating outcome. Novel therapeutic strategies are currently explored including the use of chimeric antigen receptor (CAR) T cells. However, in glioblastoma an impaired tumor infiltration by CAR T cells, antigen heterogeneity and an immunosuppressive tumor microenvironment remain significant obstacles. NK group 2D (NKG2D)-CAR T cells efficiently lyse glioma cells and confer a survival benefit of glioma-bearing immunocompetent mice upon intratumoral administration. This effect is less prominent after intravenous injection, suggesting an insufficient trafficking of CAR T cells into the tumor. Vascular endothelial growth factor receptor 2 (VEGFR2)-CAR T cells were shown to accumulate solid tumors upon intravenous administration and to have anti-glioma and anti-angiogenic activity. However, VEGFR2 expression in glioblastoma is heterogenous. Here, we generated Dual-CAR T cells targeting VEGFR2 and NKG2D ligands.

Methods:
Murine VEGFR2, NKG2D, CD19, Mock or Dual-CAR T were generated by retroviral transduction. *In vitro*, their activity was explored in co-culture assays. Glioma cells (CT-2A, GL-261) or lymphoma cells (A20) were orthotopically implanted into brains of immunocompetent mice and the infiltration of intravenously administered CAR T cells was assessed by *in vivo* fluorescence molecular tomography (FMT), *ex vivo* flow cytometry as well as 3D light-sheet microscopy (3D-LSFM).

Results:
Co-culture experiments demonstrated increased lysis of glioma cells by Dual-CAR T cells compared to VEGFR2-CAR T cells. By *ex vivo* 3D-FLSM, we observed substantial trafficking of systemically administered VEGFR2-CAR T cell into gliomas *in vivo*. Analysis of the whole 3D tumor area indicated that VEGFR2-CAR T cells extravasated and infiltrated deeper into the tumor core compared to Mock T cells. In two different glioma models, FMT imaging as well as *ex vivo* flow cytometry revealed that Dual-CAR T cells accumulated to a similar extent at the tumor site as VEGFR2-CAR T cells and around 10-fold more Dual-CAR T cells were detected compared to CAR T cells expressing the NKG2D-CAR alone. In addition, Dual-CAR T cell treatment resulted in reduced growth of orthotopically growing gliomas and significantly prolonged the survival of glioma-bearing mice compared to Mock or NKG2D-CAR or VEGFR2-CAR T cell treatment. Finally, by FMT *in vivo* imaging a higher signal of labeled systemically administered CD19-CAR T cells was observed at the site of a CNS lymphoma model if they additionally expressed the VEGFR2-CAR.

Conclusion:
Recent advances in CAR T cell optimization are mostly focused on CAR design, CAR generation and improving metabolic fitness, while improvements in CAR T cell trafficking are limited. VEGFR2-CAR T cells exhibited enhanced infiltration into the tumor site in the brain and arming of VEGFR2-CAR T cells with a NKG2D-CAR resulted in prolonged survival of glioma-bearing mice. Therefore, Dual-CAR T cells offer a versatile approach for the treatment of glioblastoma addressing two main hindrances, tumor infiltration and antigen heterogeneity. The additional CNS lymphoma model suggest that this strategy could by exploited for the treatment with CAR T cells against other brain tumor entities.

811

M. Meerang[3], M. Glettig[2], MB. Couger[1], F. Barkmann[2], V. Boeva[2], R. Bueno[1], I. Opitz[3, 4]

Pipeline establishment for reliable single nuclei RNA-sequencing analysis of banked frozen pleural mesothelioma tumors

Brigham and Women's Hospital, Boston, MA, United States[1], Department of Computer Science, ETH Zurich, Switzerland[2], Department of Thoracic Surgery, University Hospital Zurich, Switzerland[3], University of Zurich, Switzerland[4]

Introduction:
This project aims to establish a reproducible protocol for single nuclei RNA-sequencing (snRNA-seq) to assess the heterogeneity of pleural mesothelioma (PM) at the single-cell level using archived frozen tissue biobank samples across all PM histological subtypes.

Methods:
Tissue specimens from PM patients were collected and divided into two parts: one part was immediately processed for single-cell RNA sequencing (scRNA-seq), and the other part was frozen for snRNA-seq. After a minimum of 8 weeks of storage, the tissues were processed for snRNA-seq. We utilized the 10X Chromium Single Cell 3' Reagent Kit for both scRNA-seq and snRNA-seq.

Results:
Using the optimized nuclear isolation protocol, we conducted preliminary analyses of paired snRNA-seq and scRNA-seq on 7 PM patients from Zurich including 5 Epithelioid, and 2 Biphasic subtypes. We observed high-quality nuclei with high read and gene counts. Integration of snRNA-seq and scRNA-seq samples with the BBKNN by sample method showed little grouping by sequencing technology. The enrichment of both epithelioid and sarcomatoid malignant cells was detected in nuclei samples. Conversely, immune cells were underrepresented in nuclei samples. Furthermore, the integration of samples across technology showed strong grouping of cells by cell type across the protocols. These findings are further validated by data from Boston, which includes an extensive single-cell reference set for PM, derived from over 40 samples. This reference set contains 400,000 high quality cells derived from epithelioid, biphasic, and sarcomatoid surgical resected samples. In total we produced 1 billion UMIs covering the transcripts. We produced detailed transcriptomes for malignant cell populations, fibroblast, endothelial cells, chondrocytes, CD8 cytotoxic T-cells, CD4 helper T-Cells, Plasma B-cells, activated B-Cells, Natural Killer Cells, and multiple distinct populations of Macrophages.

Conclusion:
The underrepresentation of myeloid and lymphoid immune populations of snRNA-seq limits the investigation of immune heterogeneity. In addition to guiding our efforts for snRNA-seq, this sequencing project has produced a logic gated set of markers allowing us to differentiate these cell types from each other. This set is currently being used to create a 480 marker panel to allow spatial classification of all cells present in the tumor microenvironment.

812

M. Germans[7], J. Rohr[7], C. Globas[8], T. Schubert[9], A. Kaserer[3], G. Brandi[2], J. Studt[6], M. Greutmann[5], K. Geiling[4], L. Verweij[1], L. Regli[7]

Challenges in Coagulation Management in Neurosurgical Diseases: A Scoping Review, Development, and Implementation of Coagulation Management Strategies

Institut für Implementation Science in Health Care, Universität Zürich[1], Institut für Intensivmedizin, Universitätsspital Zürich[2], Klinik für Anästhesiologie, Universitätsspital Zürich[3], Klinik für Geriatrie, Universitätsspital Zürich[4], Klinik für Kardiologie, Universitätsspital Zürich[5], Klinik für Medizinische Onkologie und Hämatologie, Universitätsspital Zürich[6], Klinik für Neurochirurgie, Universitätsspital Zürich[7], Klinik für Neurologie, Universitätsspital Zürich[8], Klinik für Neuroradiologie, Universitätsspital Zürich

Introduction:
Bleeding and thromboembolic (TE) complications significantly impact outcomes in neurosurgical patients. Current guidelines fail to address the individual circumstances of neurosurgical patients, necessitating a comprehensive approach to coagulation management. This study presents a scoping review identifying knowledge gaps and introduces the COagulation MAnagement in Neurosurgical Diseases (COMAND) project aimed at reducing coagulation-related complications.

Methods:
A scoping review was conducted following the PRISMA-ScR guidelines. MEDLINE (PubMed) was searched for systematic reviews on bleeding and TE complications in neurosurgery, limited to English-language studies on adults. Two independent reviewers screened 1028 articles on bleeding and 150 on TE complications, selecting 24 and 17 relevant studies, respectively. Data extraction focused on reported incidence rates for bleeding and TE complications in neurosurgical patients. The findings were synthesized to identify gaps in current guidelines and highlight areas for future research.

Results:
The review identified significant heterogeneity in bleeding and TE risks across neurosurgical diseases. Postoperative hemorrhage risks vary from 3% in elective craniotomies to 14-33% in trauma and spontaneous intracerebral hemorrhage cases, while spinal surgery carries a postoperative bleeding risk of 0.5-1.4%. Subarachnoid hemorrhage (SAH) is associated with a high bleeding risk, particularly in cases of aneurysmal rupture, with rebleeding rates reaching up to 10% within the first 24 hours if left untreated. TE complications are also significant, with reported risks of 6.7-21% in SAH patients. TE complications occur in 3-20% of intracranial pathologies and approximately 7% in spinal surgery.
The COMAND project is an interprofessional initiative involving experts from neurosurgery, hematology, neurocritical care, anesthesiology, cardiology, geriatrics, epidemiology, and implementation science. This collaborative approach ensures that coagulation management strategies are evidence-based, feasible, and adaptable to different clinical settings. The project aims to develop individualized protocols tailored to neurosurgical conditions while integrating implementation strategies to facilitate their adoption in daily practice.

Conclusion:
Bleeding and thromboembolic complications are common in the neurosurgical population, with risks varying based on the type of disease and multiple influencing factors. Given this complexity, developing universal guidelines for coagulation management in neurosurgical patients is challenging. A more individualized approach, tailored to specific patient needs and underlying conditions, may provide better outcomes and more effective risk mitigation strategies.

813

M. Telesca[1], V. Masciovecchio[1], I. Papadopoulou[1], SA. Mohammed[1], E. Gorica[1], J. Spezzini[1], A. Mongelli[1], K. Urbanek[2], A. De Angelis[2], L. Berrino[2], L. Burkhard[1], F. Paneni[1], F. Ruschitzka[1], S. Costantino[1]

Employing Epi-drugs to Rescue Lung Microenvironmental Changes in Heart Failure with Preserved Ejection Fraction

Center for Translational and Experimental Cardiology (CTEC), Department of Cardiology, University Hospital Zurich, University of Zurich, Wagistrasse 12, 8952, Schlieren, Switzerland.[1], Università degli Studi della Campania Luigi Vanvitelli, Naples - Italy[2]

Introduction:
Heart failure with preserved ejection fraction (HFpEF) is the most common form of heart failure and is frequently complicated by the development of pulmonary hypertension (PH). The prevalence of PH in HFpEF ranges from 30% to 80%, and it is a strong predictor of mortality. Understanding changes of the lung microenvironment, namely cell-cell communications among fibroblasts, immune and endothelial cells, could unveil new targets to tackle microvascular dysfunction and PH in this setting. Epigenetic changes, namely post-translational histone modifications, are emerging as pivotal modulators of gene expression in cardiovascular disease, and their therapeutic modulation by specific epi-drugs could rescue disease phenotypes.The purpose of the study is to investigate changes of the lung microenvironment in the HFpEF lung and to test the effect of new epi-drugs on PH development.

Methods:
Mice were fed a normal-diet (ND, control) or high-fat-diet (HFD) and L-NAME for 15 weeks to induce HFpEF-related PH (HFpEF-PH). Control and HFpEF-PH mice were chronically treated with the BET protein inhibitor Apabetalone (APA) for 14 days. High resolution ultrasound imaging (Vevo 3100, Visualsonics) was employed to assess cardiac function and pulmonary pressure. Single-cell nuclei RNA sequencing (scRNA-seq) was performed in lung specimens from the different experimental groups. Primary endothelial cells (ECs) and fibroblasts (mFs) were isolated from HFpEF-PH lungs and treated with APA for 48 hours.

Results:
HFpEF mice displayed PH, as evidenced by elevated pulmonary artery pressure, increased pulmonary artery resistance, extended right ventricular wall thickness, and diminished pulmonary artery acceleration time. In vivo treatment with APA prevented PH development in HFpEF mice. To establish the cell types modulated by APA, we conducted scRNA-seq. The highest enrichment of genes whose expression was significantly correlated with echo-determined PH features was observed in mFs and mECs. Interactome analyses of our snRNAseq dataset showed that mFs are the primary source of intercellular signals in HFpEF-PH lungs. Both mECs and mFs from obese mice exhibited an altered phenotype. Specifically, mFs displayed a myo-fibroblast phenotype and altered bioenergetic profile, as shown by seahorse experiments, whereas mECs displayed defective autophagy and upregulation of NF-kB-related inflammatory genes, hypoxia-inducible factor (HIF1-α), and NADPH-oxidase-NOX4. Of note, treatment with APA rescued mECs and mFs transcriptional alterations and cell dysfunction in HFpEF-PH mice.

Conclusion:
APA can reset the lung microenvironment in a cardiometabolic model of HFpEF-PH, reducing inflammation and cellular senescence. BET inhibitors may be promising epi-drugs to treat PH in in HFpEF.

814

A. Rooney[1], Y. Yi Li[1], A. Diversi[1], K. Haldimann[1], A. Andrade Barrios[1], J. Scherrer[1], D. Albertos Torres[1], P. Göller[1], A. Egli[1]

Swab comparison for ease-of-use assessment and oral microbiota characterization

Institute of Medical Microbiology, University of Zurich, Zurich, Switzerland[1]

Introduction:
The oral microbiota is a dense and complex environment with links to health outcomes such as periodontitis and cardiovascular disease. Multiple factors may influence microbiota composition, where the influence of sample collection methods should be minimized. Our aim was to compare three different oral swabs to assess ease-of-use, DNA concentration, and microbiota composition.

Methods:
The Isohelix buccal swab with Dri-Capsules (I), the Omnigene oral swab (O), and the Zymo Research DNA/RNA Shield SafeCollect swab (Z) were evaluated. Ten healthy anonymized participants swabbed along the gum line at the base of the teeth for 30 seconds per swab. Questionnaires regarding ease-of-use were completed. Swabs were subject to DNA extraction with the Maxwell RSC Buccal Swab DNA kit and DNA concentration was measured with the Qubit Fluorometer. DNA was subject to 16S rRNA and ITS sequencing using the QIAseq 16S/ITS Screening Panel on the Illumina MiSeq. The 16S V3 and V4 hypervariable regions were analyzed for species-level alpha- and beta-diversity and were performed using QIIME2 v.2024.10.

Results:
Analyses of the 10 participants showed that participants preferred O and Z for ease-of-use and potential for limiting swab contamination. The mean post-extraction DNA concentration was low for I (0.8 ng/ml) compared to O (11.5 ng/ml) and Z (10.8 ng/ml). The mean alpha-diversity measured at the genus-level (Chao1 and Shannon Diversity Index) were 25 and 2.6 for I, 26.5 and 2.4 for O, and 30.8 and 3.1 for Z. Beta-diversity measured by Bray-Curtis dissimilarity did not demonstrate a swab-specific effect on microbiota composition.

Conclusion:
Both O and Z swabs resulted in positive ease-of-use assessments, high DNA concentrations post-extraction, and were able to differentiate individuals' oral microbiota composition with no differences in diversity measures between swabs. Considering pre-analytical quality is key for oral microbiota studies.

815

T. Vancsik[1], C. Rossel Dorca[3], M. Ronner[1], F. Schläpfer[1], LR. Herrador[3], S. Arni[1], M. Meerang[1], H. Gehart[3], I. Opitz[1, 2]

Patient-Derived Tumoroid Xenograft Models for Preclinical Validation of Therapeutics for Pleural Mesothelioma

Department of Thoracic Surgery, University Hospital of Zürich[1], Faculty of Medicine, University of Zürich[2], Institute of Molecular Health Sciences, ETH Zürich[3]

Introduction:
Pleural mesothelioma (PM) is a highly heterogeneous and aggressive cancer with limited therapeutic options. To advance personalized treatments, patient-derived tumoroid cultures that preserve the morphological and molecular characteristics of their original tumors across the epithelioid-sarcomatoid spectrum were established. High-throughput screening of these tumoroids with 3,000 FDA-approved compounds identified both common and patient-specific targets. Here, we conducted *in vivo* studies to validate the efficacy of promising therapeutic candidates using optimized tumoroid xenograft models.

Methods:
We developed orthotopic intrapleural and subcutaneous xenograft models using PM050 PM tumoroid cell line, which represents biphasic characteristics and engineered to express fluorescent and bioluminescent markers for non-invasive monitoring of disease progression. Injection parameters were optimized to achieve reproducible tumor growth kinetics. Pilot studies evaluated the therapeutic effects of romidepsin, a histone deacetylase inhibitor, and sepantronium bromide, a survivin inhibitor, in comparison to cisplatin-pemetrexed, the current standard of care. Tumor growth and drug efficacy were monitored through imaging and confirmed by histological analysis.

Results:
Both orthotopic and subcutaneous models produced detectable tumor phenotypes with growth kinetics correlating to the cell number injected. Subcutaneous grafts developed visible macroscopic tumors, while intrapleural grafts demonstrated diffuse growth patterns. Histological analysis confirmed that xenografts retained the expression of key PM markers including negative calretinin and positive vimentin, consistent with *in vitro* tumoroids and the original tumor tissue. No significant tumor size reduction was observed with therapeutic intervention with cisplatin-pemetrexed or romidepsin, whereas sepantronium bromide exhibited a trend toward tumor growth attenuation, though variability warrants further study.

Conclusion:
Our findings demonstrate the feasibility of tumoroid-based xenograft models for preclinical validation of PM therapies. The models accurately reflect disease heterogeneity and provide a robust platform for testing novel drugs. These initial results highlight the potential of targeting survivin with sepantronium bromide. Further studies to confirm the therapeutic potential of sepantronium bromide are ongoing.

816

V. Ntinopoulos[1], H. Rodriguez Cetina Biefer[1], P. Risteski[1], L. Rings[1], S. Dushaj[1], O. Dzemali[1]

Performance of an open-source, offline-capable large language model in data extraction from unstructured electronic health records

Cardiac Surgery Department, University Hospital of Zurich[1]

Introduction:
Open-source large language models may provide a solution to the data privacy issues hindering the use of large language models for processing health records. In this study we assess the performance of a recently released state-of-the-art open-source and offline-capable large language model, in data extraction from unstructured electronic health records.

Methods:
Fifty fictitious patient medical records were drafted in German and the open-source large language model (all three differently sized variants: 405B, 70B, and 8B) was provided with instructions on processing each one. Data extraction involved text-mining and classification tasks for nine variables. Two closed-source state-of-the-art large language models, were used for comparison. Large language model prompting and use were performed via online available deployments of the models.

Results:
The accuracy of the open-source large language model over all 450 requested values was 100% (no false predictions) for the 405B model, 98.6% (6 false predictions, all binary classifications) for the 70B model and 90.8% (41 false predictions, all binary classifications) for the 8B model. The accuracy of both compared closed-source large language models was 100% (no false predictions).

Conclusion:
The 405B version of the open-source large language model exhibited excellent performance, on par with the two compared closed-source models. Further research with a local offline installation of the 405B model on a computationally capable computing infrastructure using real health records is warranted to confirm these results.

817

A. Kraft[1, 2], A. Tönz[2], F. Schläpfer[2], M. Ronner[2], V. Orlowski[2], MB. Kirschner[2], V. Boeva[1, 3, 4], I. Opitz[2], M. Meerang[2]

Exosomal RNA Profiling Identifies GAS5 and Other Long Noncoding RNAs as Circulating Diagnostic Biomarkers for Pleural Mesothelioma

Department of Computer Science, Institute for Machine Learning, ETH Zurich, Zurich, Switzerland[1], Department of Thoracic Surgery, University Hospital Zurich, Zurich, Switzerland[2], ETH AI Center, ETH Zurich, Zurich, Switzerland[3], INSERM, U1016, Cochin Institute, CNRS UMR8104, Paris Descartes University, Paris, France[4]

Introduction:
Pleural mesothelioma (PM) is a rare but highly lethal cancer for which early, non-invasive diagnostic tools are critically lacking. RNAs secreted by tumor cells via exosomes are detectable in plasma and have emerged as promising biomarkers for non-invasive disease diagnosis. This study aimed to compare the RNA cargo of exosomes secreted by primary PM cells with those from non-PM cells, to identify circulating biomarkers that potentially could be used as blood-based diagnostic biomarkers for PM.

Methods:
Primary cell cultures were established from pleural effusions of 12 PM and 7 non-PM patients. Exosomes were isolated from cell culture supernatants using iZON qEV columns, followed by total RNA extraction using the mirVana PARIS kit and RNA sequencing. Sequencing reads were mapped to the human reference genome (GRCh38), and differential expression analysis was performed using DESeq2 to identify RNAs enriched in PM-derived exosomes. Candidate RNAs were validated in exosomes and plasma samples from PM and non-PM patients.

Results:
We identified 2,089 RNAs upregulated in PM-derived exosomes, with the majority comprising long noncoding RNAs (lncRNAs) (34%), pseudogenes (30%), and protein-coding genes (27%). Enriched biological processes included proliferation, protein secretion and epithelial-mesenchymal transition, all hallmarks of tumorigenesis. Among the lncRNAs, GAS5, a gene previously implicated in cancer, emerged as aparticularly promising candidate for PM diagnosis. Quantitative-PCR validation confirmed significantly higher GAS5 expression in exosomes from PM compared to non-PM samples.

Conclusion:
This study provides a comprehensive analysis of exosome-secreted RNAs in PM, identifying candidate biomarkers for blood-based diagnostic tests. Our findings underscore the critical role of the PM secretome in understanding PM biology and highlight GAS5 as a strong diagnostic candidate. We are currently validating these biomarkers in pleural effusion and plasma derived exosomes to further establish their clinical utility.

818

K. Lehmann[1], T. Schweizer[1, 2], G. Kadler[1, 3], A. Kalyanov[4], H. Walt[1], H. Essig[1]

Zirconium dental implants as optical waveguides in antimicrobial photodynamic therapy

University Hospital of Zurich, Department of Cranio-Maxillo-Facial and Oral Surgery[1], University Hospital of Zurich, Department of Dermatology[2], University Hospital of Zurich, Department of Intensive Care Medicine[3], University of Zurich and University Hospital of Zurich, Department of Neonatology, Biomedical Optics Research Laboratory[4]

Introduction:
Dental implant bacterial colonization can lead to mandibular or maxillary osteomyelitis in preexisting medication-related jaw osteonecrosis (MRONJ). Debridement, lavage and antibiotics can be effective, but concealed intraosseous prosthetic biofilm formations and antimicrobial resistance (AMR) impede successful treatment. With increasing global AMR prevalence, therapy options according to the One Health antibiotics stewardship approach are of unprecedented need to guarantee optimal future MRONJ treatment outcome. Antimicrobial photodynamic therapy (aPDT) combined with optical waveguides could eradicate those biofilms without the risk of AMR, thus aligning with the One Health approach. Therefore, this study investigates the waveguiding function of light transmitting Zirconium (ZrO2) dental implants in aPDT with Titanium (TAV) implants as a control.

Methods:
In-vitro grown Staphylococcus epidermidis biofilms on zirconium (n=115) and titanium (n=100) implants were treated for 1.5 minutes with 1, 10, 100 µg/ml methylene blue (MB) photosensitizer or H2O as a control before red light illumination (670 nm) from above with 0, 15, 30 (15 J/cm2 each from above and below), 45, 90 J/cm2 intensity. The CFU number after 1 minute of sonication, overnight agar plate incubation at 37° and divided by the H2O and 0 J/cm2 control CFU number determined the surviving bacteria. Furthermore, light absorption, intensity transmission and polarization were investigated in zirconium dental implants with 3.5, 4.1, 4.5, 5 mm diameters.

Results:
Increasing MB concentration and radiation intensity decreased CFU in both implant groups. At 10 µg/ml MB for 15, 30, 45, 90 J/cm2radiation, 74, 84, 95, 77% bactericidal effect for zirconium substantially differed from titanium with 70, 36, 47, 60%. Additionally, zirconium dental implants demonstrated a characteristic absorption spectrum with 2.3*10-5 red light intensity transmission/cm2 and no detectable polarization.

Conclusion:
Zirconium dental implant waveguiding in aPDT showed a strong bactericidal effect, strengthening the vision for a clinical application in infected dental implants. The optical characteristics of ZrO2 seem to be superior to those of TAV and enable future research to explore practical implementation as waveguides in MRONJ therapy. The successful clinical use of this biofilm-directed aPDT has the potential to reduce the need for antibiotic prescription, thus advancing the One Health approach of antibiotic stewardship.

819

Z. Germuskova[3], E. Pronzini[3], T. Roloff[3], E.M. Broens[4], K. Søgaard[1], F. Renzi[2], A. Egli[3]

Emerging evidence of antimicrobial resistance in Capnocytophaga canimorsus and the implications for empiric treatment choices

Aalborg University Hospital[1], University of Namur[2], University of Zurich[3], Utrecht University[4]

Introduction:
Capnocytophaga species, particularly *C. canimorsus*, are common colonizers of the oral cavity of dogs and cats and can cause severe infections in humans following animal bites. Penicillins, such as amoxicillin, are a frequent empiric antibiotic choice for bite-wound infections, often paired with β-lactamase inhibitors like clavulanic acid. However, the emergence of antimicrobial resistance (AMR) in these bacteria poses a significant clinical challenge. Due to their slow growth and fastidious nature, species identification and antibiotic susceptibility testing (AST) is often not feasible, necessitating reliance on empiric therapy. We aimed to determine the prevalence of AMR in *Capnocytophaga* isolated from human infections and animal oral microflora.

Methods:
Through the Global *Capnocytophaga* Consortium, we retrospectively collected *Capnocytophaga* isolates from human infections and from animals (dogs and cats) across 12 countries. AST was performed on 85 strains, including the *C. canimorsus* ATCC 35979 type strain, using the agar dilution method with amoxicillin and amoxicillin-clavulanic acid solid media plates. A subset of strains was whole genome sequenced (WGS) to identify potential AMR genes (Illumina, 150nt, paired-end).

Results:
In preliminary testing of 85 strains using the agar dilution method, we observed two distinct population of strains with different susceptibilities to amoxicillin: wild-type (MIC50 = 0.5mg/L), representing 82% of the tested strains, and non wild-type (MIC50 = 32mg/L), representing 18% of all strains. Addition of clavulanic acid resulted in a 4 to 7-fold reduction in the MIC values of the non-wild type population. WGS revealed the non wild-type strains are enriched for the presence of *blaOXA-347* gene, a putative β-lactamase. The 85 strains are currently under investigation to verify the potentially resistant phenotype and elucidate the genotype-phenotype relationship in these isolates, with the total number of strains tested expected to reach 250 as the study progresses.

Conclusion:
Our findings indicate a high prevalence of potential amoxicillin resistance in *Capnocytophaga canimorsus*, suggested by elevated MIC values in a subset of strains, correlating with the presence of the *blaOXA-347* gene. However, further phenotypic susceptibility testing suggests that clavulanic acid partially restores amoxicillin efficacy, emphasizing the role of β-lactamase inhibitors in treatment. The tested *C. canimorsus* isolates were recovered from wound infections, bloodstream infections, and independently from oral microflora of dogs and cats, underscoring the widespread presence of potential amoxicillin resistance. Ongoing investigations with an expanded strain collection will provide insights into the genotype-phenotype relationship. These findings point to the urgent need to investigate global distribution patterns of AMR in *Capnocytophaga* using standardized methods, and caution against overreliance on empiric therapy after dog bites.

820

F. Davidhi[2], F. Costa[2], D. Ledergerber[1], I. Indiveri[3], L. Imbach[1], J. Sarnthein[2]

Event-based seizure detection in iEEG using neuromorphic hardware

Swiss Epilepsy Center, Klinik Lengg[1], University Hospital of Zürich[2], University of Zurich and ETH Zurich[3]

Introduction:
Accurate seizure monitoring is critical for patient management, yet current methods, such as seizure diaries, are often unreliable. Chirps are iEEG frequency patterns that are associated with seizures. Neuromorphic hardware, with its low power consumption and real-time processing capabilities, is a promising platform to detect these patterns. Using chirps and neuromorphic engineering, we aim to perform real-time seizure detection in intracranial EEG (iEEG).

Methods:
We analysed iEEG data to identify chirps. In pre-recorded iEEG data from one patient, we filtered in 6 frequency bands in the range 0-40 Hz. We then employed a software Asynchronous Delta Modulation (ADM) encoder for encoding analog waveforms in two streams of UP/DOWN events. These events were used as input spikes in an SNN implemented on a neuromorphic chip processor (Costa et al. Nature Communications 2024;15(1):3255.). Each frequency band is mapped on a neural population that inhibits all others aside from the next one, in order from high to low frequency. This results in a network able to detect monotonic chirps in the iEEG data. The lowest frequency population of the network connects to an output chirp-counting population to reliably detect chirps, and thereby seizures.

Results:
In 48 consecutive hours of one iEEG channel from one patient, we detected all 40 seizures (sensitivity = 100%) with one false detection (false detection rate = 0.021 per hour). For 4 hours of iEEG, the mean processing duration was 4 hours and 55 seconds (standard deviation = 41.72 seconds).

Conclusion:
These findings highlight the feasibility of real-time chirp-based seizure detection using a spiking neural network implemented on neuromorphic hardware, showing potential for real-time seizure monitoring in human iEEG. This work is supported by the Swiss National Science Foundation (204651).

821

D. Dimakopoulos[1], JJB. Teurlings[1], D. Ledergerber[3], L. Imbach[2, 3], J. Sarnthein[1, 2]

Human ripples underlying working memory lateralize to healthy hippocampus

Department of Neurosurgery, University Hospital Zürich[1], Neuroscience Center Zürich (ZNZ), University of Zürich and ETH Zürich[2], Swiss Epilepsy Center, Klinik Lengg, Zürich[3]

Introduction:
Short high-frequency oscillatory events (physiological ripples) in the hippocampus are known to occur during encoding and retrieval of episodic memories in animals and humans. Physiological ripples are distinct from epileptic high frequency oscillations that indicate the epileptogenic zone (Dimakopoulos et al. Brain 2025; online) and whose rate is not modulated by task performance (Boran et al. Front Hum Neurosci. 2021;15:613125). The hippocampus contributes to the network involved in working memory processing but the role of ripples in working memory is yet unknown.

Methods:
We detected ripples from electrodes implanted bilaterally in the hippocampal CA1 region of 15 neurosurgical patients (7 male) performing a verbal working memory task that separates the stages of the trial (encoding, maintenance and retrieval) (Dimakopoulos et al. Elife 2022;11:e78677). We determined the ripple rate during the trial stages and recorded patients' responses. After patients underwent resective epilepsy surgery, we classified seizure outcome as seizure free (ILAE 1) or seizure recurrence (ILAE 2-6).

Results:
In 24078 ripples across 3452 trials, we find that ripples cluster early during the encoding stage and, most prominently, while items were retrieved when participants engaged in response by button press. The ripple rate was higher for trials with correct response than for incorrect response ($P = .002$). All 10 patients with a higher ripple rate (0.2 IQR 0.18 0.24 ripples/s) in the non-resected hippocampus achieved postsurgical seizure freedom (ILAE 1) and the opposite was true for all 5 patients with ILAE 2-6 (OR 231 CI [4 13304], $P < 0.001$ chi-square test).

Conclusion:
The clustering suggests that ripples mediate both encoding and retrieval of working memory items in the functional (but not the epileptic) hippocampus. This highlights the distinction between epileptic high frequency oscillations and physiological ripples involved in a cognitive task. A non-functional hippocampus may serve as a predictor of postsurgical seizure freedom. (SNSF 204651).

822

V. Mavrodiev[1], C. Bockisch[1], W. Weber[1, 2], F. Fierz[2]

Investigating differences in the early visual response to a moving visual field in patients with visual dependency

Department of Neurology, University Hospital Zurich, Switzerland[1], Department of Ophthalmology, University Hospital Zurich, Switzerland[2]

Introduction:
Our goal was to study the discrepancies in the early visual response between patients with visual dependency and healthy controls. We utilized the ocular following responses (OFRs) to moving visual fields as well as the participants' ability to suppress eye movements when instructed. OFRs are quick eye movements that track sudden movements of a textured pattern.

Methods:
The prospective data was collected from 30 healthy subjects and 29 participants with or without vestibulardisorders reporting visual dependency. The subjects were seated in front of a projection screen. A field of dots was projected on the screen, including a moving central visual field with four different radii of visual angle or a moving annular visual field with a stationary center. Two sets of instructions were given: the first one allowed the subjects to follow the moving portion of the dots, and the second one instructed them to fixate a flashing cross in the center without allowing their eyes to move with the dots. Using a video eye tracker, the eye velocity was recorded.

Results:
We quantified the early eye movement response as the velocity 200 msec after the pattern movement started. We quantified the early eye movement response as the velocity 200 msec after the pattern movement started. Eye velocity when the central region moved increased when the region size became larger, reaching peak velocity of about 5°/s for patients and 4°/s for control subjects. When the surrounding dots moved, eye velocity was highest (1-2 °/s) when the central region was small and went to 0°/s when the whole screen was stationary. While there is a trend for patients to have shorter reactions times to the moving visual field, this was not significant

Conclusion:
Subjects with visual dependency exhibited an enhanced ocular following response velocity and an enhanced response to smaller-sized stimuli compared to healthy controls. When given fixation instructions, they showed a decreased ability to suppress the OFR. The findings may contribute to a better clinical characterization of patients with visual dependency, thus forming the basis for targeted treatment approaches.

823

V. Mavrodiev[1], C. Bockisch[1], K. Weber[1, 2], F. Fierz[2]

Vestibular rotation cancellation perception by vision in patients with increased visual dependency

Department of Neurology, University Hospital Zurich, Switzerland[1], Department of Ophthalmology, University Hospital Zurich, Switzerland[2]

Introduction:
Our goal was to investigate differences in patients with visual dependancy compared to healthy controls utilizing perceptual measures of self-movement in situations where visual motion and vestibular signals give conflicting information.

Methods:
Recruitment was conducted at the outpatient clinic of the University Hospital Zurich. Prospective data was collected from 31 healthy individuals as well as 24 subjects with increased visual dependency. Subjects were passively rotated in space and exposed to visual stimulation that conflicted with the actual motion and the motion sensed by the vestibular system. Subjects indicated their perceived direction of self-motion. We measured how long it takes for the perception of self-motion, initially dominated by vestibular signals, to transition into being dominated by visual signals. This was carried out by a rotating chair, moving independently of a patterned drum around the chair. Runs with various conditions were performed - movement of the chair in darkness, movement of the chair and the drum with the same speed with lights on (cancellation trial) as well as movement of the chair and drum in the same direction but with different speeds with lights on (reverse trial).

Results:
When rotating in the dark, patients and control subjects perceived rotation for a similar amount of time, on average (11.3 s for controls, 11.7 s of patients, t=0.4, p=0.67, df= 54), suggesting that the vestibular response to the slow yaw rotations in our groups were similar. When the surround was visible but stationary, perceived rotation increased to about 14 s for both patients and controls but declined as the visual surround (and the visual-vestibular conflict) speed increased. When the visual surround moved at twice the speed of the person rotation, the average duration of perceived rotation was 4.2s for patients and 3.8s for controls.

Conclusion:
On average, patients with visual dependency did not show greater reliance on visual cues when visual and vestibular self-motion stimuli conflict. We could not measure a quantifiable difference in the perception of movement when putting the vestibular and the visual systems in conflict.

824

C. Steinack[3], P. Baumgartner[2], GM. Monsch[4], D. Schneiter[4], S. Oh[1], E. Samara[5], I. Opitz[4], C. Clarenbach[3], S. Ulrich[3], M. Kohler[3], T. Gaisl[3]

Impact of Robotic-Assisted Bronchoscopy with Integrated Cone-Beam CT on Stage Shift in Peripheral Pulmonary Lesions at a Lung Cancer Centre

Section of Interventional Pulmonology, David Geffen School of Medicine, University of California, Los Angeles, Los Angeles, California[1], Universitätsspital Zürich, Klinik für Innere Medizin, Zurich, Switzerland[2], Universitätsspital Zürich, Klinik für Pneumologie, Zurich, Switzerland[3], Universitätsspital Zürich, Klinik für Thoraxchirurgie, Zurich, Switzerland[4], Universitätsspital Zürich, Radiation Protection Unit, Zurich, Switzerland[5]

Introduction:
Robotic-assisted bronchoscopy (RAB) with integrated Cone Beam Computed Tomography (CBCT) may enhance diagnostic yield for small peripheral pulmonary lesions (PPLs) without a bronchus sign and may have implications for lung cancer management. This study evaluates the first six months of RAB with CBCT at a tertiary center.

Methods:
This prospective cohort included patients undergoing RAB (ION endoluminal system) with integrated CBCT (Cios Spin) and cryobiopsy as clinically deemed necessary by four operators. Diagnostic yield was assessed per ATS2024 criteria (intermediate definition), with a 12-month follow-up (currently ongoing).

Results:
A total of 141 patients (mean age 68.6±9.5 years, 57.1% male) with 213 PPLs (median short axis 10 mm [IQR 7–14], long axis 11 mm [9–16]) were included. 31 (14.6%) lesions had a positive bronchus sign and 49 (23.1%) lesions were pure ground-glass-opacities. Median procedure time per lesion was 37 minutes [IQR 26–54], requiring an average of 1.25 CBCT spins/lesion (median dose-area product 6.1 Gy·cm²). Diagnostic yield was 89.3%, with a 1.4% pneumothorax rate. In 9.3% a resection was possible during the same anesthesia-event. Follow-up of 13 lesions (6.1%) is ongoing. Compared to the prior six years, center-wide lung cancer diagnoses (incl. other diagnostic modalities) increased by +69%, and stage IA diagnoses by +291%.

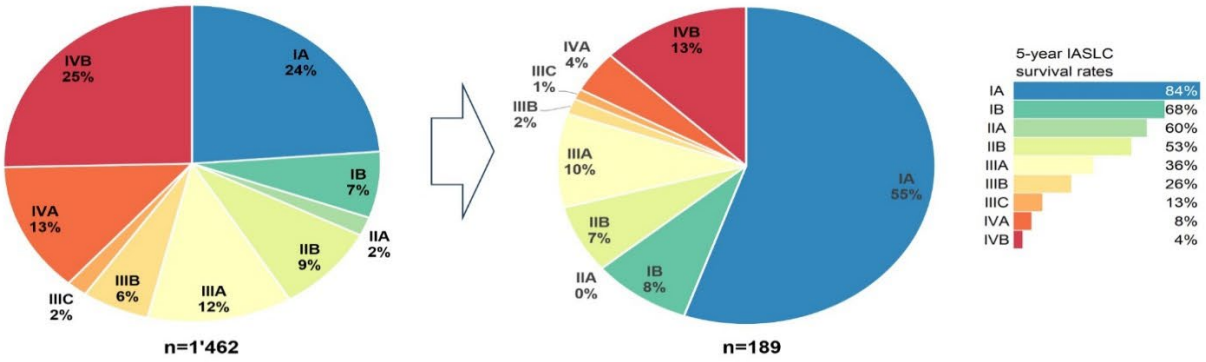
IVB 25%
IA 24%
IB 7%
IVA 13%
IIA 2%
IIB 9%
IIIB 6%
IIIC 2%
IIIA 12%
n=1'462
IVA 4%
IVB 13%
IIIC 1%
IIIB 2%
IIIA 10%
IA 55%
IIB 7%
IB 8%
IIA 0%
n=189
5-year IASLC survival rates
IA 84%
IB 68%
IIA 60%
IIB 53%
IIIA 36%
IIIB 26%
IIIC 13%
IVA 8%
IVB 4%

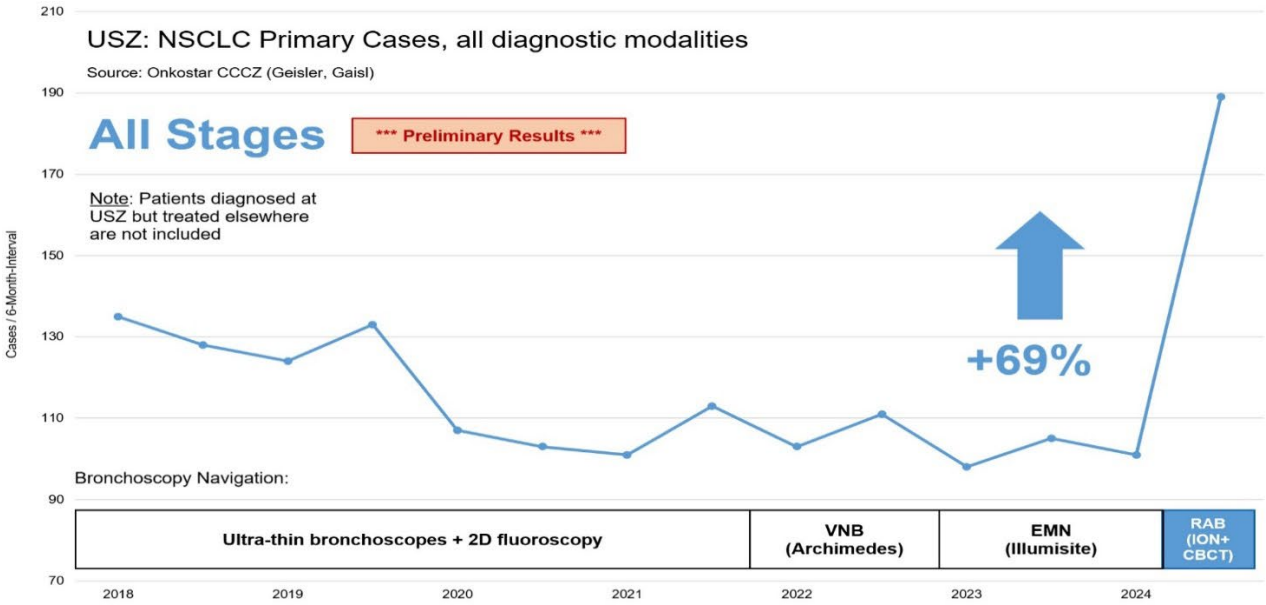
USZ: NSCLC Primary Cases, all diagnostic modalities
Source: Onkostar CCCZ (Geisler, Gaisl)
All Stages
*** Preliminary Results ***
Note: Patients diagnosed at USZ but treated elsewhere are not included
+69%
Cases / 6-Month-Interval
Bronchoscopy Navigation:
Ultra-thin bronchoscopes + 2D fluoroscopy
VNB (Archimedes)
EMN (Illumisite)
RAB (ION+ CBCT)
2018
2019
2020
2021
2022
2023
2024

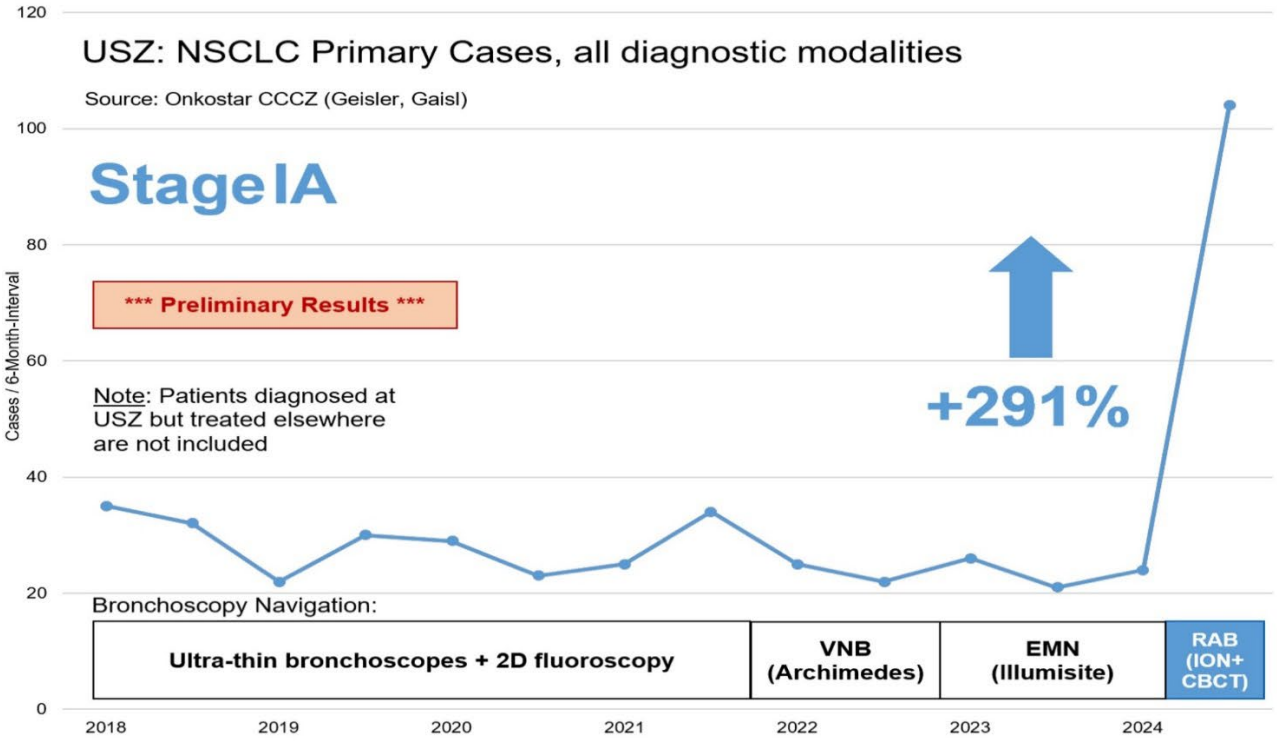
USZ: NSCLC Primary Cases, all diagnostic modalities
Source: Onkostar CCCZ (Geisler, Gaisl)
Stage IA
*** Preliminary Results ***
Note: Patients diagnosed at USZ but treated elsewhere are not included
+291%
Cases / 6-Month-Interval
Bronchoscopy Navigation:
Ultra-thin bronchoscopes + 2D fluoroscopy
VNB (Archimedes)
EMN (Illumisite)
RAB (ION+ CBCT)
2018
2019
2020
2021
2022
2023
2024

Conclusion:
RAB with integrated CBCT is a safe, efficient, and highly effective technique, offering excellent diagnostic yield even for subcentimeter lesions without a bronchus sign. This approach complements conventional bronchoscopy and has the potential to facilitate earlier lung cancer detection, thereby contributing to a stage shift in lung cancer diagnosis.

825

J. Epprecht[6], B. Siedentop[6], M. Papadimitriou-Olivgeris[7, 8], P. Monney[4], M. Frank[5], B. Ledergerber[6], G. Tzimas[4], P. Tozzi[2], M. Kirsch[2], M. van Hemelrijck[3], O. Dzemali[1, 3], B. Hasse[6]

No gender disparities in surgical treatment of infective endocarditis: a Swiss multicenter study

Center for Translational and Experimental Cardiology (CTEC), Department of Cardiology, University Hospital of Zurich, University of Zurich[1], Department of Cardiac Surgery, Lausanne University Hospital and University of Lausanne[2], Department of Cardiac Surgery, University Hospital Zurich and University of Zurich[3], Department of Cardiology, Lausanne University Hospital and University of Lausanne[4], Department of Cardiology, University Hospital Zurich and University of Zurich[5], Department of Infectious Diseases and Hospital Epidemiology, University Hospital Zurich and University of Zurich[6], Infectious Diseases Service, Cantonal Hospital of Sion and Institut Central des Hôpitaux (ICH), Sion[7], Infectious Diseases Service, Lausanne University Hospital and University of Lausanne[8]

Introduction:
Registry-based studies have consistently shown that women are less likely to receive surgical treatment for infective endocarditis (IE), although the underlying causes remain unclear. This disparity is concerning, as patients with surgical indications who do not undergo surgery face worse outcomes. This study aimed to evaluate whether women treated at two Swiss university hospitals were less likely to receive surgery despite having an established indication, whether the reasons for withholding surgery differed between sexes, and whether female sex was associated with a worse prognosis.

Methods:
This retrospective and prospective study included patients treated for IE at USZ or CHUV between 2014 and 2024. Surgical indications were assessed by a multidisciplinary team using the 2015 ESC guidelines. Logistic regression models were used to adjust for potential confounding factors. To assess survival, Kaplan-Meier analysis stratified by sex and surgical treatment was employed.

Results:
Among 1108 IE patients included, 272 (24.5%) were women. A surgical indication was identified in 48.5% of female patients (n=132) and 49.9% of male patients (n=417), with surgery performed in 77.3% and 77.0% of these cases, respectively. The most frequent reasons for not performing surgery were multimorbidity (4.8% in women vs. 5.9% in men), advanced age (4.0% vs. 3.5%), and neurologic contraindications (2.9% vs. 2.4%), with no difference between sexes. Logistic regression analyses revealed no evidence of an association between female gender and failure to undergo indicated surgery (unadjusted odds ratio [OR] 0.98, 95% confidence interval [CI] 0.61-1.55; adjusted OR [aOR] 0.69, 95% CI 0.39-1.19). Factors associated with not receiving surgery included a higher Charlson Comorbidity Index (>3: aOR 5.6, 95% CI 3.19-10.0), ongoing intravenous drug use (aOR 3.95, 95% CI 1.75-8.90), prosthetic valve IE (aOR 3.23, 95% CI 1.92-5.50), double valve IE (aOR 2.53, 95% CI 1.27-5.03), sepsis at presentation (aOR 1.87, 95% CI 1.17-2.99), and higher age (aOR 1.43 per 10 years older, 95% CI 1.18-1.74). Patients with aortic valve IE were less likely to forgo surgery (aOR 0.35, 95% CI 0.20-0.61), as were patients treated in Zurich vs. Lausanne (aOR 0.61, 95% CI 0.38–0.98). Investigating underlying reasons for this significant center effect, such as clinical protocols, resources, and patient characteristics, could provide further insight into this disparity. There was no difference in 1-year survival in female vs. male patients overall (73.6% vs. 74.8%, log-rank test p=0.5). Failure to undergo indicated surgery was associated with a significantly lower 1-year survival of 39.6% compared to no surgical indication (81.6%) or surgical indication with surgery (86.8%, log-rank test p=<0.001). There was no difference in survival between sexes in these subgroups.

Conclusion:

At these two Swiss university hospitals, female gender was not associated with a higher risk of indicated surgery being withheld. Further research is warranted, particularly in settings with limited access to cardiac surgery.

826

C. Steinack[3], P. Baumgartner[2], G. Monsch[4], D. Schneiter[4], S. Oh[1], E. Samara[5], I. Opitz[4], C. Clarenbach[3], S. Ulrich[3], M. Kohler[3], T. Gaisl[3]

Robotic-Assisted Bronchoscopy with Integrated Cone-Beam CT vs. Conventional Bronchoscopy for Diagnosing Peripheral Pulmonary Lesions: An Open-Label Randomized Controlled Trial

Section of Interventional Pulmonology, David Geffen School of Medicine, University of California, Los Angeles, Los Angeles, California[1], Universitätsspital Zürich, Klinik für Innere Medizin, Zurich, Switzerland[2], Universitätsspital Zürich, Klinik für Pneumologie, Zurich, Switzerland[3], Universitätsspital Zürich, Klinik für Thoraxchirurgie, Zurich, Switzerland[4], Universitätsspital Zürich, Radiation Protection Unit, Zurich, Switzerland[5]

Introduction:
Robotic-assisted bronchoscopy (RAB) with integrated cone-beam computed tomography (CBCT) represents a cutting-edge approach for diagnosing hard-to-access peripheral pulmonary lesions (PPLs). Despite its potential, direct comparisons with conventional bronchoscopy (CB) are lacking.

Methods:
In this investigator-initiated, single-center, open-label randomized trial, adult patients with PPLs were randomized 1:1 to undergo either CB with ultra-thin bronchoscopes and 2D fluoroscopy or RAB+CBCT (Ion endoluminal system, Cios Spin). Cryoprobes were used in all procedures, conducted by two interventional pulmonologists performing >450 procedures annually. The primary endpoint, diagnostic yield, was defined per ATS 2024 consensus criteria (intermediate definition). Trial registered at ClinicalTrials.gov (NCT06489678).

Results:
From June to November 2024, 78 patients with 127 PPLs were randomized to CB (39 patients) and RAB+CBCT (39 patients). Median lesion diameter was 11 mm [IQR 9–16], 18 (14.2%) lesions had a positive bronchus-sign, and 35 (27.6%) lesions were classified as pure ground-glass opacities. Diagnostic yield was 14.3% (9/65) for CB and 89.1% (49/62) for RAB+CBCT, yielding an absolute difference of 74.8% (95% CI, 62.8–86.7%, p<0.001). Among non-diagnostic CB cases, 95.6% (44/46) were successfully diagnosed through subsequent RAB+CBCT, either during the same anesthesia event or a separate procedure. Overall, 68 (53.5%) cases were diagnosed with lung cancer (50 [39.4%] with stage IA). The overall rate of adverse events were similar in both groups (p=0.09). 12-month follow-up for 7 (5.5%) lesions is ongoing.

Conclusion:
RAB with integrated CBCT offers a significantly higher diagnostic yield than CB, positioning it as a pivotal tool for effective early lung cancer diagnosis and a potential driver of stage shift in disease management.

Programm und Abstracts:

www.usz.ch/docr

Organisation und Kontakt

Universitätsspital Zürich
Direktion Forschung und Lehre
Rämistrasse 100
8091 Zürich

+41 43 253 01 10
dfl@usz.ch

Anmeldung und Kosten

Es ist keine Anmeldung nötig.
Die Teilnahme ist kostenlos.

Video-Aufzeichnung

Die Veranstaltung findet vor Ort statt. Alle Beiträge werden gefilmt und im Anschluss an die Veranstaltung online aufgeschaltet.

Veranstaltungsort

Universitätsspital Zürich
Grosser Hörsaal OST
via Eingang PATH:
Schmelzberstrasse 12
8091 Zürich

Anreise

Tramlinien 6, 9, 10 bis Haltestelle
ETH/Universitätsspital

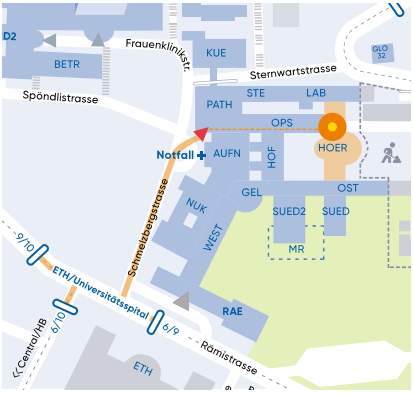

Folgen Sie dem USZ unter

05.25